Fall 1-1-2019

Liquid Chromatography - Mass Spectrometric Analysis of Clinicallyand Pharmacologically Relevant Molecules

Raghavi Kakarla
Cleveland State University

LIQUID CHROMATOGRAPHY - MASS SPECTROMETRIC ANALYSIS OF CLINICALLY AND PHARMACOLOGICALLY RELEVANT MOLECULES

RAGHAVI KAKARLA

Bachelor of Pharmacy

Andhra University

April 2009

Master of Pharmacy in Pharmaceutical Analysis

Acharya Nagarjuna University

October 2011

Submitted in partial fulfillment of requirements for the degree

DOCTOR OF PHILOSOPHY IN CLINICAL-BIOANALYTICAL CHEMISTRY

at the

CLEVELAND STATE UNIVERSITY

December 2019

This dissertation of RAGHAVI KAKARLA, Candidate for Doctor of Philosophy

in Clinical-Bioanalytical Chemistry for the

Department of Chemistry and College of Graduate Studies,

CLEVELAND STATE UNIVERSITY

has been approved by

Dissertation Chairperson, Dr. Baochuan Guo, 10-23-2019

Department of Chemistry

Dissertation Committee Member, Dr. Aimin Zhou, 10-18-2019

Department of Chemistry

Dissertation Committee Member, Dr. Xue-Long Sun, 10-23-2019

Department of Chemistry

Dissertation Committee Member, Dr. John F Turner, 10-23-2019

Department of Chemistry

Dissertation Committee Member, Dr. Chandrasekhar Kothapalli, date

Department of Chemical and Biomedical Engineering

Student's Date of Defense

Dedicated to my parents Sushma Rani, Satyanarayana

&

my beloved husband, Ravikiran

ACKNOWLEDGMENTS

I will forever be thankful to my advisor, *Dr. Baochuan Guo* without whom this dissertation would not have been possible. I am grateful for his invaluable guidance, encouragement and support throughout my Ph.D. program. His technical advice and mentorship have taught me innumerable lessons and insights on the workings of research. The past six years in his lab will remain a crucial part in my career.

My sincere thanks to my thesis committee members, *Drs. Aimin Zhou, Xue-Long Sun, John F Turner* and *Chandrasekhar Kothapalli* for their time and suggestions that enriched my work. I thank *Dr. Xiang Zhou* for training and helping with handling of analytical instruments and *Dr. Jerry Mundell* for his support and encouragement during my teaching assignments. I also thank Cleveland State University for providing facilities that made this work possible.

My heartfelt thanks to the members of our lab, especially *Rama, Ravali* and *Rebecca,* for their constant support and fruitful discussions. I also thank *Vasavi, Karthik, Rohan, Ruhan, Gang, Snigdha, Norah, Viharika, Shashank, Chandana* and other fellow graduate students for their company and support.

I am forever grateful to my parents *Sushama Rani* and *Satyanarayana* for their unconditional love and support. I won't be what I am now, without them. I am greatly indebted to my husband *Ravikiran* for his untiring love, patience, and support throughout this journey. I am thankful to my sister *Bhargavi* and brother-in-law, *Somasekhar* for their constant support. I am thankful to my niece, *Kamala* who filled my life with joy. I am very lucky to have the best of in-laws, *Vani, Raghurambabu, Kavitha* and *Praveen* who inspire me with their love and wisdom. I also thank *Vijitha, Sindu, Vasudha, Mounika, Sravya,* other family members and friends who always believed in me and supported me.

LIQUID CHROMATOGRAPHY - MASS SPECTROMETRIC ANALYSIS OF CLINICALLY AND PHARMACOLOGICALLY RELEVANT MOLECULES

RAGHAVI KAKARLA

ABSTRACT

Liquid Chromatography-Mass Spectrometry is an advanced analytical technique that offers high sensitivity and specificity and has been increasingly used for analysis of a wide variety of compounds including clinically and pharmacologically relevant molecules. In this dissertation we describe qualitative and quantitative liquid chromatographic mass spectrometric methods to analyze both small molecules and larger macromolecules that provide useful insights into diagnosis and management of several diseases. An LC-MS(/MS) analytical method includes extraction of analytes of interest from the matrix followed by liquid chromatographic separation and mass spectrometric detection. Chapter I describes pre-analytical workflows and sample pretreatment techniques and theories underlying LC-MS and instrumentation that are relevant to this work. The first chapter also describes the process of method development followed by validation guidelines for quantitative bio-analytical assays. Chapter II describes a novel, rapid, and simple quantitative mass spectrometric method for endogenous molecules in human bile that are associated with Cholangiocarcinoma and Cholelithiasis. The method was designed and validated to overcome problems suffered by conventional methods such as time-consuming extraction steps, carryover and unavailability of blank bile by employing simple dilution, flow injection and standard addition to matrix effects respectively. In Chapter III, a quantitative LC-MS/MS method was developed and validated for the determination of an antitumor drug in mouse brain to support an investigation to study the effectiveness of

intracerebral microdialysis as an alternative route of administration. This method describes a two-step extraction process using Proteinase K and ethanol protein precipitation to overcome the low recovery and high matrix effects faced by previously reported methods. Chapter IV describes investigation of feasibility of employing a less commonly used proteolytic enzyme, aspartic acid N endopeptidase, in the digestion of prothrombin for qualitative LC-MS analysis. This study could be employed to study distribution of variants of des-gamma-carboxy-prothrombin, a biomarker which is elevated in hepatocellular carcinoma and vitamin K deficiency to further identify a more specific variant(s) as a biomarker. Finally, this dissertation is concluded with recommendations for qualitative and quantitative LC-MS research methodology based on the findings herein and future directions implicated by the impact of this work.

TABLE OF CONTENTS

LIST OF TABLES

LIST OF FIGURES

CHAPTER I

INTRODUCTION

1.1 General introduction and scope of research

Liquid Chromatography-Mass Spectrometry is a hyphenated analytical technique that unites the separation power of liquid chromatography with the detection capability of mass spectrometry. It not only enables analysis of analytes in liquid phase but also offers high sensitivity and specificity and thus is being increasingly utilized for qualitative and quantitative analyses of small and large molecules such as biomarkers and drugs in biological matrices. Biomarkers are biological molecules that indicate the presence and progress of a disease and are important tools that aid in detection, diagnosis and treatment of diseases. LC-MS is regarded as the analytical gold standard for quantification of small molecules in the clinical laboratory as it provides superior specificity compared to widely employed techniques such as immunoassays and HPLC [1]. In addition to small molecule biomarkers, protein biomarkers are also being studied extensively because in contrast to gene-based biomarkers they provide more meaningful and clinically relevant information. The changes that take place during and after protein expression such as altered expression, post translational modifications, structure, function, interactions, etc. may stimulate or

effect underlying mechanisms of many diseases including cancer. Proteomics revolves around identification and understanding these changes and many attempts are being made to identify biomarkers based on expressed proteins [2]. Proteins are made up of amino acids varying in number and sequence and hence differ in their molecular structures and physiochemical properties which allows for their separation and identification. With the emergence of mass spectrometry, LC-MS has advanced as a major analytical tool for proteomics analyses owing to its sensitivity, selectivity, accuracy and throughput [3].

Pharmacological studies provide important information related to safety and efficacy of drugs and hence play a significant role in drug development [4]. When a drug is administered into the body, the physicochemical and biochemical properties of the drug and biophysical properties of the body dictate the fate of the drug. As most drugs are exogenous, they do not have an appropriate biodistribution profile in the body unlike endogenous molecules. Thus, their distribution is mostly systemic and lacks selectivity which leads to unwanted side effects and is especially the case with cytotoxic anticancer drugs. In order to improve safety, various targeted delivery systems and alternate routes of administration are being investigated as promising alternatives to maximize therapeutic efficacy and minimize systemic toxicity [5]. In order to evaluate the potential of the targeted drug delivery systems, their biodistribution needs to be evaluated using analytical methods that provide accurate quantification. LC-MS/MS has become the most commonly used technique for pharmacokinetic studies as it not only offers accurate quantification of drug/metabolite based on molecular weight but also provides structural information pertaining to metabolism of the drug [6].

In this dissertation we describe qualitative and quantitative liquid chromatographic mass spectrometric methods to analyze small and large molecules that provide useful insights into diagnosis and management of various diseases. In general, LC-MS(/MS) analysis includes extraction of analyte of interest from the matrix followed by liquid chromatographic separation and mass spectrometric detection. In this chapter, we provide a brief background on LC-MS, various sample preparation techniques for small molecules and proteins, underlying principles and instrumentation, overview of method development and validation.

Chapter II describes a simple method for high throughput analysis of glycocholic acid and unconjugated bilirubin in human bile. High levels of glycocholic acid and unconjugated bilirubin in bile are found to be associated with Cholangiocarcinoma and Cholelithiasis respectively. Because of the hydrophobic nature of these metabolites, current methods require time-consuming extraction steps and are prone to column carryover in order to separate these from interfering matrix components. Furthermore, it is virtually impossible to prepare a blank bile matrix that does not contain these analytes. Therefore, we employed a dilute-and-shoot flow-injection mass spectrometric method to quantify glycocholic acid and unconjugated bilirubin in bile using standard addition. Bioanalytical method validation has also been performed in accordance with FDA guidelines using clinical samples.

Chapter III focuses on a sample preparation method for LC-MS/MS analysis of an anticancer drug, Temozolomide in mouse brain. Brain tumor treatment is not as successful as the treatment of other tumors due to the systemic toxicity that limits the amount of

Temozolomide administered orally or intravenously. A potential strategy to combat systemic toxicity is targeted drug delivery through intracerebral microdialysis which needs to be investigated in animal models using a good analytical method prior to human clinical trials. Unfortunately, current methods that quantify Temozolomide in mouse brain suffer from poor extraction methods that result in high matrix effects (220%) and low recovery (63%) and are not reliable for analysis. Hence, we have developed a sample preparation with two-step extraction process that improved recovery to 82% and reduced to matrix effects within 15%.

In Chapter IV, we focus on evaluating the feasibility of digestion of a protein prothrombin with an unconventional protease called Aspartic acid N endopeptidase for in order to elucidate the distribution of variants of abnormal prothrombin in two different disease states. Biosynthesis of prothrombin requires post translational carboxylation of ten glutamic acid residues present in its Gla domain. However, in Vitamin K deficiency and hepatocellular carcinoma, carboxylation is defective leading to elevated levels of variants of abnormal prothrombin called Des-gamma-carboxy-prothrombin. Those variants that are elevated in hepatocellular carcinoma are also elevated in Vitamin K deficiency and therefore lead to false positive results as immunoassays cannot distinguish between them. An investigation of distribution of variants of the protein in both conditions might lead to the discovery of a specific biomarker for hepatocelluar carcinoma. This could be achieved by digesting the protein to produce a peptide that contains all the ten glutamic acid residues (modified or unmodified) and analyzing them using LC-MS. The main goal of this study is to evaluate the feasibility of using Aspartic acid N endopeptidase to digest prothrombin. We have optimized the proteolytic digestion of prothrombin and compared the digestion

efficiency of the enzyme to that of Trypsin because the latter is the most commonly used in LC-MS proteomic workflows.

1.2.1 High Performance Liquid Chromatography

High performance liquid chromatography is a separation technique and has a wide variety of applications including qualitative/quantitative analyses and chemical purification. HPLC separates components in a sample based on their affinities towards mobile and stationary phases. Reverse Phase HPLC is a commonly used mode of HPLC which separates analytes by using a non-polar stationary phase and a polar mobile phase. Fig.1.1 shows the schematic diagram of a typical HPLC system. A solvent reservoir holds mobile phase that comprises of a mixture of solvents (like methanol, water, acetonitrile, along with a suitable buffer) and is degassed and pumped pulse-free into an analytical column at a controlled flow rate. A specified volume of a sample is injected and carried by the mobile phase into the column. The column consists of relatively hydrophobic particles which act as stationary phase to retain compounds. As mobile phase passes through the column, components in the sample are eluted at different times depending on their affinity towards the stationary and mobile phases. The degree and time of separation is dictated by various factors like pKa of the compound, pH, organic modifier of the mobile phase, flow rate, chemical nature and particle size of the stationary phase. Ultra-High Pressure Liquid Chromatography (UHPLC) is a recent development and superior version of HPLC that operates at high pressures and utilizes a HPLC column packed with sub-2μ sized particles. UPLC provides improved resolution, speed of separation and is being increasingly used for bioanalysis to separate proteins, peptides, metabolites, drugs etc.

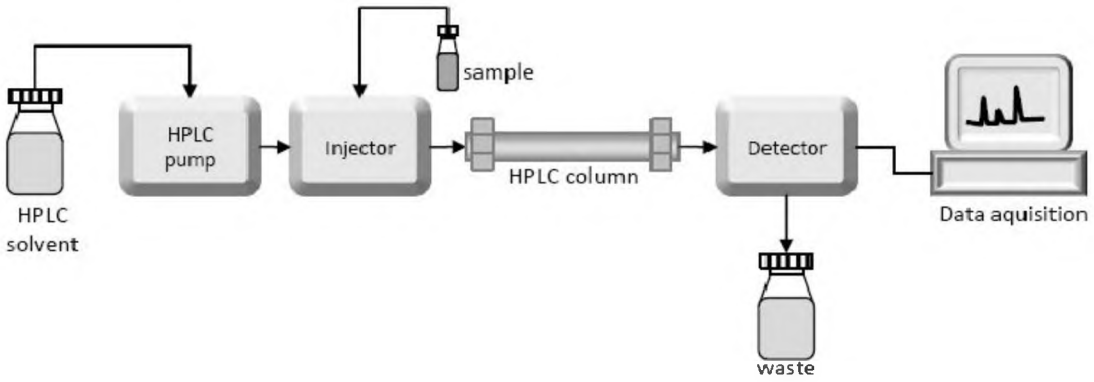

Figure 1. 1 Schematic diagram of a typical HPLC system [7]

1.2.2 Mass Spectrometry

Mass spectrometry is a detection technique that generates gaseous ions and separates analytes based on their mass to charge ratios (m/Z). It not only provides accurate molecular weight information but also helps in structure elucidation of molecules. With its highly specific and sensitive analytical capabilities, it has become a powerful tool for bioanalysis. Liquid Chromatography Mass Spectrometry (LC-MS) is a hyphenated technique that combines the separating power of liquid chromatography with the analytical capabilities of mass spectrometry. The high selectivity offered by mass spectrometry enables accurate quantitation even if all analytes are not chromatographically resolved. This makes quantitation feasible even without the use of a chromatographic column to separate the analyte and is termed flow-injection mass spectrometry (FI-MS). Chapter II describes the use of FI-MS/MS for quantification of endogenous molecules in bile in chapter II. The basic components of a mass spectrometer are ion source, mass analyzer and a detector.

1.2.2.1 Ionization source

The incoming components from HPLC are in liquid state at atmospheric pressure and must be converted into gaseous ions for analysis. To achieve this, various ion sources can be used as interfaces between HPLC and MS such as electro spray ionization (ESI), atmospheric pressure chemical ionization (APCI) and atmospheric pressure photo ionization (APPI). Electrospray ionization (ESI) is the most commonly coupled ionization source for the analysis of non-volatile biomolecules. ESI is a soft ionization technique and is widely used owing to its ability to ionize small molecules as well as large molecules.

Electrospray ionization occurs by the formation of charged droplets followed by desolvation finally leading to the production of gas phase ions. As illustrated in fig. 1.2, a positive or negative electric field is applied at the spray needle tip which produces ions in liquid state. Repulsive forces between the ions push them towards the surface increasing the charge density even more. When repulsive forces become higher than the surface tension of the droplets, they are ejaculated as a stream into the desolvation zone forming a 'Taylor cone' at the end of the spray needle. A heating gas causes the solvent to evaporate thereby shrinking the droplet and increasing the charge density further. The droplet becomes unstable with increasing charge density and finally breaks apart into smaller stable droplets when the repulsive forces exceed 'Raleigh limit'. Desolvation and fission of droplets continue to occur till each droplet has a single ion. In case of large molecules such as proteins or large peptides, ions may contain multiple charges which reduces the m/Z to be within the measurable range, thus allowing the detection of large molecules. ESI can be done both in positive mode in which mostly protonation occurs resulting in the formation of $[M+H]^+$ ions and in negative mode which results in de-protonation producing $[M-H+]^-$ ions. Protonation and deprotonation can be facilitated by addition of a buffer based on the chemical nature of the analyte.

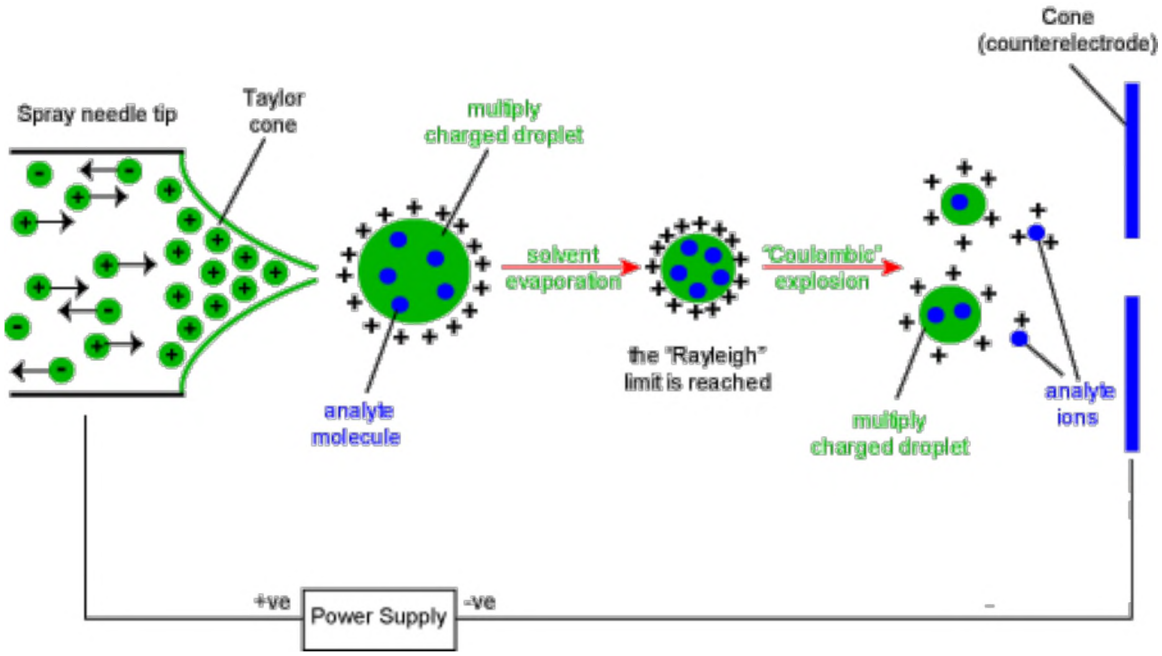

Figure 1. 2 Mechanism of electrospray ionization [8]

1.2.2.2 Mass analyzer

The ions generated in the source are separated in the mass analyzer according to their mass to charge ratio (m/Z). There are different types of mass analyzers that vary in mass range limit, speed of analysis, mass accuracy and resolution. In this dissertation, a triple quadrupole mass analyzer (Q-TRAP) was used for qualitative and quantitative analyses. Quadrupole mass analyzers consist of four parallel rods made of inert metal arranged radially as shown in fig. 1.3. A set of fixed DC and alternating Rf potentials are applied to the rods which create electric fields in which ions travel in helical trajectories. Only those ions with certain mass to charge (m/Z) have stable trajectories and pass through the quadrupoles to reach the detector, while other hit the quadrupoles and fail to reach the detector. Thus, Rf voltage can be varied to separate ions according to their mass to charge ratios (m/Z). Quadrupole analyzers are inexpensive, offer high sensitivity and specificity but have limited mass range. A triple quadrupole mass spectrometer (QqQ) consists of three quadrupoles in tandem as shown in fig 1.3 with first and last quadrupole functioning as mass filters with a collison cell in between. The first quadrupole (Q1) filters ions of specified m/Z which are fragmented in the collision cell (q2) in the presence of an inert gas like nitrogen while the third quadrupole (Q3) scans selected fragment ions of certain m/Z. This type of scan is called as multiple reaction monitoring (MRM) and is preferred method for quantitation as it offers high specificity and sensitivity.

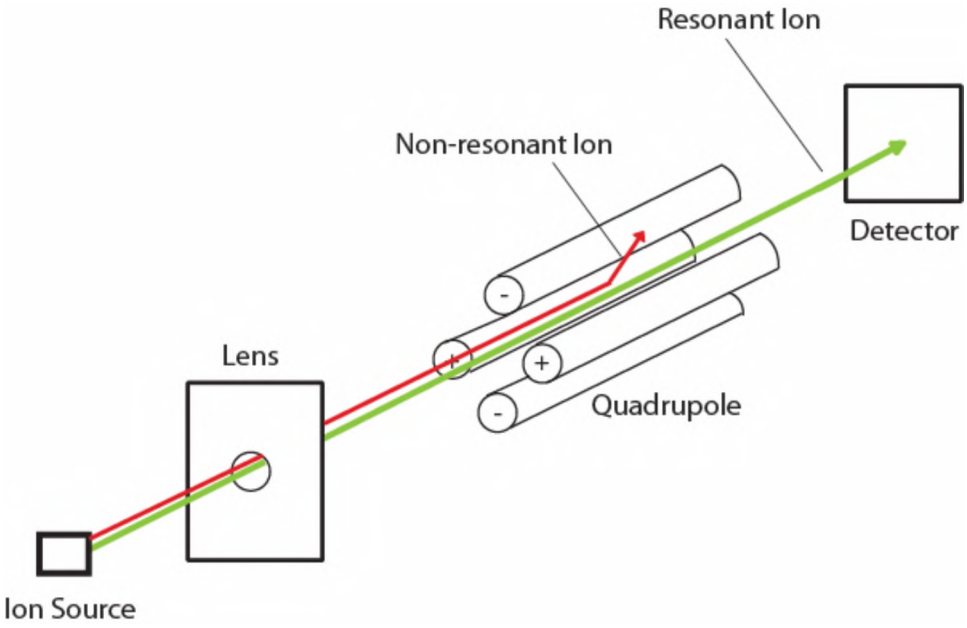

Figure 1. 3 Schematic diagram of a quadrupole [9]

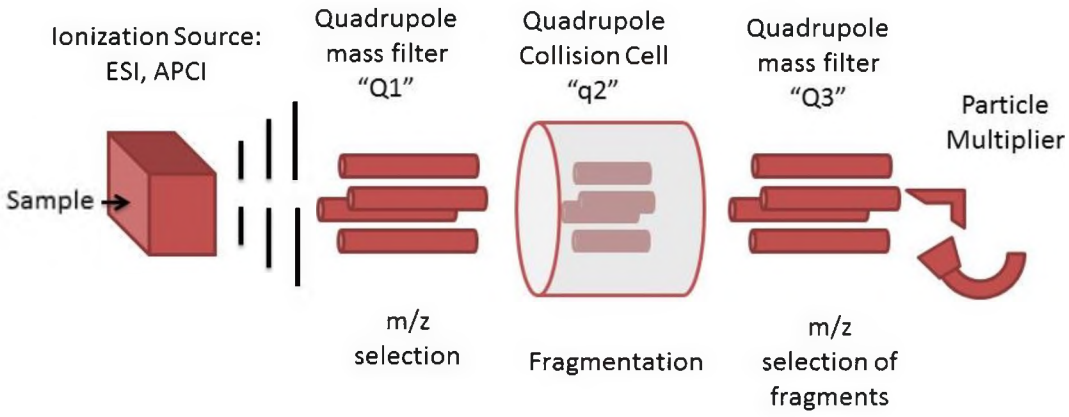

Figure 1. 4 Multiple reaction monitoring in triple quadrupole [10]

1.2.2.3 Detector

Ions passing through the mass analyzer are drawn into the detector. An electron multiplier is one of the most commonly used detectors in mass spectrometers and functions based on secondary electron emission from a series of dynodes. Each ion that strikes a dynode ejects more electrons which in turn strike the next dynode thus creating an 'electron pulse'. The cumulative signal of electron pulses is displayed as total count of ions per second.

1.2 Pre-analytical workflow for analysis of clinically relevant molecules

1.3.1 Biological sample pre-treatment

In bioanalysis, analytes are present in a variety of biological specimen that are common such as plasma, serum and urine, less common such as bile, cerebrospinal fluid, specialized such as stool, dried blood spots or very specialized like tissue and secretions. Each specimen differs from one another in terms of chemical constitution and complexity of the matrix. The components present along with the analyte(s) in a biological/clinical sample are proteins, lipids, salts, and other endogenous compounds that can significantly influence the analytical method [11]. They tend to co-elute with the analyte and compete for limited space on droplet surface during electro spray ionization resulting in matrix effects such as ion suppression or ion enhancement. Furthermore, they can also foul the column, affecting analyte peak shape, produce ghost peaks and high levels of background

noise. Hence samples must be pretreated to isolate analyte as much as possible from the matrix components prior to LC-MS analysis. Cleaner samples produce more robust results, increased sensitivity and selectivity. This is achieved by one or a combination of different sample pretreatment techniques depending on the chemical nature, concentration of analyte, matrix in which analyte is present, stability of analyte, potential interferences, specific challenges such as sensitivity, throughput and more. For small molecules, sample pre-treatment is done by dilution, protein precipitation, liquid-liquid extraction and solid phase extraction. The discussion has been limited to those techniques relevant to this research, which include dilution, protein precipitation, and solid phase extraction.

1.3.1.1 Dilute and Shoot

Dilute-and-shoot is the simplest sample pre-treatment method in which a suitable solvent is added to the sample followed by centrifugation. The supernatant is then subjected to LC-MS/MS analysis. Dilution not only facilitates high throughput analyses in a clinical laboratory setting, but also is reported to reduce matrix effects significantly by decreasing the concentration of matrix components in the sample [12]. However, dilute-and-shoot technique is only suitable for less complex samples such as bile, urine and saliva and in which concentration of analyte is fairly high compared to those of matrix components and can be quantified even after dilution.

1.3.1.2 Protein precipitation

Protein precipitation is one of the common sample pretreatment methods for biological specimen in which proteins are present in higher concentrations such as blood, serum, tissue etc. Proteins can contaminate or block HPLC columns and cause significant matrix effects if not removed. Addition of protein precipitating agents disrupts the hydration layer surrounding individual proteins and causes them to aggregate as illustrated in fig. 1.5. The sample is then centrifuged at high speeds so that aggregated proteins form a pellet at the bottom which can be easily separated. Organic solvents such as methanol, ethanol and acetonitrile are among the most commonly used organic solvents for protein precipitation. They decrease the dielectric constant of the protein solution, which increases the electrostatic interactions between proteins resulting in protein aggregation [13]. Strong acids such as perchloric acid and trichloroacetic acid form insoluble salts with the amine groups of the proteins and precipitate proteins [14]. Ammonium sulfate is also a widely used protein precipitating agent at high concentrations of <0.15 M. Salt ions compete with proteins for water molecules exposing hydrophobic regions of proteins that are less soluble in water. This process is called 'salting out' [15]. Other protein removal agents include metal ions such as Zinc sulfate and ultrafiltration. Protein precipitation is not only simple and cost effective but is also reported to decrease phospholipids from serum and plasma samples [11]. However, protein precipitation as such might not be sufficient enough to minimize matrix effects and is combined with other sample pretreatment techniques to achieve much more cleaner samples.

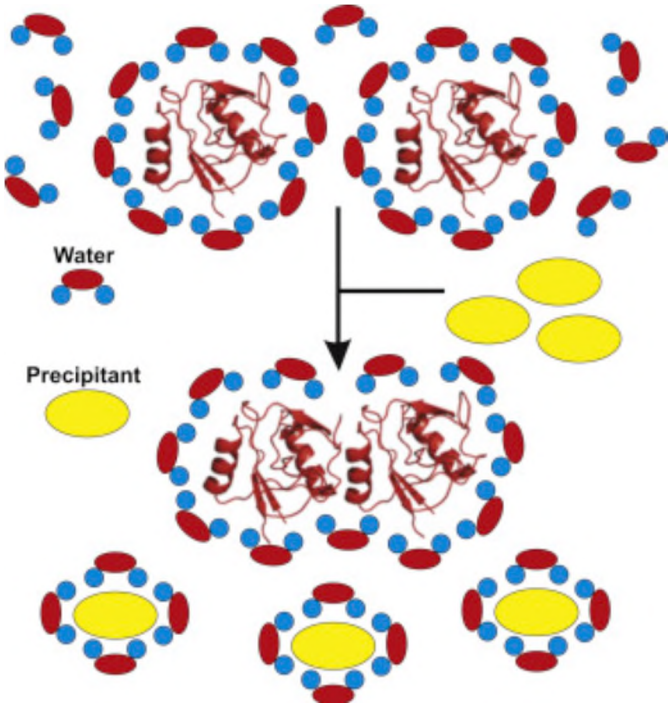

Figure 1. 5 Mechanism of protein precipitation [16]

1.3.1.3 Solid Phase Extraction

Solid-phase extraction has been proven to be a reliable and versatile method for the selective extraction and enrichment of a variety of analytes in biological matrices. The principle of solid phase extraction is same as that of liquid chromatography; analyte from solution is purified by sorption onto a solid-phase cartridge containing stationary phase made of silica, C18, C8, C4, phenyl, etc. followed by elution of the analyte with a solvent appropriate for instrumental analysis. In this work, we have employed a ZipTip based solid phase extraction for removing salts and other unwanted chemicals in the sample prior to LC-MS analysis. ZipTip contains solid sorbent, typically made of C18 material embedded in a pipette tip. SPE is performed stepwise as shown in fig. 1.6.

- *Conditioning*: Sorbent is activated by wetting/ conditioning first with an organic solvent followed by an aqueous buffer.
- *Loading:* Sample is then loaded into the ziptip and the analyte along with other interfering molecules bind to the sorbent.
- *Washing:* A buffer solution (typically composed of water and a modifier) is used to wash the sorbent to remove undesirable, co-retained interfering molecules, leaving the analyte molecules bound to the sorbent.
- *Eluting:* Finally, the analyte molecules are eluted from the sorbent with a solvent of higher elution strength comprising of appropriate percent of organic solvent and buffer.

SPE not only reduces matrix effects significantly but can also be used to concentrate the analyte after extraction.

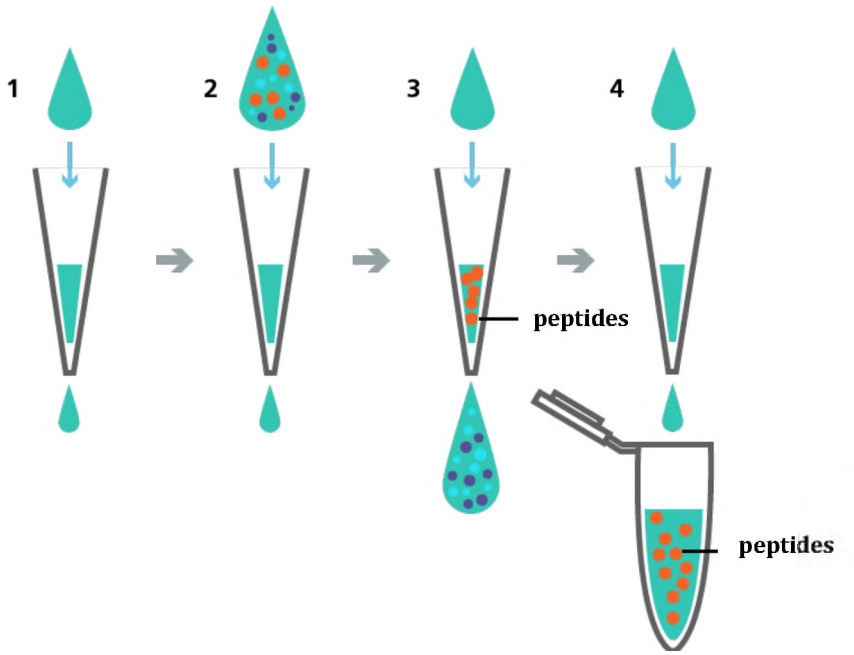

Figure 1. 6 Solid phase extraction using ZipTip

1.3.2 Enzymatic digestion for proteomic analysis (middle-down approach)

There are two fundamental LC-MS based approaches in proteomics that are used to identify different variants of proteins. In top-down approach, intact proteins are ionized and analyzed directly by using high-resolution mass spectrometers. However, top-down analysis is challenging and is not a good choice for proteins larger than 50 kDa as the dynamic range of instruments is limited, the resulting spectra from multiply charged ions is much complex and requires expensive high-resolution instruments such as like FT-ICR, hybrid ion trap FT-ICR, and hybrid ion trap–orbitrap or tribid quadrupole-orbitrap mass analyzers [17]. In bottom-up proteomics (also known as shotgun proteomics), proteins are cleaved into peptides less than 3 kDa, typically by Trypsin, separated by SDS PAGE and/or by HPLC and subjected to MS analysis. This approach is robust, ensures high throughput and is the most widely used approach as it is based on the analysis of peptides that produce more simpler spectra than intact proteins. However, Trypsin produces peptides that are sometimes too short and the sequence coverage might not be efficient which is not ideal for investigating PTMs. Middle-down proteomics, a newly emerging approach involves proteolysis using unconventional enzymes to produce longer peptides within 3-10 kDa range and offer the advantages of both top-down and bottom-up approaches. Differences in all the three workflows is illustrated in Fig 1.7. Middle-down proteomics permits better sequence coverage and facilitates the identification of neighboring PTMs as longer peptides are analyzed. The workflow of middle-down proteomics is similar to that of bottom-up except that Trypsin is replaced by other proteolytic enzymes like Asp-N and Glu-C that have fewer cleavage sites than Trypsin [18]. Efficient proteolysis of proteins

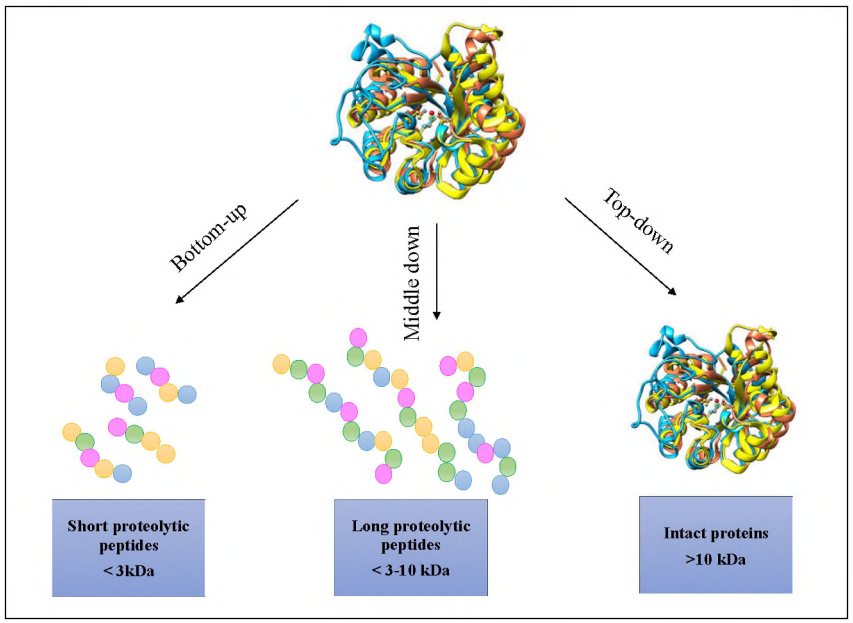

Figure 1. 7 Various analytical workflows in proteomics

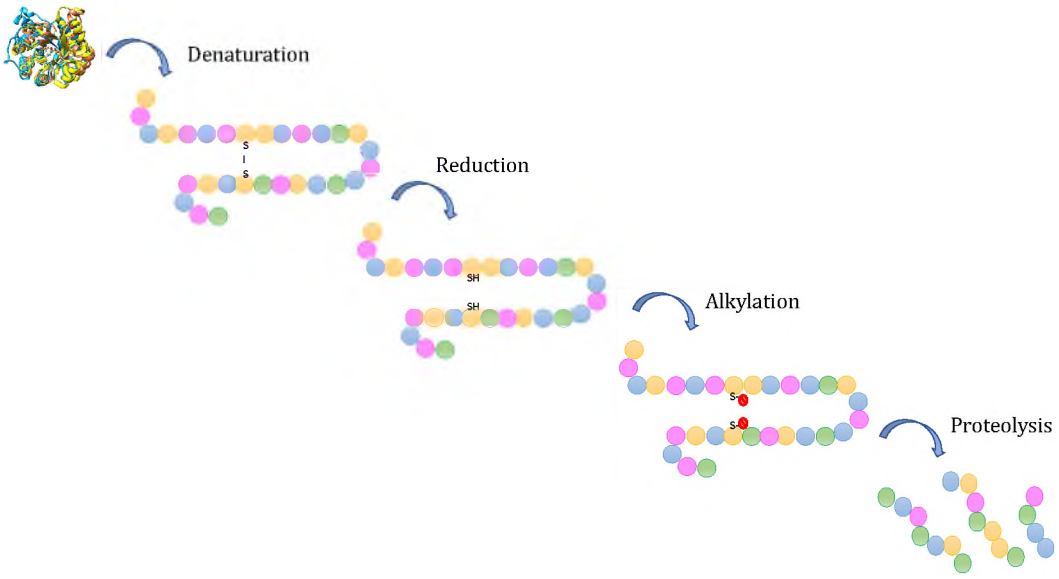

Figure 1. 8 Denaturation, reduction and alkylation steps before performing digestion

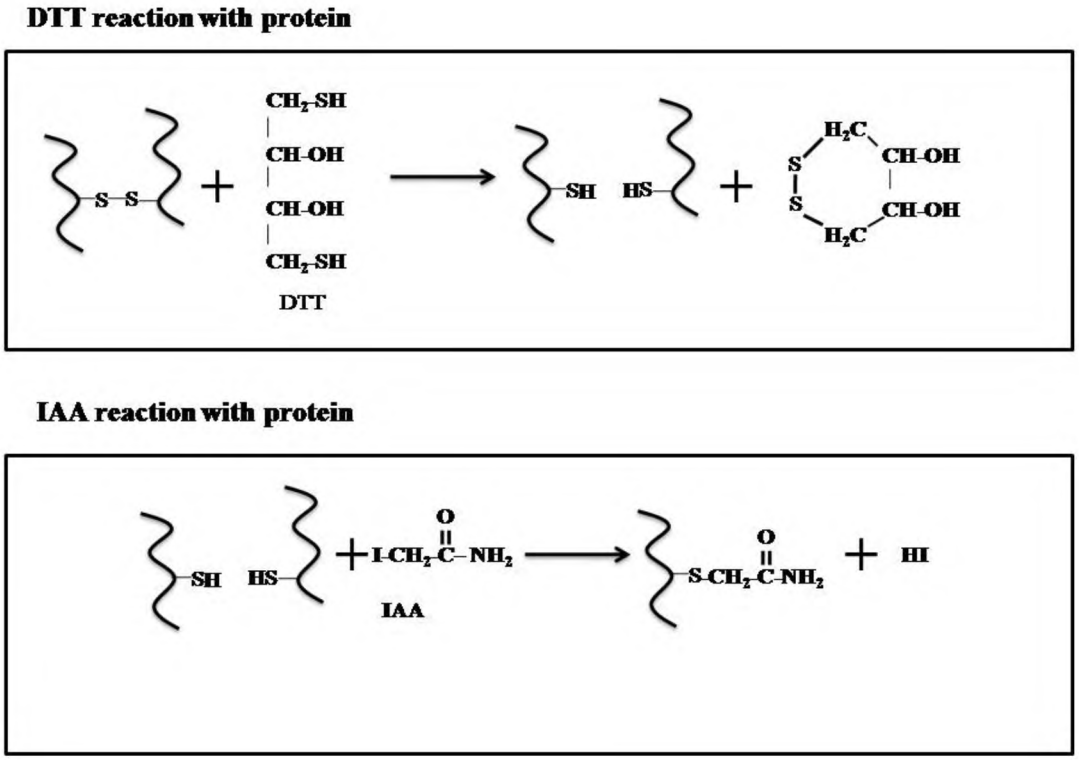

Figure 1. 9 Chemical reactions of reduction and alkylation at cysteine residues [19]

into peptides is a key step in bottom-up and middle-down proteomic workflows. Proteolysis is performed by using proteolytic enzymes or chemicals and is usually more efficient when proteins are converted to polypeptides that are more accessible to enzymes for digestion. This is achieved through a sequence of steps involving denaturation, reduction and alkylation as illustrated in fig. 1.8. Proteins are first denatured by treating with 6-8M urea, 6M guanidine hydrochloride or detergents which disrupt hydrophobic interactions causing the protein to unfold. This is followed by reduction with 5-15 mM dithiothreitol (DTT) or 5-50 mM tris(2-carboxyethyl) phosphine (TCEP) which reduce disulfide linkages between cysteine residues that are retained after denaturation, to thiol groups as shown in fig 1.9. Reformation of disulfide bonds is prevented by alkylation with Iodoacetamide (IAA) which adds carbamidomethyl group as shown in fig 1.9. IAA is added at a concentration of approximately three times to that of DTT. After alkylation, a suitable buffer is added to reduce the concentration of denaturing agent and pH favorable for the protease to have maximal activity to digest the protein. This is followed by addition of protease at an optimal enzyme-to-protein ratio and incubated at 37 °C for 1-18 hours. After sufficient time, digestion is stopped by acidifying the digest by the addition of formic or trifluoroacetic acid, as lowering the pH will inactivate, or quench the enzyme. Resultant peptides are then extracted and analyzed.

1.5 Method development

LC-MS method development is an iterative process in which some of the steps are optimized further to achieve desired results. Method development requires the knowledge

of composition of sample matrix, chemical properties of analyte, expected concentration range of the analyte etc. Fig. 1.10 shows the general steps involved in method development. In general, the first step is optimization of an MS/MS method to monitor MRM channels. This is done by manually infusing the standard solution of analyte(s) and the IS separately into the electrospray ionization source of the mass spectrometer. Depending on the response of the mass spectrometer, a suitable polarity (positive or negative mode) is chosen and source dependent parameters are optimized. The most abundant molecular ion is chosen as precursor ion which is fragmented by optimizing the compound dependent parameters such as collision energy. The most abundant or unique fragment is chosen as a product ion for quantification whilst the second most abundant is chosen for evaluating specificity of the method. Once the mass spectrometric parameters are optimized for analytes and the IS, an LC method is developed. Typically, a C18 HPLC column is chosen for most separations although other stationary phases such as phenyl, C8 and HILIC among others etc. are also used, depending on the hydrophobicity of the analyte of interest. In one of our projects we have flow-injected samples into the mass spectrometer without using a HPLC column in order to prevent the highly hydrophobic analytes sticking to the column which further leads to carry over. Chromatographic parameters such as mobile phase composition, elution profile, flow rate, run time, column temperature etc. are optimized until desired separation and peak shapes are obtained. Optimization of MS and LC parameters is followed by development (and simplification when possible) of sample preparation. Samples are pretreated by dilution, protein precipitation, liquid-liquid extraction, solid phase extraction etc. Finally, the method is validated after it has been optimized further to obtain desired sensitivity and specificity.

Figure 1. 10 Flowchart of analytical method development and optimization

1.5 Quantitative Method Validation

Once developed, bio-analytical methods are validated to ensure that the data is reliable by addressing crucial concerns such as accuracy, precision, specificity, selectivity, linearity (range in measurements that provide reliable data), sensitivity, effect of sample collection, and storage on the data. The U.S. FDA recommends validation of bioanalytical methods and provides detailed guidance with the aid of calibrators and quality controls and defines reference limits for some of the parameters.

Calibrators or calibration standards are biological matrices to which a known amount of analyte has been spiked and are used to plot calibration curves from which concentrations of analytes in quality control samples and study samples are determined. A set of calibrators consists of a blank or double blank (does not contain analyte or internal standard) a zero calibrator or single blank (does not contain analyte but contains internal standard) and six non-zero calibrators covering the quantitation range, lower and upper limits. Quality control is a biological matrix with a known quantity of analyte that is used to monitor the performance of a bioanalytical method. Three levels of quality controls such as low-quality control (LQC), medium-quality control (MQC) and high-quality control (HQC), are freshly prepared for evaluating various validation parameters.

1.5.1 Calibration curve

Linearity refers to the relationship between the instrument response and the calibration standards within the intended quantitation range. A calibration range should be

chosen based on the range expected in the study. The simplest model that describes the concentration-response relationship, suitable weighing factor and regression equation must be used. Accuracy and precision of calibrators should be determined using a minimum of six non-zero calibrators, a zero calibrator and a blank. %RE and %CV of non-zero calibrators should be ± 15% of the nominal concentration except LLOQ which can be ± 20% of the nominal concentration.

1.5.2 Specificity and Selectivity

The extent to which a method can evaluate the analyte in the biological matrix without interferences from matrix components is defined as selectivity. Specificity is the ability of the method to unambiguously evaluate the analyte in the presence of other components such as impurities, degradation products, matrix components etc. Selectivity is determined by analyzing blank samples of appropriate biological matrix from at least six individual sources. Specificity is evaluated for interference by cross reacting molecules, concomitant medications etc.

1.5.2 Carryover

Carryover is defined as the appearance of the analyte in a sample from the previous sample. FDA recommends that carry over should be eliminated during the stage of method development. It is usually determined by injecting a double blank after running the upper

limit of quantification. The instrument response should be <20% of the LLOQ in the double blank at the retention time of the analyte.

1.5.3 Sensitivity

Sensitivity, also called the lower limit of quantitation (LLOQ) is defined as the lowest analyte concentration in the biological matrix that can be quantified with acceptable accuracy and precision. FDA recommends that the analyte response at the LLOQ should be five times greater than or equal to zero, referred to as the calibrator/single blank. Accuracy and precision of the LLOQ should be ± 20% of nominal concentration determined form five replicates on same day and five different days.

1.5.4 Accuracy and Precision

Accuracy is defined as the degree of closeness of determined value to the nominal or true value under proposed conditions. Precision is defined as closeness of agreement among a series of measurements obtained from multiple sampling of the same homogenous sample under the proposed conditions. Accuracy and Precision are determined on the same day (Intra-day) and five different days (Inter-day) by evaluating five sets of three QCs for percentage relative error (%RE) and percent coefficient of variance (%CV). FDA recommends that %RE should be ± 15% of nominal concentration and %CV ± 15% for three QCs.

1.5.5 Recovery

Recovery is defined as the extraction efficiency of an analytical method reported as % of known amount of an analyte carried through the sample extraction and processing steps of the method. Recovery need not be 100% but should be optimized to ensure that the recovery of analyte and IS should be consistent and reproducible. Absolute and relative recoveries of analyte are assessed by comparing responses of analyte (absolute recovery) and response ratios of analyte and IS (relative recovery) in extracted samples to those in extracts of blank samples spiked with analyte and IS after extraction.

1.5.6 Matrix effect

Matrix effect is defined as the effect on the method caused by components in a study sample other than the analyte. The components in the matrix when co-eluting with the analyte, tend to compete with analyte molecules for ionization resulting in either ion suppression or enhancement. Moreover, the matrix effects vary between samples, as matrix composition in biological samples is varied, making the assay difficult to control for these interferences. FDA recommends that bioanalytical methods using LC-MS/MS must be assessed and accounted for matrix effects. The absolute matrix effect of analyte is determined by comparing the response of analyte in extracted biological sample matrix with that of analyte in neat solution. The relative matrix effect is determined by comparing the response ratio of analyte and IS to that of analyte in extracted biological sample matrix with the response ratio of analyte and IS analyte in neat solution.

1.5.7 Stability

Stability is the measure of intactness of the analyte in the biological matrix under proposed storage and use conditions relative to the starting material for given time intervals. Stability studies are performed by comparing the responses of QCs against freshly prepared samples in different conditions covering exposure in autosampler, benchtop, freeze-thaw cycles in addition to stability of stock solution and long-term stability. FDA recommends accuracy of ± 15% of nominal concentration at two QC levels.

1.6 Conclusion

The use of LC-MS for qualitative and quantitative analysis of clinically relevant molecules and drugs has been rapidly increasing owing to the technique's sensitivity and selectivity. In this chapter, a brief background on analysis of small and large molecules, theories and instrumentation of HPLC and mass spectrometry, pre-analytical workflows, method development and quantitative method validation guidelines stated by the US FDA has been discussed and the application of these area of analytical science are presented in the coming chapters.

1.7 References

[1] S. K. Grebe and R. J. Singh, "LC-MS/MS in the Clinical Laboratory – Where to From Here?," *Clin. Biochem. Rev.*, vol. 32, no. 1, pp. 5–31, Feb. 2011.

[2] P. R. Srinivas, M. Verma, Y. Zhao, and S. Srivastava, "Proteomics for Cancer Biomarker Discovery," *Clin. Chem.*, vol. 48, no. 8, pp. 1160–1169, Aug. 2002.

[3] G. Chen and B. N. Pramanik, "LC-MS for protein characterization: current capabilities and future trends," *Expert Rev. Proteomics*, vol. 5, no. 3, pp. 435–444, Jun. 2008.

[4] D. K. Walker, "The use of pharmacokinetic and pharmacodynamic data in the assessment of drug safety in early drug development," *Br. J. Clin. Pharmacol.*, vol. 58, no. 6, pp. 601–608, Dec. 2004.

[5] R. A. Kudgus, C. A. Walden, R. M. McGovern, J. M. Reid, J. D. Robertson, and P. Mukherjee, "Tuning Pharmacokinetics and Biodistribution of a Targeted Drug Delivery System Through Incorporation of a Passive Targeting Component," *Sci. Rep.*, vol. 4, p. 5669, Jul. 2014.

[6] E. Want, B. J. Compton, T. Hollenbeck, and G. Siuzdak, "The application of mass spectrometry in pharmacokinetics studies," *J. Spectrosc.*, vol. 17, no. 4, pp. 681–691, 2003.

[7] S. Czaplicki, "Chromatography in Bioactivity Analysis of Compounds," 2013, pp. 99–122.

[8] "Bristol University - High Performance Liquid Chromatography Mass Spectrometry (HPLC/MS)." [Online]. Available: http://www.bristol.ac.uk/nerclsmsf/techniques/hplcms.html. [Accessed: 10-Oct-2019].

[9] "Figure 1.4: Schematic Diagram of a Quadrupole Mass Analyser. Ionisation...," *ResearchGate*. [Online]. Available: https://www.researchgate.net/figure/Schematic-Diagram-of-a-Quadrupole-Mass-Analyser-Ionisation-occurs-at-the-source-Ions_fig3_303384278. [Accessed: 10-Oct-2019].

[10] "File:Triple quadrupole schematic.jpeg," *Wikipedia*. 11-Oct-2015.

[11] C. Bylda, R. Thiele, U. Kobold, and D. A. Volmer, "Recent advances in sample preparation techniques to overcome difficulties encountered during quantitative analysis of small molecules from biofluids using LC-MS/MS," *Analyst*, vol. 139, no. 10, pp. 2265–2276, 2014.

[12] H. Stahnke, S. Kittlaus, G. Kempe, and L. Alder, "Reduction of matrix effects in liquid chromatography-electrospray ionization-mass spectrometry by dilution of the sample extracts: how much dilution is needed?," *Anal. Chem.*, vol. 84, no. 3, pp. 1474–1482, Feb. 2012.

[13] "Protein Precipitation - an overview | ScienceDirect Topics." [Online]. Available: https://www.sciencedirect.com/topics/chemistry/protein-precipitation. [Accessed: 21-Aug-2019].

[14] C. Polson, P. Sarkar, B. Incledon, V. Raguvaran, and R. Grant, "Optimization of protein precipitation based upon effectiveness of protein removal and ionization effect in liquid chromatography-tandem mass spectrometry," *J. Chromatogr. B Analyt. Technol. Biomed. Life. Sci.*, vol. 785, no. 2, pp. 263–275, Mar. 2003.

[15] P. T. Wingfield, "Protein Precipitation Using Ammonium Sulfate," *Curr. Protoc. Protein Sci. Editor. Board John E Coligan Al*, vol. APPENDIX 3, p. Appendix-3F, May 2001.

[16] P. Novák and V. Havlíček, "4 - Protein Extraction and Precipitation," in *Proteomic Profiling and Analytical Chemistry (Second Edition)*, P. Ciborowski and J. Silberring, Eds. Boston: Elsevier, 2016, pp. 51–62.

[17] Tim Wehr, "Top-Down versus Bottom-Up Approaches in Proteomics," *LCGC North America*, vol. 24, no. 9, pp. 1004–1010, Sep. 2006.

[18] A. Cristobal, F. Marino, H. Post, H. W. P. van den Toorn, S. Mohammed, and A. J. R. Heck, "Toward an Optimized Workflow for Middle-Down Proteomics," *Anal. Chem.*, vol. 89, no. 6, pp. 3318–3325, 21 2017.

[19] "NPTEL WEB COURSE – ADVANCED CLINICAL PROTEOMICS," p. 16.

CHAPTER II

DEVELOPMENT AND VALIDATION OF A DILUTE AND SHOOT FLOW INJECTION TANDEM MASS SPECTROMETRY METHOD FOR THE QUANTIFICATION OF GLYCOCHOLIC ACID AND UNCONJUGATED BILIRUBIN IN HUMAN BILE

2.1. Introduction

2.1.1. Cholangiocarcinoma and Glycocholic acid

Cholangiocarcinoma (CCA) or bile duct cancer arises from the epithelial lining of intra-hepatic and extra-hepatic bile ducts. CCA is one of the most aggressive forms of malignancies and around 8000 Americans are diagnosed annually [1]–[3]. Early diagnosis of CCA is challenging due to its late clinical presentation and difficulties in early detection. Current diagnostic methods lack the ability to distinguish benign from malignant tumors. For example, imaging techniques such as ultrasonography, computed tomography (CT), and magnetic resonance imaging (MRI) reveal bile duct blockage, but they are

inefficient in differentiating the blockage caused by benign scarring or a malignant tumor [1].

Glycocholic acid (GCA) is a conjugated bile acid produced from cholic acid. A significant increase in the concentration of GCA has been observed in the bile of patients with CCA, compared with those with benign biliary tract diseases [2], [4]. Because bile and its constituents are directly in contact with the biliary epithelium, it could be an ideal biological fluid for detection of CCA [4].

2.1.2. Cholelithiasis and Unconjugated Bilirubin

Cholelithiasis or gall stone disease effects approximately 6% of men and 9% of women in the United States and is the primary cause for hospital admissions related to gastroenterology [5]. Gall stones are anomalous lumps precipitating from bile and are classified into cholesterol gall stones (mostly comprised of cholesterol) and pigment gall stones (comprised of calcium complexes of bilirubin). Though it is a benign condition, cholelithiasis could be a risk factor for life threatening diseases like cardiovascular disease and cancer [6]. Cholelithiasis is mostly asymptomatic and the existence of gallstones is only revealed during an ultrasound.

Unconjugated bilirubin (UBL) is a toxic metabolite of heme and is usually excreted in bile after conjugation in the liver. In healthy conditions, UBL is present in very low proportions in bile. However, studies have established that deconjugation occurs in bile catalyzed by bacterial enzymes or non-enzymatic hydrolysis resulting in the formation of

more UBL [7],[8]. Higher proportion of UBL in bile is considered as a risk factor for Cholelithiasis as UBL is found to act as a nidus for the formation of cholesterol gall stones [9]. UBL has also been identified as a component of biliary sludge that precedes the formation of pigment stones [10]–[12]. UBL in bile could be a potential biomarker of Cholelithiasis that requires further investigation to evaluate its potential.

Nevertheless, bile was not until recently a preferred biological fluid for clinical analysis because sampling of bile required surgery. Advances in imaging techniques like endoscopic retrograde cholangiopancreatography (ERCP) now makes it possible to sample bile without surgical intervention. A thorough literature survey revealed a TLC and a HPLC method to determine Bilirubin and a LC-MS method to determine GCA in human bile respectively [7], [13], [14]. HPLC and TLC methods lack the specificity and accuracy offered by mass spectrometry methods. Although LC-MS has unparalleled sensitivity and accuracy, it suffers from various obstacles due to highly hydrophobic nature of bile acids and matrix components that complicate its quantification. First, current methods require time-consuming extraction steps in order to separate GCA or UBL from interfering matrix components. Furthermore, because analytes strongly bind to the C18 reverse phase columns strongly, it is necessary to frequently wash the column vigorously, which is not practical in a clinical setting. Finally, it is virtually impossible to create a blank bile matrix that does not contain GCA and UBL.

To overcome these problems, we employed dilute-and-shoot flow-injection MS/MS (for short, FI-MS/MS) to quantify GCA and UBL simultaneously in bile, for which standard addition calibration is also utilized. The high concentrations of GCA and UBL in bile allow dilution of bile by as much as 800,000 times to minimize matrix effects [12].

Diluted sample is then injected directly into the ionization source without LC separation, avoiding column contamination and the problem of carryover. Sample preparation and run time are also substantially minimized by using a FI-MS/MS method, whilst maintaining quantification accuracy and precision [15], [16]. Moreover, we utilized a standard-addition method for calibration, which not only does not require a blank matrix that is virtually impossible to obtain, but also minimizes matrix effects. In standard addition, solutions containing different concentrations of analyte are directly added to aliquots of the sample [17]. Thus, any change in signal intensity between the sample and the spiked samples will only result from change in analyte concentration and hence matrix effects are minimized. Bioanalytical method validation has been conducted in accordance with FDA guidelines [18].

2.2. Experimental

2.2.1. Chemicals

Glycocholic acid ($C_{26}H_{43}NO_6$) was purchased from Sigma Aldrich, (St. Louis, MO, USA). Bilirubin ($C_{33}H_{35}N_4O_6$ 99%) was purchased from Acros Organics (Geel, AN, Beligium). Dehydrocholic acid ($C_{24}H_{34}O_5$, >98%) was a reference standard purchased from USP (Rockville, MD, USA). HPLC grade methanol and Dimethyl sulfoxide (DMSO) was purchased from EMD Millipore Corporation (Billerica, MA, USA) and Alfa Aesar (Ward Hill, MA, USA) respectively. Deionized water was obtained from Barnstead D3750 Nano Pure water purification system by Thermo Scientific (Waltham, MA, USA). Bile samples were obtained from four volunteers at Mississippi State University.

2.2.2. Instrumentation

Quantification was performed by liquid chromatography coupled to a triple quadrupole-tandem mass spectrometer. The Shimadzu HPLC unit (Columbia, MD, USA) consisted of binary pumps (Nexera LC-30 AD), degasser (a DUG20A3R), autosampler (SIL-30 AC), column oven (CTO-10AVP) and a controller (CBM 20A). The AB SCIEX 5500 QTRAP mass spectrometer (Toronto, Canada) was equipped with an electrospray ionization probe, triple quadrupole and a syringe pump. The instrument operation, acquisition and processing of data was performed using AB SCIEX Analyst software.

2.2.3. Flow Injection

Flow injection of GCA, UBL and IS was performed isocratically at 30°C with a carrier solvent comprising of 90% methanol at a flow rate of 0.3 mL/min. It should be noted that a LC column was not used for separation. A 10 µL volume of the sample from the autosampler vials was injected into the system and data was acquired for a run time of 2.5 min per sample.

2.2.4. Tandem mass spectrometry

Mass spectrometric analysis was performed in negative electrospray ionization (ESI^-) mode. Source and compound dependent parameters were optimized and the conditions were as follows: curtain gas: 30 psi; ion spray voltage: -4500V; ion spray

temperature: 400°C; ion source gases: 1 and 2 to 20 psi; declustering potential: -110 V; entrance potential: -14 V; collision energy: -53 eV (GCA), -40 eV (UBL), and -44 eV (IS) and cell exit potential: -25 eV. Quantitation of GCA and UBL was achieved in multiple reaction monitoring (MRM) mode. The selected precursor-product ion pairs for GCA, UBL and IS were *m/Z* 464.1 → 74, 583.6 → 285.3 and 401.2 → 249.1 respectively.

2.2.5. Preparation of stock and working solutions

Stock solutions of GCA and IS were prepared separately in appropriate volumes of methanol and UBL in DMSO to obtain concentrations of 1mg/mL. All stock solutions were stored at -20°C. The working standard solutions of GCA and UBL (2.5, 5, 10, 20, 30, and 40 µg/mL for calibrators and 6.3, 14.1, 32 for quality controls (QCs)) were prepared by serial dilution in methanol. A working solution of IS (20 µg/mL) was prepared by diluting the stock solution of IS with methanol.

2.2.6. Preparation of bile samples by dilution

Bile samples were thawed to room temperature and vortexed for 2 minutes. 2 µL of each bile sample was diluted to 8mL with methanol, vortexed for 2 min and centrifuged at 14000 rpm for 20 minutes. A pooled bile sample (mixture of 4 lots of human bile samples) was also treated in a similar way to yield diluted pooled bile. The supernatants obtained after centrifugation were used to prepare calibrators and quality controls as described below.

2.2.7. Preparation of calibrators for standard addition

Calibrators (12.5, 25, 50, 100, 150 and 200 ng/mL) were prepared by spiking each working standard solution (2.5, 5, 10, 20, 30 and 40 µg/mL) with 5 µL of diluted pooled human bile (prepared as mentioned above). A single blank was prepared without spiking the diluted pool bile with working standard solution. To ensure that the analyte concentration in the sample was within the linear range and not below the LLOQ, an 'initial spike' of 5 µL of 5 µg/mL of GCA and UBL were spiked into all the calibrators. The volume of the solutions was then made up with methanol, vortexed, centrifuged at 14000 rpm for 20 min and the supernatant was transferred to an autosampler vial for analysis.

2.2.8. Preparation of quality controls (QCs)

Quality controls (QCs) (31.3, 70.7 and 160 ng/mL) were prepared by spiking working standard solutions of GCA and UBL (6.3, 14.1 and 32 µg/mL) with 5 µL of diluted pooled human bile and treated the same way as calibrators.

2.3. Results and Discussion

2.3.1. Method Development

2.3.1.1. Multiple Reaction Monitoring

Detection of GCA, UBL and IS was carried out using a triple quadrupole mass spectrometer. Since both GCA, UBL and IS have carboxylic acid side chains, negative ion mode was chosen for ionization. Multiple reaction monitoring (MRM) was utilized to ensure specific quantification by reducing the interference of other molecules present in the bile. Experimentally, the most abundant ion was selected as precursor ion which was subjected to collision-induced dissociation (CID). CID produces fragment ions and the most abundant fragment ion was chosen as product ion for quantification. The precursor and product ions selected for this study are shown in fig 2.1. The peaks at 464.1 Da 401.2 and 583.3 Da represent precursor ions and the peaks at 74.0, 249.1 and 285.2 represent product ions for GCA, IS and UBL respectively. Specifically, the transitions used in MRM were 464.1 $\rightarrow$ 74.0 for GCA, 401.2 $\rightarrow$ 249.1 for IS and 583.3 $\rightarrow$ 285.2 for UBL. To ensure that only analytes and no other ions were quantified, we also monitored additional transitions (qualifiers) of GCA (m/Z 464.1 $\rightarrow$ 402.4) and (583.6 $\rightarrow$ 241.2) UBL as for increased confidence in identifying the target analytes.

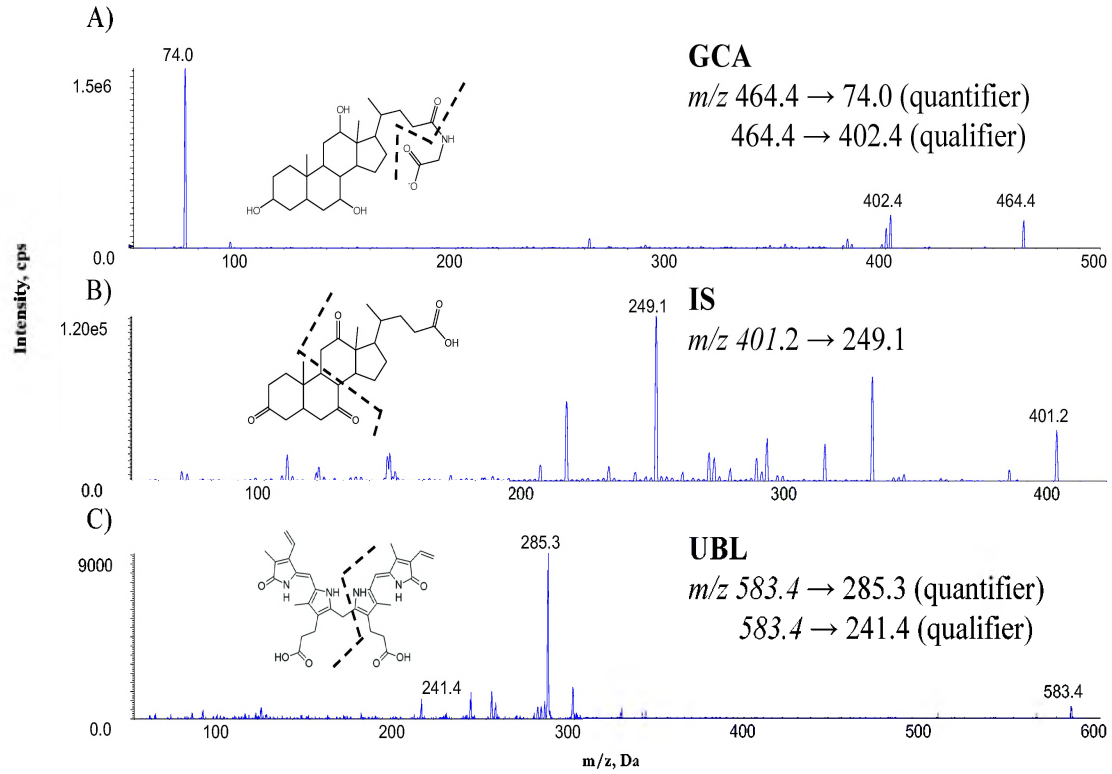

Figure 2. 1 The MS/MS spectra of and proposed fragmentation pattern of (A) GCA (B) IS (C) UBL in negative electrospray ionization mode.

2.3.1.2. Sample Preparation and Flow injection

Because GCA, UBL and IS are highly hydrophobic, they can bind to C18 materials very strongly materials very strongly, resulting in carry over, which poses a problem when a column is used for separation. Hence, we employed a flow injection strategy to avoid this issue by eliminating the use of a column. This was possible considering that the concentrations of GCA and UBL in bile are very high, meaning that these analytes can still be detected even after substantial dilution of bile, and most importantly, such simple dilution may be sufficient enough to avoid matrix effects when the separation column is not used. Clearly, another benefit of dilution is that no extraction method is needed to first retrieve the analytes from bile before analysis. Hence, bile is substantially diluted and then directly injected (without any sample preparation) into the mass spectrometer. A carrier solvent comprising of 90% methanol carried the injected sample as a plug into ESI of mass spectrometer at a flow rate of 0.3 mL/min. We found that our method was reproducible, evidenced by the fact that the detection signals were consistently detected at the same time window in every run. The typical flow injection detection signals of GCA, IS and UBL were displayed in fig. 2.2.

2.3.1.3. Standard addition

To quantify GCA and UBL in bile using a traditional calibration curve method, a blank bile matrix without the analytes is required. However, it is virtually impossible to obtain such blank matrix, as charcoal stripping, currently used not only removes GCA and UBL from bile, but also removes other matrix components. As a consequence, the actual

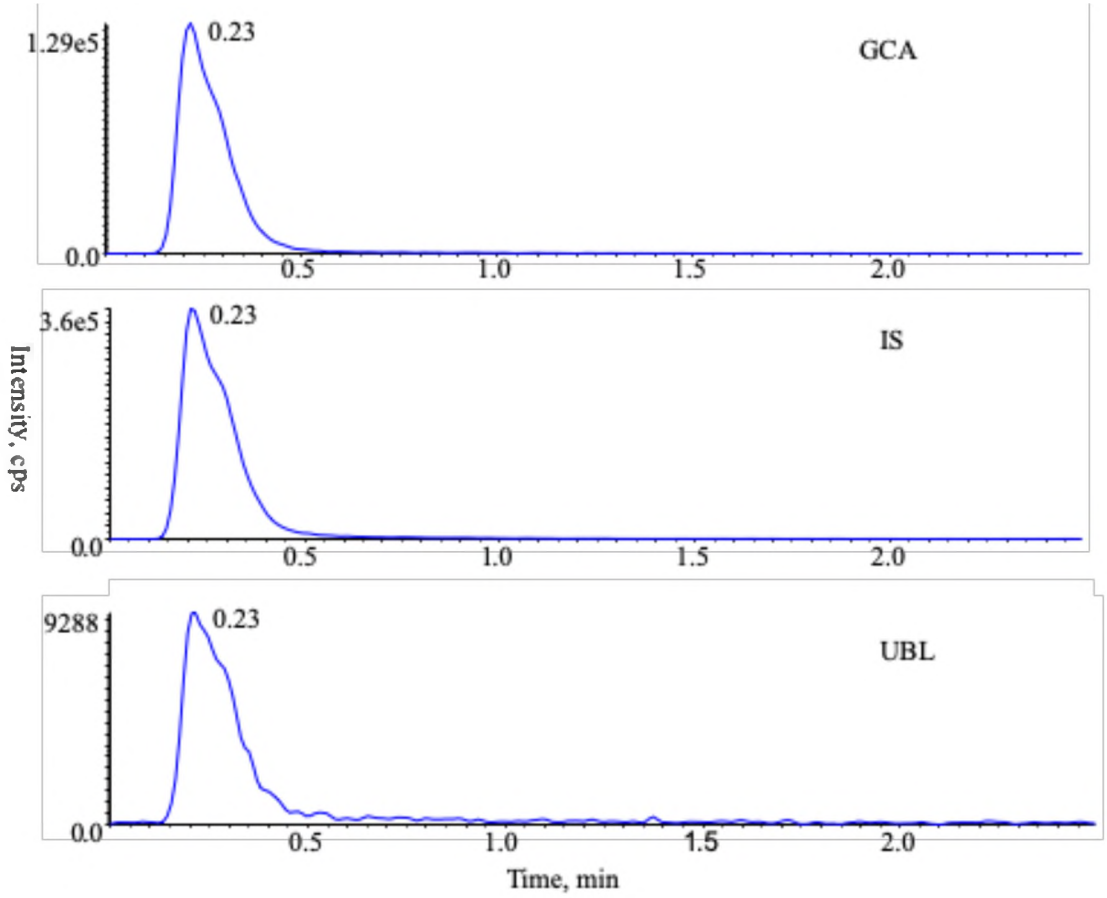

Figure 2. 2 Extracted flow-injection chromatograms of GCA, IS and UBL (from top to bottom) in MRM mode

composition of matrix after charcoal stripping is altered, not reflecting the true nature of the bile sample [19]. Standard addition is the method of choice for quantitation when an endogenous amount of analyte is "inherently" present in matrix [17], [20], [21]. In our method, we employed standard addition to generate the calibration curve, which was constructed using bile samples spiked with standard GCA and UBL solutions by plotting the peak area ratio of analytes to IS vs the concentration of analytes added. The absolute value of the x-axis intercept corresponds to the concentration of the analytes in a bile sample.

2.3.2. Method Validation

The method was validated for linearity, accuracy, precision, matrix effects, LLOQ and carryover according to the FDA bioanalytical method guidelines.

2.3.2.1. Linearity of standard addition calibration curve

A linear relationship between the concentration of analytes and the peak area ratio (the product ion intensities of GCA and UBL to product ion intensity of IS) was determined using pooled and individual human bile lots by plotting standard addition calibration curves. To evaluate linearity, five replicates of analyte spiked bile calibrators at 12.5, 25, 50, 100, 150, 200 ng/mL and single blank were analyzed. The chromatograms are displayed in fig. 2.2. Standard addition-calibration curves were plotted for pooled human bile and individual lots with peak area ratios vs concentration using weighing factor of 1/x. The

Table 2. 1 Linearity data of calibrators in pooled bile samples (n=3)

Spiked concentration (ng/mL)	GCA			UBL		
	Determined concentration (ng/mL)	% RE	% CV	Determined concentration (ng/mL)	% RE	% CV
12.5	12.04 ± 2.45	-3.7	20.37	11.03 ± 2.93	-11.78	20.27
25	26.73 ± 5.26	6.9	19.66	21.87 ± 5.08	-12.53	33.13
50	50.95 ± 5.80	1.9	11.39	37.98 ± 0.85	-24.03	10.56
100	97.63 ± 4.08	-2.4	4.18	106.25 ±9.04	6.25	19.91
150	133.17 ± 6.90	-11.2	5.18	150.17±10.69	0.11	20.00
200	217.17 ±10.60	8.6	4.88	224.67±29.54	12.33	38.61

% RE (percent relative error) = [(determined concentration − spiked concentration)/(spiked concentration)] x 100
% CV (percent coefficient of variation) = (standard deviation/mean) x 100

A

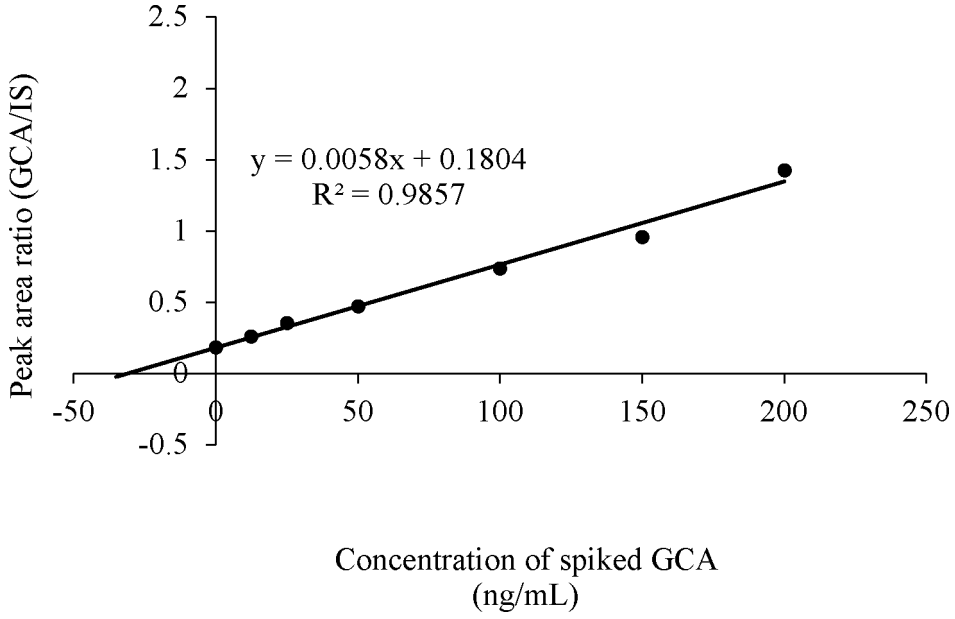

B

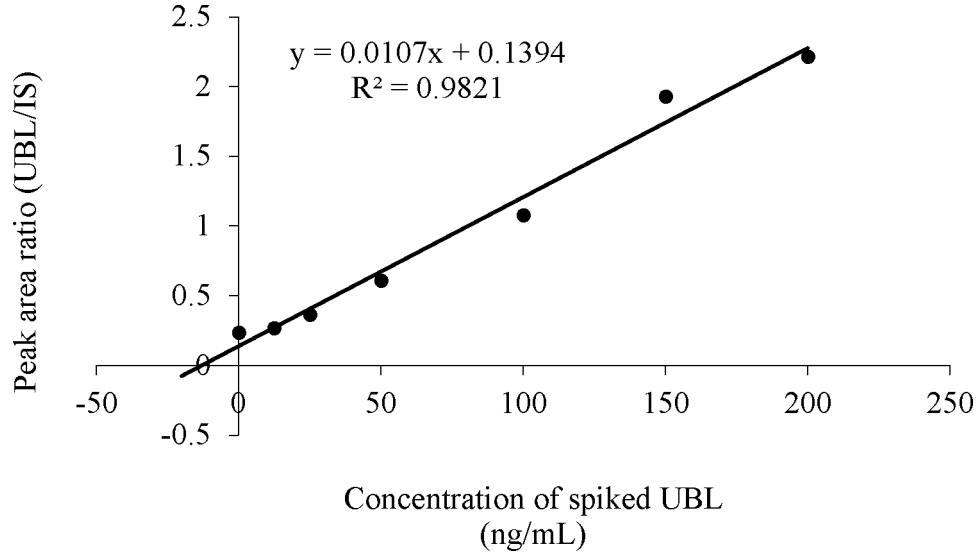

Figure 2. 3 Standard-addition calibration plot of A) GCA and B) UBL in pooled human bile from four lots. The x-axes intercepts correspond to the actual concentration of GCA and UBL

correlation coefficients of standard addition curves of GCA and UBL were found to be 0.9857 and 0.9821 respectively as shown in fig. 2.3. The accuracy and precision values were tabulated in table 1.1. %RE was found to be within the limit (±20% for LLOQ and ±15% for remaining calibrators) for GCA and UBL for all of the calibrators except third calibrator of UBL. The precision values of second calibrator of GCA and five calibrators of UBL were above the limit (±20% for LLOQ and ±15% for remaining calibrators).

2.3.2.2. Accuracy and Precision

The accuracy of a method defines the closeness of mean test concentration determined by the method to the actual concentration of the analyte and is expressed as percent relative error (%RE). Precision of a method defines the closeness of individual concentrations of analyte to one another and is expressed as percent coefficient of variation (%CV). Accuracy and precision of our method were evaluated by analyzing five replicates of QCs at 31.25, 70.71 and 160 ng/mL on the same day (intra-day) and in five separate days (inter-day). The data for intra-day and inter-day accuracy and precision were presented in Tables 2.2 and 2.3. Accuracy was expressed as % RE and precision was expressed as %CV. For GCA, the intra-day accuracy was within -1.44 – 18.1 and % RE of inter-day was within 9.02-14.8. The intra-day precision of GCA was within 11.45-12.53 while % CV of inter-day for five replicates on five separate days was 6.50-11.60. The intra-day accuracy for UBL was between 5.99 – 21.42 while inter-day accuracy was within 10.69-20.96. The intra-day precision of UBL ranged from 13.18 – 23.78 and inter-day precision was within 10.68 – 24.04. The above data suggests that the method has reasonable accuracy and

Table 2. 2 Intra-day accuracy and precision of GCA and UBL in pooled bile (n=5)

QC Level	Spiked concentration (ng/mL)	GCA			UBL		
		Determined concentration ± SD (ng/mL)	% RE	% CV	Determined concentration ± SD (ng/mL)	% RE	% CV
LQC	31.25	33.08 ± 6.56	5.86	12.53	24.89 ± 8.26	21.42	13.18
MQC	70.71	83.51 ± 9.73	18.1	11.45	69.28 ±19.81	9.41	23.78
HQC	160.00	157.7 ±16.70	-1.44	12.34	149.62±42.61	5.99	22.15

Intra-day accuracy and precision were determined at three QC levels using five lots of pooled bile on same day.

% RE (percent relative error) = [(determined concentration − spiked concentration)/(spiked concentration)] x 100

% CV (percent coefficient of variation) = (standard deviation/mean) x 100

Table 2. 3 Inter-day accuracy and precision of GCA and UBL in pooled bile (n=5)

QC Level	Spiked concentration (ng/mL)	GCA			UBL		
		Determined concentration ± SD (ng/mL)	% RE	% CV	Determined concentration ± SD (ng/mL)	% RE	% CV
LQC	31.25	33.57 ± 6.2	14.80	9.02	24.43 ±14.95	21.96	10.68
MQC	70.71	69.61± 31.28	9.52	11.60	69.41 ± 1.72	10.69	24.04
HQC	160.00	141.8 ±18.38	12.03	6.50	142.50 ±7.22	10.93	20.38

Inter-day accuracy and precision were determined at three QC levels using five lots of pooled bile on five different days.
% RE (percent relative error) = [(determined concentration − spiked)/(spiked)] x 100
% CV (percent coefficient of variation) = (standard deviation/mean) x 100

precision as most of %RE and %CV values were within the 15% limit set by the FDA and some values of UBL were slightly over the limit.

2.3.2.3. Matrix effect

The presence of other components in a biological sample can lead to matrix effects (such as ion suppression or enhancement) and bile does contain high concentrations of various other molecules. Hence, both absolute and relative matrix effects on our method were determined by comparing the peak area ratios of five replicates of QCs in bile samples and solvent. Absolute matrix effects were determined by comparing the peak areas of analytes in diluted bile samples and in neat solutions at three QCs. Relative matrix effects were determined by comparing the peak area ratios of GCA/IS and UBL/IS in diluted bile samples and in neat solutions at three QCs. The data are presented in table 2.4. The absolute and relative matrix effects were expressed as %ME. The absolute matrix effect of GCA was within 91.65 - 98.99% while relative matrix effects was 87.35 – 94.78%. The absolute and relative matrix effects of UBL were within 86.77 - 91.85% and 88.93 – 98.24% respectively. The data suggest that the use of dilution and standard addition has held the matrix effects on both the analytes within the 15% limit set by the FDA guidelines.

Table 2. 4 Absolute and relative matrix effects of GCA and UBL in pooled bile (n=5)

QC Level	Spiked concentration (ng/mL)	GCA		UBL	
		Absolute matrix effect ± SD	Relative matrix effect ± SD	Absolute matrix effect ± SD	Relative matrix effect ± SD
LQC	31.25	98.99 ± 10.37	94.78 ± 9.45	91.85 ±11.90	92.13 ± 13.08
MQC	70.71	96.36 ± 5.32	87.35 ± 3.54	90.33 ± 9.33	98.24 ±17.30
HQC	160.0	91.65 ± 4.87	91.66 ± 7.90	86.77 ± 7.48	88.93 ± 24.73

Matrix effect was determined at three QC levels using five lots of pooled bile.
Absolute matrix effect = (mean peak area of analyte in diluted bile)/(mean peak area of analyte in neat solution).
Relative matrix effect = (mean peak area of analyte/IS in diluted bile)/(mean peak area of analyte/IS in neat solution).

2.3.2.4. Lower limit of quantification

In our method, the lower limit of quantification (LLOQ) was defined as the concentration of GCA and UBL in the lowest calibrator (12.5 ng/mL) used to construct the standard addition calibration curve. We have conducted a study to examine reproducibility of quantitation at the LLOQ level of 12.5 ng/mL, which was achieved by quantifying GCA and UBL in five replicates of pooled bile samples containing 12.5 ng/mL. It was found that the % CV for GCA and UBL were less than 20%, suggesting that our method is sensitive enough to reproducibly detect GCA and UBL at a concentration as low as 12.5 ng/mL. It must be noted that no study was conducted to determine whether our method can detect analytes at the level of less than 12.5 ng/mL.

2.3.2.5. Carry over

Carry over problem is often associated with the column-based method, where the analyte from earlier analyzed samples can stick to the column, affecting analysis of the samples that are analyzed thereafter. This is particularly problematic with bile that contains high concentrations of various highly hydrophobic molecules including GCA and UBL. Although our method does not use any column, we did conduct a study to examine whether any bile molecules including GCA and UBL can stick to autosampler and tubing, leading to carry over, and thus affecting the accuracy of our method. This was achieved by immediately quantifying a blank sample (solvent) after injecting analytes at 200 ng/mL concentration (upper limit of quantitation). It was found that our method was not subjected to carry over as expected.

2.3.3. Quantification of GCA in Human Bile Samples

After developing and validating our method, we applied it to quantify GCA and UBL in human bile samples collected from four individuals. However, we do not know if samples were obtained from healthy individuals or diseased patients. It was found that our method could detect and differentiate the analyte and IS signals from the background noise in most of the samples. The standard addition curves were constructed for each of all the four bile samples. The results obtained from four human bile samples was listed in Table 2.5. The concentration of GCA was found to range from 4.53- 23.95 mM which was almost within 5.04 - 55.04 mM range reported in a study determined using LCMS method [13]. The concentration of UBL in bile reported in our study 5.07 – 54.98 mM while one UBL in one of the samples was found to be below LLOQ. However, these values were higher than the levels, 0.01 -0.150 mM, 0.005 -0.013 μM, 0.014 -0.181 μM as reported previously using TLC and HPLC methods [9], [22].

Table 2. 5 Concentration of GCA and UBL in four human bile samples

Human bile sample	Concentration of GCA (mM)	Concentration of UBL (mM)
Subject 1	4.53	5.54
Subject 2	24.95	54.98
Subject 3	9.96	5.07
Subject 4	21.48	<LLOQ

2.4. Conclusion

We have successfully developed a dilute-and-shoot flow injection MS/MS method for the quantification of GCA and UBL in human bile using standard addition. Our method has been validated for linearity, accuracy, precision, matrix effects, LLOQ and carryover, according to the FDA guidelines. This method offers several benefits for clinical use. First, it does not require tedious sample purification prior to analysis. Our method utilizes simple dilution for sample preparation, while not compromising on sensitivity even after 800, 000-fold dilution. Second, our method is accurate and precise without the use of LC separation, eliminating the carryover problem that which would otherwise require frequently washing to maintain the column condition. Third, our method does not necessitate blank bile matrix that is virtually impossible to obtain but is required for the conventional quantitation method. In addition, our method is fast with a run time of only 2.5 min, enabling high throughput analyses of over 500 samples a day. To the best of our knowledge, this is the first flow injection MS/MS method developed for quantifying GCA and UBL in human bile.

2.5 References

[1] T. Janvilisri, K. Leelawat, S. Roytrakul, A. Paemanee, and R. Tohtong, "Novel Serum Biomarkers to Differentiate Cholangiocarcinoma from Benign Biliary Tract Diseases Using a Proteomic Approach," *Disease Markers*, 2015. [Online]. Available: https://www.hindawi.com/journals/dm/2015/105358/. [Accessed: 09-Oct-2019].

[2] X. Xu *et al.*, "Identification of bile biomarkers of biliary tract cancer through a liquid chromatography/mass spectrometry-based metabolomic method," *Mol. Med. Rep.*, vol. 11, no. 3, pp. 2191–2198, Mar. 2015.

[3] "Key Statistics About Bile Duct Cancer." [Online]. Available: https://www.cancer.org/cancer/bile-duct-cancer/about/key-statistics.html. [Accessed: 09-Oct-2019].

[4] A. W. Sharif *et al.*, "Metabolic profiling of bile in cholangiocarcinoma using in vitro magnetic resonance spectroscopy," *HPB*, vol. 12, no. 6, pp. 396–402, Aug. 2010.

[5] J. Tanaja and J. M. Meer, "Cholelithiasis," in *StatPearls*, Treasure Island (FL): StatPearls Publishing, 2018.

[6] L. M. Stinton and E. A. Shaffer, "Epidemiology of gallbladder disease: cholelithiasis and cancer," *Gut Liver*, vol. 6, no. 2, pp. 172–187, Apr. 2012.

[7] J. Fevery, N. Blanckaert, P. Leroy, R. Michiels, and K. P. Heirwegh, "Analysis of bilirubins in biological fluids by extraction and thin-layer chromatography of the intact tetrapyrroles: application to bile of patients with Gilbert's syndrome,

hemolysis, or cholelithiasis," *Hepatol. Baltim. Md*, vol. 3, no. 2, pp. 177–183, Apr. 1983.

[8] W. Spivak, D. DiVenuto, and W. Yuey, "Non-enzymic hydrolysis of bilirubin mono- and diglucuronide to unconjugated bilirubin in model and native bile systems. Potential role in the formation of gallstones," *Biochem. J.*, vol. 242, no. 2, pp. 323–329, Mar. 1987.

[9] M. K. Dutt, G. M. Murphy, and R. P. H. Thompson, "Unconjugated bilirubin in human bile: the nucleating factor in cholesterol cholelithiasis?," *J. Clin. Pathol.*, vol. 56, no. 8, pp. 596–598, Aug. 2003.

[10] S. P. Lee and J. F. Nicholls, "Nature and composition of biliary sludge," *Gastroenterology*, vol. 90, no. 3, pp. 677–686, Mar. 1986.

[11] T. H. Magnuson, K. D. Lillemoe, G. E. Peoples, and H. A. Pitt, "Oral calcium promotes pigment gallstone formation," *J. Surg. Res.*, vol. 46, no. 4, pp. 286–291, Apr. 1989.

[12] "Unconjugated bilirubin, and the hydrolysis of conjugated bilirubin, in gallbladder bile of patients with cholelithiasis - Gastroenterology." [Online]. Available: https://www.gastrojournal.org/article/0016-5085(78)90358-X/fulltext. [Accessed: 09-Oct-2019].

[13] S. Perwaiz, B. Tuchweber, D. Mignault, T. Gilat, and I. M. Yousef, "Determination of bile acids in biological fluids by liquid chromatography-electrospray tandem mass spectrometry," *J. Lipid Res.*, vol. 42, no. 1, pp. 114–119, Jan. 2001.

[14] W. Spivak and W. Yuey, "Application of a rapid and efficient h.p.l.c. method to measure bilirubin and its conjugates from native bile and in model bile systems. Potential use as a tool for kinetic reactions and as an aid in diagnosis of hepatobiliary disease," *Biochem. J.*, vol. 234, no. 1, pp. 101–109, Feb. 1986.

[15] R. Alagandula, X. Zhou, and B. Guo, "A dilute-and-shoot flow-injection tandem mass spectrometry method for quantification of phenobarbital in urine," *Rapid Commun. Mass Spectrom. RCM*, vol. 31, no. 1, pp. 39–46, Jan. 2017.

[16] S. C. Nanita and L. G. Kaldon, "Emerging flow injection mass spectrometry methods for high-throughput quantitative analysis," *Anal. Bioanal. Chem.*, vol. 408, no. 1, pp. 23–33, Jan. 2016.

[17] X. Cai, Y. Liu, X. Zhou, U. Navaneethan, B. Shen, and B. Guo, "An LC-ESI-MS method for the quantitative analysis of bile acids composition in fecal materials," *Biomed. Chromatogr. BMC*, vol. 26, no. 1, pp. 101–108, Jan. 2012.

[18] C. for D. E. and Research, "Bioanalytical Method Validation Guidance for Industry," *U.S. Food and Drug Administration*, 22-Jan-2019. [Online]. Available: http://www.fda.gov/regulatory-information/search-fda-guidance-documents/bioanalytical-method-validation-guidance-industry. [Accessed: 09-Oct-2019].

[19] W. J. Griffiths and J. Sjövall, "Bile acids: analysis in biological fluids and tissues," *J. Lipid Res.*, vol. 51, no. 1, pp. 23–41, Jan. 2010.

[20] P. Basilicata, N. Miraglia, M. Pieri, A. Acampora, L. Soleo, and N. Sannolo, "Application of the standard addition approach for the quantification of urinary benzene," *J. Chromatogr. B*, vol. 818, no. 2, pp. 293–299, Apr. 2005.

[21] S. Ito and K. Tsukada, "Matrix effect and correction by standard addition in quantitative liquid chromatographic–mass spectrometric analysis of diarrhetic shellfish poisoning toxins," *J. Chromatogr. A*, vol. 943, no. 1, pp. 39–46, Jan. 2002.

[22] W. Spivak and M. C. Carey, "Reverse-phase h.p.l.c. separation, quantification and preparation of bilirubin and its conjugates from native bile. Quantitative analysis of the intact tetrapyrroles based on h.p.l.c. of their ethyl anthranilate azo derivatives," *Biochem. J.*, vol. 225, no. 3, pp. 787–805, Feb. 1985.

CHAPTER III

DEVELOPMENT AND VALIDATION OF AN LC-MS/MS METHOD FOR DETERMINATION OF TEMOZOLOMIDE IN MOUSE BRAIN FOLLOWING INTRACEREBRAL MICRODIALYSIS

3.1. Introduction

Temozolomide (TMZ) is an anticancer pro-drug that has been approved by the US Food and Drug Administration for treatment of newly diagnosed glioblastoma multiforme (GBM) in adults. GBM is a grade IV brain tumor effecting 10 per 100,000 people across the world. This form of cancer has very poor prognosis and patients usually die within few months after diagnosis [1]. Administration of TMZ with concurrent radiation therapy followed by a maintenance dose has been found to increase the life span of GBM patients from 12.1 to 14.6 months [2,3]. At physiological pH, TMZ hydrolyzes spontaneously to Methyl-(trazen-1-yl) imidazole-4-carboxamide (MTIC) which further dissociates to form Diazomethane. Diazomethane is reactive and methylates guanine at the O^6 position forming 'methylated guanine-thymine' mismatches and double-stranded breaks, eventually leading to apoptosis of the cell.

However, GBM remains incurable because administration of TMZ via intravenous and oral routes delivers only 35-39% of the drug to the tumor site owing to poor permeability and abnormal vasculature of brain tumors [4,5]. Furthermore, if higher dose of TMZ is administered to increase drug delivery, it leads to systemic toxicity worsening the already compromised lifestyle of the patient. One potential alternative for effective treatment is targeted drug delivery by intracerebral microdialysis in which TMZ is perfused directly into the brain tumor region through a semipermeable microdialysis probe [6]. However, microdialysis is mostly utilized as a sampling technique rather than a drug delivery procedure [7-9]. To assess the potential of intracerebral microdialysis as an alternative route of administration, a good analytical method is required to quantitate TMZ first in animal models. Goldwirt et al. and Liu et al described LC-MS methods for determining TMZ in mouse brain following intraperitoneal administration and focused ultrasound treatment respectively [10-11]. However, these methods were only partially successful in extracting TMZ from mouse brain. Though no validation data was published by Liu et al., Goldwirt et al. reported a mean recovery of 63% and mean matrix effects of 220 %. Therefore, in this work, our aim is to improve recovery of TMZ and minimize matrix effects of mouse brain tissue for LC-MS/MS quantitation. We hypothesize that poor extraction of TMZ could be attributed to lack of a lysis buffer and incomplete protein precipitation. Hence, we augmented homogenization with the help of a lysis buffer, Proteinase K to release TMZ from mouse brain tissue and achieved a mean recovery of 82%. We were also able to curtail matrix effects to <15% by precipitating proteins in mouse brain tissue with ethanol. In this study we describe a detailed LC-MS/MS method

development and validation to determine TMZ in mouse brain following intracerebral brain microdialysis.

3.2. Experimental

3.2.1. Chemicals

Temozolomide ($C_6H_6N_6O_2$, >98%), Theophylline (as an internal standard, IS, $C_7H_8N_4O_2$, 99%), formic acid (CO_2H_2, 98%), ammonium acetate ($C_2H_7NO_2$, 99.99%) and HPLC grade ethanol were purchased from Sigma Aldrich (St. Louis, MO, USA). HPLC-grade methanol was obtained from Alfa Aesar (Ward Hill, MA, USA). Proteinase K was purchased from Qiagen (Hilden, Germany). Deionized water was obtained from Barnstead D3750 nano pure water purification system by Thermo Scientific (Waltham, MA, USA). Mice brain samples were obtained and shipped after 12 hours following intracerebral microdialysis of TMZ.

3.2.2. Preparation of stock solutions and mobile phase

The standard stock solution of TMZ (1 mg/mL) was prepared by dissolving an appropriate amount of TMZ in known volume of acidic methanol consisting of ammonium acetate (10 mM)- methanol (1:4 v/v) (pH 3.5). The standard stock IS solution (1 mg/mL) was prepared by dissolving an appropriate amount of IS in known volume of methanol. Both the standard stock solutions were stored at -20 °C in separate glass vials. The working

standard solutions for calibrators (2.04, 6.80, 34.0, 68.0, 170 and 340 μg/mL) and for quality controls (6.12, 40.8 and 272 μg/mL) were prepared by serial dilution of the stock solution with mobile phase A. These working standards were used to prepare mouse brain calibrators and quality controls. The working standard solution of IS (34.0 μg/mL) was prepared by diluting the standard stock solution of IS with methanol.

Mobile phase A (pH 3.5) was prepared by dissolving 500 μL of formic acid and ammonium acetate (equivalent to 10 mM) in 100 mL of water and making up the volume to 500 mL. Mobile phase B consisted of 100% methanol.

3.2.3. Preparation of calibrators and quality controls

TMZ mouse brain calibrators (1.02, 3.40, 17.0, 34.0, 85.0 and 170 μg/g) and QCs (3.06, 20.4 and 136 μg/g) were prepared by spiking 10 μL of working standard solutions of TMZ to 20 mg aliquots of blank mouse brain and treated the same way as study samples.

3.2.4. Mouse brain sample preparation

To 20 mg slices of homogenized frozen mouse brain, 10 μL of IS solution (34 μg/mL), 10 μL of formic acid and 40 μL of Proteinase K solution (20 mg/mL) were added, vortexed for 1 minute and incubated at 37 °C for 1 hour. 270 μL of Ethanol was added to the lysed samples and incubated at -20 °C for 1 hour to allow protein precipitation. The samples were then centrifuged at 14000 rpm for 10 minutes. 50 μL of the supernatant was

transferred into an autosampler vial and the volume was made upto 1 mL with mobile phase A for subsequent LC-MS/MS analysis.

3.2.5. Instrumentation

High performance liquid chromatography was performed on Shimadzu HPLC unit (Columbia, MD, USA) which consisted of binary pumps (Nexera LC-30 AD), degasser (a DUG20A3R), autosampler (SIL-30 AC), column oven (CTO-10AVP) and a controller (CBM 20A). Mass spectrometric detection was carried out in AB SCIEX 5500 QTRAP mass spectrometer (Toronto, Canada) equipped with electrospray ionization (ESI) probe and a syringe pump. The instrument operation, acquisition and processing of data was performed using AB SCIEX Analyst software (version 1.6.1).

3.2.5.1. Liquid Chromatography

Chromatographic separation of TMZ and IS was achieved at 30 °C on a Waters symmetry® C18 column (2.1 mm x 150 mm x 3.5 µ). Mobile phase A comprised of formic acid and 10 mM ammonium acetate (pH 3.5) (0.1/100, v/v) and mobile phase B consisted of methanol. The elution program was as follows: 5% B (initial), 5-30% B (2 min), 30% B (2 min), 30-90% B (2 min), 90-5% B (2 min) and 5% B (1 min). The flow rate was set at 0.4 mL min^{-1} and the run time was 8 minutes.

3.2.5.2. Mass spectrometry

Mass spectrometric detection was carried out in positive electrospray ionization mode by utilizing multiple reaction monitoring feature of triple quadrupole. The source and compound dependent parameters were optimized by manual infusion of TMZ and IS solutions separately into the ionization source. The source dependent parameters were as follows: curtain gas at 30 psi; collision assisted dissociation gas at high; ion spray voltage at 5500 V; source temperature at 100 °C; sheath gas at 10 psi and desolvation gas at 10 psi. The compound dependent parameters were as follows: declustering potential at 150 V; entrance potential at 10 V; collision energy at 15 eV (TMZ), 25 eV (IS) and collision cell exit potential at 20 V (TMZ), 10 V (IS). The mass transitions for TMZ were *m/z* 195.1 – 138.1 (quantifier) 195.1 – 138.1 (qualifier) and for IS was 181.1 – 124.1.

3.3. Results and Discussion

3.3.1. Method development

3.3.1.1. Analyte and IS

Temozolomide chemically 4-methyl-5-oxo-2,3,4,6,8-pentazabicyclo[4.3.0]nona-2,7,9-triene-9-carboxamide, has a molecular weight of 195.138 g/mol. It is stable at pH <5 and labile at pH >7 with a pKa value of 10.51 [12]. Theophylline was selected as internal

standard not only because of its structural similarity to TMZ, but also because it was significantly less expensive than the deuterated analogs of TMZ. Theophylline is chemically 1,3-Dimethyl-3,7-dihydro-1H-purine-2,6-dione with a molecular weight of 180.164 g/mol. Theophylline has a pKa value of 7.82 and is stable in the pH range of 1-12 [13-14].

3.3.1.2. Mass spectrometric detection

Detection of TMZ and IS was carried out using a triple quadrupole mass spectrometer. Since TMZ and IS readily protonated in the acidic mobile phase, positive electrospray mode was chosen for ionization. As shown in fig. 3.1, TMZ and the IS generated protonated precursor ions $[TMZ + H]^+$ at *m/z* 195.1 and $[IS + H]^+$ at *m/z* 181.1 respectively in the ionization source. These precursor ions were further fragmented in the collision cell into product ions at *m/z* 138.1 and 110.0 for TMZ and at *m/z* 124.1 for the IS. Quantitation was done in multiple reaction monitoring (MRM) mode with mass transitions of *m/z* 195.1 → 138.1 for TMZ and *m/z* 181.1 → 124.1 for the IS. To ensure that only TMZ and no other ions were quantified, we also monitored an additional transition of *m/z* 195.1 → 110.0 as a qualitative transition for increased confidence in identifying the target analyte.

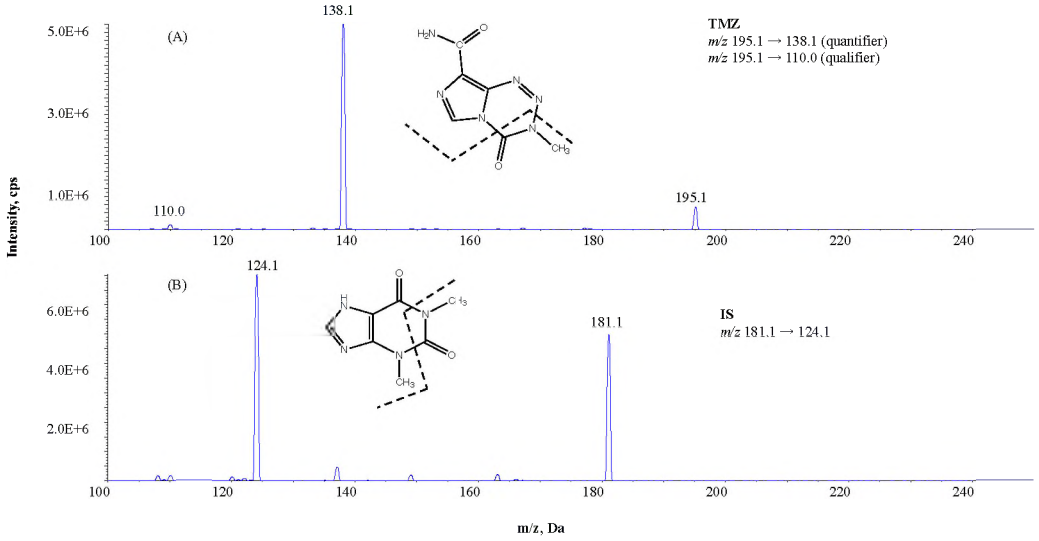

Figure 3. 1 The mass spectra of TMZ and IS along with their probable fragmentation pattern in ESI+ mode. (A) Precursor ion of TMZ - m/z 195.1, product ions of TMZ - m/z 138.1 (quantifier) and 110.0 (qualifier). (B) Precursor ion of IS - m/z 181.1, product ion of IS - m/z 124.1.

3.3.1.3. Liquid chromatographic separation

Since TMZ and IS are hydrophobic, reverse phase C-18 columns were chosen for chromatographic separation in a HPLC unit. Columns such as Agilent Poroshell 120 EC-C18 column (Agilent Technologies Inc., Santa Clara, CA, USA), Phenomenex Luna® C18 column (Phenomenex Inc., Torrance, CA, USA) and Waters Symmetry® C18 column (Waters Corporation, Milford, MA, USA) were experimented. Among them Waters Symmetry® C18 column demonstrated best peak shape and symmetry and hence was chosen for analytical separation. Because TMZ degrades at pH >5, mobile phase A was maintained at pH 3.5 using 10 mM ammonium acetate and 0.1% formic acid which also helped in improved ionization. Methanol was used as organic solvent to provide optimum strength for eluting TMZ and IS from the C-18 column.

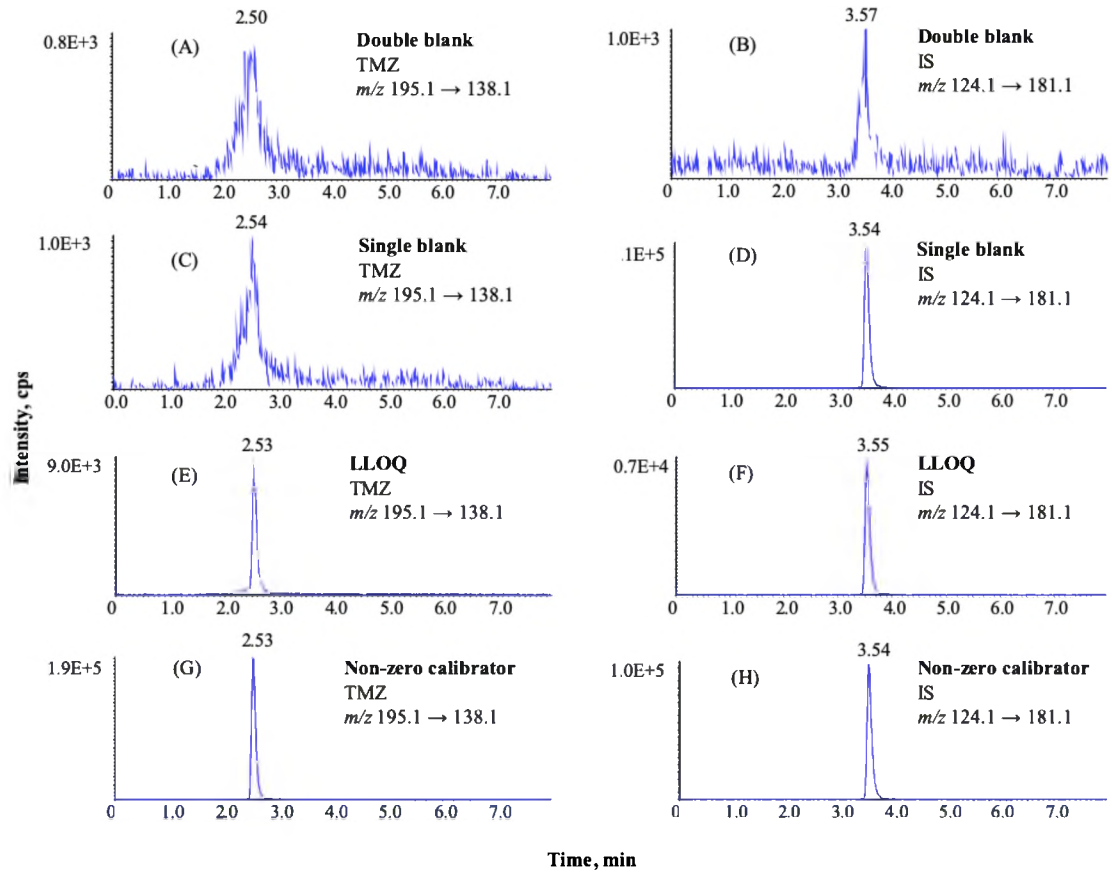

Figure 3. 2 The LC-MS/MS chromatograms of TMZ and IS in mouse brain. Double blank (TMZ and IS absent) chromatograms of (A) TMZ quantifier (B) IS. Single blank (TMZ absent and IS at 17 μg g^{-}) chromatograms of (C) TMZ quantifier (D) IS. LLOQ (TMZ at 1.02 μg $g^{-}$and IS at 17 μg g^{-}) chromatograms of (E) TMZ quantifier (F) IS. Calibrator (TMZ at 17 μg $g^{-}$and IS at 17 μg g^{-}) chromatograms of (G) TMZ quantifier (H) IS.

3.3.1.4. Sample preparation

The first step in sample preparation was addition of 10 μL of formic acid to prevent hydrolysis of TMZ at pH < 5 by maintaining a ~pH 3.5. Next, in order to achieve high percent recovery of TMZ, we tested homogenization with various lysis buffers such as SDS, RIPA, guanidine hydrochloride and Proteinase K out of which Proteinase K gave the best results. We further optimized the volume by treating equal weight frozen brain aliquots with 0.4, 4 and 40 μL of Proteinase K and incubated at 37 °C for 1 hour. 40 μL of Proteinase K treated sample produced most clear solution and hence was chosen for sample preparation.

In addition to water, mouse brain consists of about 25% proteins, 11% phospholipids and 4% cholesterol [15]. Protein precipitation is one of the common sample preparation methods to remove proteins from the sample matrix [16,17]. However, Goldwirt et al.'s method suffered from severe matrix effects of about 220% possibly due to incomplete removal of proteins from the matrix. The amount of zinc sulfate used was lower than the recommended ratio of 2:1 (zinc sulfate to matrix) which might have resulted in incomplete protein precipitation [18]. Additionally, zinc sulfate was also believed to precipitate drug molecules along with proteins present in tissues [19]. To address this issue, we evaluated alternative protein precipitating agents, trifluoro acetic acid (TFA) and ethanol.

Equal weight frozen brain aliquots were first acidified with formic acid, spiked with TMZ, IS and lysed with Proteinase K. For TFA protein precipitation, one set of the above samples was treated with 40 μL of TFA, diluted with 130 μL of water and incubated at 4°C

for 1 hour. The second set of samples was treated with 270 μL of ethanol and incubated at -20 °C for 1 hour. All samples were then centrifuged and processed the same way as described in section 2.4. Thereafter, the peak area ratios of both sample sets were compared against those of neat solution (without matrix). The peak area ratios of ethanol treated samples were consistent with negligible matrix effects and suggested higher recovery compared to those of TFA treated samples. Hence ethanol was chosen for protein precipitation.

3.3.2. Method validation

The LC-MS method was validated in accordance with the guidelines established by the US FDA for industry on bioanalytical method validation [20].

3.3.2.1. Selectivity and specificity

Specificity is defined as the ability to measure exclusively TMZ in the presence of other components in addition to matrix components. To ensure specificity, in addition to *m/z* 195.1 → 138.1 (quantifier), another mass transition *m/z* 195.1 → 110.0 (qualifier) was monitored throughout the analysis.

Selectivity is defined as the ability of the method to determine analyte in the sample without interferences from matrix components. To evaluate selectivity, six double blanks and single blanks from six different mouse brains were analyzed. for interferences at retention times of TMZ and IS. As shown in Fig.2, tiny peaks were detected at the retention

time of TMZ and IS in double and single blanks, but they are insignificant as their peak area was < 10% of that of LLOQ.

3.3.2.2. Linearity and Lower limit of quantitation (LLOQ)

The relationship between concentration of TMZ in the calibrators and detector response was studied in the range of 1.02 – 170 μg/g. A standard calibration curve for TMZ was constructed using a double blank, a single blank and six non-zero calibrators in mouse brain matrix (1.02, 3.40, 17.0, 34.0, 85.0 and 170 μg/g). The peak area ratios of TMZ to IS were plotted against the concentrations of TMZ in mouse brain calibrators with 1/x as weighing factor. The equation derived from the calibration curve was $y = 0.0356x + 0.2771$ with a correlation coefficient of 0.9975. As shown in table 3.1, the accuracy and precision for all calibrators were within limit (20% for the LLOQ and 15% for other non-zero calibrators) except ULOQ which was slightly higher.

Lower limit of quantitation (LLOQ) is defined as the lowest analyte concentration in the matrix that can be determined with acceptable accuracy and precision. The absolute peak area of TMZ at 1.02 μg/g i.e., the LLOQ was more than five times of the absolute peak area of TMZ in double and single blanks as required by the US FDA. The LLOQ was further evaluated in five different mouse brain samples on the same day and five different days for intra and inter-day accuracy and precision respectively. As shown in table 3.2, accuracy and precision of LLOQ were 6% and 15% respectively which were below the 20% limit set by the FDA.

Table 3. 1 Linearity of TMZ from six non-zero calibrators in three mouse brain samples measured over three different days (n=3).

Spiked concentration (µg/g)	Determined concentration ± SD (µg/g)	%RE	%CV
1.02	0.97 ± 0.13	- 5	11
3.40	3.27 ± 0.12	- 4	14
17.0	19.2 ± 0.45	13	14
34.0	37.0 ± 2.03	9	8
85.0	88.2 ± 3.30	4	14
170	162 ± 3.76	- 5	17

%RE (percent relative error) = [(determined concentration − spiked concentration)/(spiked concentration)] x 100
%CV (percent coefficient of variation) = (standard deviation/mean) x 100

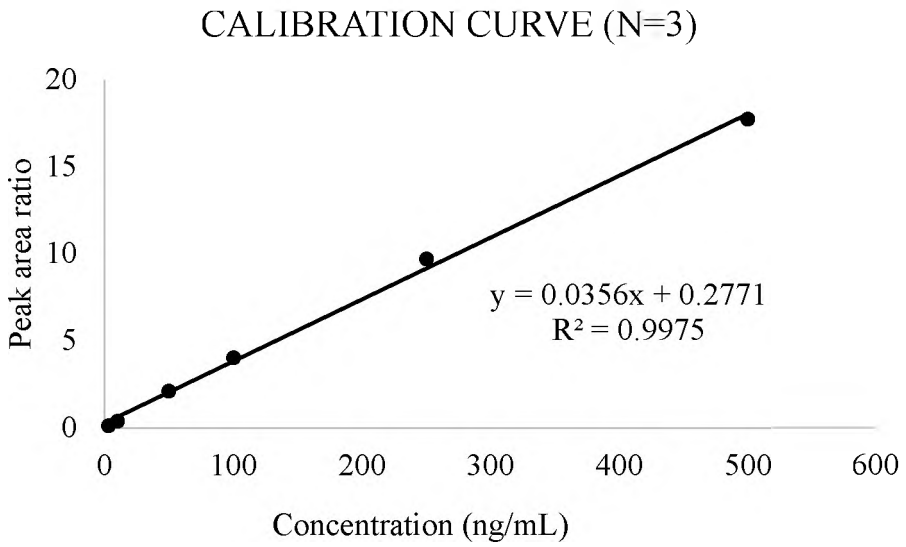

Figure 3. 3 Calibration curve of TMZ (n=3)

Correlation coefficient, $R^2 = 0.9975$

Table 3. 2 Lower limit of quantitation (LLOQ) of TMZ determined in five individual mouse brain samples on the same day and five different days (n=5).

LLOQ Spiked concentration (µg/g)	Intra-day			Inter-day		
	Determined concentration ± SD (µg/g)	%RE	%CV	Determined concentration ± SD (µg/g)	%RE	%CV
1.02	1.06 ± 0.05	4	5	1.09 ± 0.07	6	15

%RE (percent relative error) = [(determined concentration − spiked concentration)/(spiked concentration)] x 100

%CV (percent coefficient of variation) = (standard deviation/mean) x 100

3.3.2.3. Accuracy and precision

Accuracy is defined as the degree of closeness of the determined value to the true value. Precision is defined as the closeness of agreement among series of measurements obtained from multiple sampling of the same homogeneous sample. For this study, we estimated intra-day and inter-day accuracy and precision in three QCs at three concentrations (3.06, 20.4 and 136 μg/g) prepared from five individual mouse brains. Intra-day accuracy and precision were determined by five sets of three QCs prepared from five individual mouse brains on the same day. Inter-day accuracy and precision were determined by five sets of three QCs prepared from five individual mouse brain samples on five different days. As shown in table 3.3, intra-day accuracy expressed as %RE was ≤ 7% and precision expressed as %CV was ≤ 3%. The inter-day accuracy was ≤ 6% and precision was ≤ 10 %. It should be noted that even though analyses were done using QCs from five individual mouse brain samples, all values were well below the 15% limit set by the FDA demonstrating the accuracy and precision of the method.

Table 3. 3 Accuracy and precision of TMZ in five individual blank mouse brain samples measured on the same day and five different days (n=5).

QC level	Spiked concentration (µg/g)	Intra-day				Inter-day		
		Determined concentration ± SD (µg/g)	%RE	%CV		Determined concentration ± SD (µg/g)	%RE	%CV
LQC	3.06	3.13 ± 0.05	2	2		3.27 ± 0.13	4	10
MQC	20.4	19.0 ± 0.63	-7	3		19.2 ± 0.66	- 6	10
HQC	136	137 ± 4.64	1	3		141 ± 4.87	2	9

%RE (percent relative error) = [(determined concentration − spiked concentration)/(spiked concentration)] x 100

%CV (percent coefficient of variation) = (standard deviation/mean) x 100

3.3.2.4. Matrix effect and recovery

Matrix effect is defined as the effect on the method caused by other components in a study sample except the analyte. For this study, we evaluated the absolute and relative matrix effects in five individual mouse brain samples in three QCs at three concentrations (3.06, 20.4 and 136 μg/g). The absolute matrix effect of TMZ was determined by calculating the percentage of mean peak area of TMZ at three concentrations in extracted mouse brain matrix over mean peak area of TMZ in neat solution. The relative matrix effects were evaluated by calculating percentage of mean peak area ratio of TMZ and IS at three concentrations in the extracted mouse brain matrix over that of TMZ and IS in neat solution. As shown in table 3.4, the absolute matrix effects were within 85-108% and relative matrix effects were within 96-102%. All the values were below the 15% limit set by the FDA suggesting that we have successfully addressed the matrix effect issue suffered by Goldwirt et al.'s method by using ethanol to precipitate out proteins.

Recovery is defined as the extraction efficiency of the method, expressed as percentage of the known amount of the analyte carried through the extraction steps of the method [21]. Recovery was studied by assessing the absolute and relative recoveries in two individual mouse brain samples in three QCs at three concentrations (3.06, 20.4 and 136 μg/g). Absolute recovery was estimated by calculating the percentage mean peak area of TMZ spiked in mouse brain matrix before extraction over that of TMZ spiked in extracted mouse brain matrix. Relative recovery was evaluated by calculating the percentage of mean

Table 3. 4 Absolute, relative and IS matrix effect in five individual mouse brain samples (n=5).

Mouse brain sample	QC level	Spiked concentration (µg/g)	Absolute matrix effect (%)	IS matrix effect (%)	Relative matrix effect (%)
1	LQC	3.06	97 ± 4.67	98 ± 1.57	98 ± 4.23
	MQC	20.4	98 ± 2.29	101 ± 1.85	98 ± 0.76
	HQC	136	98 ± 1.30	102 ± 0.99	96 ± 1.37
2	LQC	3.06	96 ± 1.16	97 ± 2.06	99 ± 3.25
	MQC	20.4	94 ± 1.20	95 ± 2.51	98 ± 3.14
	HQC	136	90 ± 0.84	89 ± 1.33	101 ± 0.84
3	LQC	3.06	106 ± 1.77	104 ± 3.76	102 ± 5.35
	MQC	20.4	94 ± 0.55	94 ± 0.32	100 ± 0.31
	HQC	136	85 ± 1.57	82 ± 0.45	103 ± 2.13
4	LQC	3.06	108 ± 2.71	111 ± 2.35	98 ± 1.53
	MQC	20.4	95 ± 2.40	98 ± 0.41	97 ± 2.72
	HQC	136	91 ± 0.13	94 ± 1.18	97 ± 1.19
5	LQC	3.06	103 ± 2.69	101 ± 0.87	102 ± 2.97
	MQC	20.4	99 ± 1.50	101 ± 1.96	99 ± 3.34
	HQC	136	92 ± 0.55	91 ± 1.27	100 ± 1.17

Absolute matrix effect = [(mean peak area of TMZ in extracted mouse brain/mean peak area of TMZ in neat solution)] x 100.
IS matrix effect = [(mean peak area of IS extracted mouse brain /mean peak area of IS in extracted neat solution)] x 100.
Relative matrix effect = [(mean peak area ratio of TMZ/IS in extracted mouse brain/mean peak area ratio of TMZ/IS in neat solution)] x 100.

Table 3. 5 Absolute, relative and IS recovery in two individual mouse brains (n=2).

Mouse brain sample	QC level	Spiked concentration (µg/g)	Absolute Recovery (%)	IS Recovery (%)	Relative Recovery (%)
1	LQC	3.06	80 ± 0.03	71 ± 0.01	113 ± 0.05
	MQC	20.4	85 ± 0.02	78 ± 0.02	109 ± 0.02
	HQC	136	79 ± 0.01	72 ± 0.00	109 ± 0.02
2	LQC	3.06	81 ± 0.00	67 ± 0.02	121 ± 0.03
	MQC	20.4	84 ± 0.02	78 ± 0.01	108 ± 0.02
	HQC	136	84 ± 0.02	77 ± 0.02	108 ± 0.02

Absolute recovery = [(mean peak area of TMZ in mouse brain/mean peak area of TMZ in extracted mouse brain matrix)] x 100.
IS recovery = [(mean peak area of IS in mouse brain/mean peak area of IS in extracted mouse brain matrix)] x 100.
Relative recovery = [(mean peak area ratio of TMZ/IS in mouse brain/mean peak area ratio of TMZ/IS in extracted mouse brain matrix)] x 100.

peak area ratio of TMZ and IS spiked in mouse brain matrix before extraction over that of TMZ and IS spiked in the extracted mouse brain matrix.

As shown in table 3.5, the mean absolute recovery was 82% and mean relative recovery was 111%. These values were higher than those reported by Goldwirt et al. who reported a mean recovery of 63% suggesting that our method has improved the recovery of TMZ from mouse brain by 19% which could be attributed to the use of a lysis buffer to aid in homogenization.

3.3.2.5. Stability studies

Stability is defined as the measure of intactness of analyte in the sample matrix under specific storage and use conditions relative to the starting material for given time intervals. Studies were conducted to assess stock solution, autosampler, benchtop and freeze-thaw cycle stabilities. The stability of TMZ in the autosampler, benchtop and freeze thaw samples was expressed as percentage of measured mean peak area ratio of TMZ to IS against those of TMZ to IS in freshly prepared samples. Stock solution stability was assessed by keeping the stock solution (1 mg/mL) of TMZ at room temperature (25 °C) on bench top for 12 hours before diluting it to 10 and 100 ng/mL. Bench top and autosampler stability studies were performed by leaving QCs on bench top at 25 °C for 12 hours and autosampler at 15 °C respectively. Three freeze-thaw cycles were conducted by freezing QCs at -20 °C for 12 hours followed by thawing them unassisted at 25 °C.

Table 3. 6 Stability studies of TMZ under various test conditions (n=3).

Test conditions	Sample	Nominal Concentration	Temperature	Duration	% Recovery ± SD
Bench top	Stock solution	10 ng/mL	25 °C	12 h	116 ± 0.02[a]
	Stock solution	100 ng/mL			125 ± 0.04[a]
Bench top	LQC	3.06 µg/g	25 °C	12 h	100 ± 0.04[b]
	HQC	136 µg/g			102 ± 0.05[b]
Autosampler	LQC	3.06 µg/g	15 °C	18 h	109 ± 0.06[b]
	HQC	136 µg/g			90 ± 0.04[b]
Freeze-thaw cycles	LQC	3.06 µg/g	-20 to 25 °C	Frozen for 12 h	123 ± 0.08[b]
	HQC	136 µg/g			116 ± 0.04[b]

[a] %Recovery = [mean peak area of TMZ in stability sample/ mean peak area of TMZ in fresh sample] x 100.

[b] %Recovery = [mean peak area ratio of TMZ/IS in stability sample/ mean peak area ratio of TMZ/IS in fresh sample] x 100.

The stability of samples under various test conditions described above was expressed as percent recovery (%RE) and were presented in table 3.6. Stock solution showed a recovery of 116% when diluted to 10 ng/mL and 125 % when diluted to 100 ng/mL indicating that it should not be stored at room temperature for more than 12 hours. The %RE of QCs were $\leq$ 10% suggesting that QCs were stable for 12 hours at bench top and 18 hours in the autosampler. The %RE for LQC was 2% higher than the 20% limit set by FDA signifying that freezing and thawing QCs should be kept under three cycles.

3.3.2. Method application

The above method has been applied to determine TMZ in eight mouse brain samples subjected to intracerebral micro dialysis. As shown in table 3.7, the concentration of TMZ in the eight brain samples collected after 12 hours was below LLOQ. While no data was available on pharmacokinetics of intracerebral microdialysis of TMZ in mice brain, Goldwirt et al. published a concentration-time profile where concentration of TMZ reached almost zero at 4 hours after intra peritoneal administration. This suggests that TMZ could have been possibly converted into its metabolites long before the sample have been collected. Hence, we conducted another study by injecting 40 μg of TMZ into a mouse brain using a 1cc syringe fitted with a 31 g, 5/16inch needle (similar gauge size as that of the microdialysis probe) and analyzed it immediately. The determined amount was 39.55 μg with a percent recovery of 99%.

3.4. Conclusion

In conclusion, a high recovery yielding LC-MS/MS method for quantitative determination of TMZ in mouse brain has been developed and validated for the first time. The method consisted of two-step extraction process involving a lysis buffer for homogenization and protein precipitation with ethanol, both crucial for achieving 82% recovery and matrix effects within 15%. The method developed was applied to study samples and might be useful in determining the amount of TMZ in mouse brain in order to evaluate intra cerebral microdialysis as a potential alternate route of administration.

3.5 References

[1] F. Hanif, K. Muzaffar, K. Perveen, S.M. Malhi, & S.U.Simjee, Glioblastoma multiforme: A review of its epidemiology and pathogenesis through clinical presentation and treatment, Asian Pac J Cancer Prev. 18 (2017) 3-9.

[2] M.H. Cohen, J.R. Johnson, R. Pazdur, Food and Drug Administration Drug approval summary: temozolomide plus radiation therapy for the treatment of newly diagnosed glioblastoma multiforme, Clin Cancer Res. 11 (2005) 6767-6771.

[3] R. Stupp, W.P. Mason, M.J. Van Den Bent, M. Weller, B. Fisher, M.J. Taphoorn, K. Belanger, A.A. Brandes, C. Marosi, U. Bogdahn, J. Curschmann, R.C. Janzer, S.K. Ludwin, T. Gorlia, A. Allgeier, D. Lacombe, J.G. Cairncross, E. Eisenhauer, R.O. Mirimanoff, Radiotherapy plus concomitant and adjuvant temozolomide for glioblastoma, N Engl J Med. 352 (2005) 987-996.

[4] L. Reyderman, P. Statkevich, C.M. Thonoor, J. Patrick, V.K. Batra, M. Wirth, Disposition and pharmacokinetics of temozolomide in rat, Xenobiotica. 34 (2004) 487-500.

[5] H. Holback, Y. Yeo, Intratumoral drug delivery with nanoparticulate carriers, Pharm Res. 28 (2011) 1819-1830.

[6] G. Boschi & J.M. Scherrmann, Microdialysis in mice for drug delivery research, Adv Drug Deliv Rev. 45 (2000) 271-281.

[7] R. Grossman, B. Tyler, M.A. Rudek, E. Kim, P. Zadnik, U. Khan, J.O. Blakeley, A.P. Pathak, H. Brem, Microdialysis measurement of intratumoral temozolomide concentration after cediranib, a pan-VEGF receptor tyrosine kinase inhibitor, in a U87 glioma model, Cancer Chemother Pharmacol. 72 (2013) 93-100.

[8] J. Portnow, B. Badie, M. Chen, A. Liu, S. Blanchard, T.W. Synold, The neuropharmacokinetics of temozolomide in patients with resectable brain tumors: potential implications for the current approach to chemoradiation, Clin Cancer Res. 15 (2009) 7092-7098.

[9] C.J. Peer, L. Ronner, L. Rodgers, C.M.L. McCully, K.E. Warren, W.D. Figg, Quantification of temozolomide in nonhuman primate fluids by isocratic ultra-high performance liquid chromatography-tandem mass spectrometry to study brain tissue penetration following intranasal or intravenous delivery, Separations, 3 (2016) 4.

[10] L. Goldwirt, N. Zahr, R. Farinotti, C. Fernandez, Development of a new UPLC-MSMS method for the determination of temozolomide in mice: application to plasma pharmacokinetics and brain distribution study, Biomed Chromatogr. 27 (2013) 889-893.

[11] H.L. Liu, C.Y. Huang, J.Y., Chen, H.Y.J. Wang, P.Y. Chen, K.C. Wei, Pharmacodynamic and therapeutic investigation of focused ultrasound-induced blood-brain barrier opening for enhanced temozolomide delivery in glioma treatment, PLoS One. 9 (2014).

[12] Wishart DS, Feunang YD, Guo AC, Lo EJ, Marcu A, Grant JR, Sajed T, Johnson D, Li C, Sayeeda Z, Assempour N, Iynkkaran I, Liu Y, Maciejewski A, Gale N, Wilson A,

Chin L, Cummings R, Le D, Pon A, Knox C, Wilson M. DrugBank 5.0: a major update to the DrugBank database for 2018. Nucleic Acids Res. 2017 Nov 8. https://www.drugbank.ca/drugs/DB00853, (accessed on 02.06.2018).

[13] Wishart DS, Feunang YD, Guo AC, Lo EJ, Marcu A, Grant JR, Sajed T, Johnson D, Li C, Sayeeda Z, Assempour N, Iynkkaran I, Liu Y, Maciejewski A, Gale N, Wilson A, Chin L, Cummings R, Le D, Pon A, Knox C, Wilson M. DrugBank 5.0: a major update to the DrugBank database for 2018. Nucleic Acids Res. 2017 Nov 8. https://www.drugbank.ca/drugs/DB00277 (accessed on 02.06.2018).

[14] J.L. Cohen, Analytical Profiles of Drug Substances, Academic Press, New York, 1975.

[15] G.A. Jamieson, D.M. Robinson, Mammalian cell membranes: responses of plasma membranes, first ed., Butterworths, London, 1977.

[16] R.R. Voggu, X. Zhou, B. Su, B. Guo, A simple and rapid LC-MS/MS Method for the determination of BMCL26 a novel anti-parasitic Agent in rat plasma, J Anal Bioanal Tech. 6 (2015) 265.

[17] R.R. Voggu, R. Alagandula, X. Zhou, B. Su, B. Zhong, B. Guo, A rapid LC-MS/MS method for quantification of CSUOH0901, a novel antitumor agent, in rat plasma, Biomed Chromatogr. 29 (2015) 797-802.

[18] C. Polson, P. Sarkar, B. Incledon, V. Raguvaran, R. Grant, Optimization of protein precipitation based upon effectiveness of protein removal and ionization effect in liquid chromatography–tandem mass spectrometry, J. Chromatogr. B. 785 (2003) 263-275.

[19] A. Negrusz, G. Cooper, Clarke's Analytical Forensic Toxicology, second ed., Pharmaceutical press, London, 2013.

[20] U.S. Food, Drug Administration Bioanalytical method validation, guidance for industry, 2018, Available from: https://www.fda.gov/downloads/drugs/guidances/ucm070107.pdf. (accessed on 02.06.2018).

[21] F. Chow, A. Ocampo, P. Vogel, S. Lum, N. Tran, Current challenges for FDA-regulated bioanalytical laboratories performing human BA/BE studies; Part III: selected discussion topics in bioanalytical LC/MS/MS method validation, The Quality Assurance Journal: The Quality Assurance Journal for Pharmaceutical, Health and Environmental Professionals. 12 (2009) 22-30.

CHAPTER IV

INVESTIGATION OF THE APPLICABILITY OF DIGESTION USING ASPARTIC ACID N ENDOPEPTIDASE FOR IDENTIFICATION OF VARIANTS OF DES-GAMMA-CARBOXY PROTHROMBIN BY LC-MS

4.1. Introduction

Hepatocellular carcinoma (HCC) is the second leading cause of cancer related deaths in the world and is the fifth most common cancer with over half a million cases diagnosed a year globally [1]. HCC is usually diagnosed at late stages and patients are reported to have a maximum post-diagnostic survival period of five years [2]. Infection with hepatitis B or C viruses, alcohol-related cirrhosis and non-alcoholic steatohepatitis are found to be major risk factors of HCC [3]. Symptoms of HCC include right upper quadrant pain, weight loss, jaundice, palmar erythema, gynecomastia, portal hypertension, anemia, etc. [4]. Management of HCC is dependent on the nature of tumor, ranging from surgical resection, liver transplantation during initial stages to chemotherapy in late stages [2]. HCC screening is performed by using ultrasound of the liver which is challenging because of differences in the interpretations among radiologists and by magnetic resonance imaging

which is expensive [2], [4]. Alfa feto protein (AFP) and Des-gamma-carboxy-prothrombin (DCP) also known as PTB induced by Vitamin K absence-II (PIVKA-II) have been investigated and widely used as tumor markers for HCC [5]–[19].

4.1.1 Biosynthesis of DCP from prothrombin precursor

prothrombin (PTB) or clotting factor II is an important protein involved in the coagulation of blood. It has a molecular weight of 72 kDa and is present at a concentration of approximately 0.1 mg/mL in the plasma of healthy individuals [20]. In the coagulation cascade, prothrombinase complex converts PTB to thrombin which converts soluble fibrinogen to insoluble fibrin ultimately leading to coagulation of blood. PTB is a single chain glycoprotein comprising of 579 amino acid residues which are arranged into gamma carboxyglutamic (Gla) domain (residues 1-46), kringle-1 (residues 65-143), kringle-2 (residues 170-248) and protease domain comprising of A chain (residues 285-320) and catalytic B chain (residues 321-579) [21]. In the Gla domain of PTB, there are present ten post translationally modified glutamic acid residues located at 6, 7, 14, 16, 19, 20, 25, 26, 29 and 32 positions. Under physiological conditions, prothrombin precursor (622 amino acids) is converted to PTB (579 amino acids) by post translational carboxylation and removal of a signal peptide and a propeptide in the lumen of the endoplasmic reticulum of liver cells before its secretion into the blood. [22]. During this process, glutamic acid residues (Glus) present in the Gla domain are converted to γ-carboxy glutamic acid residues (Glas) by a Vitamin K dependent enzyme, γ-glutamyl carboxylase as shown in fig 4.1.

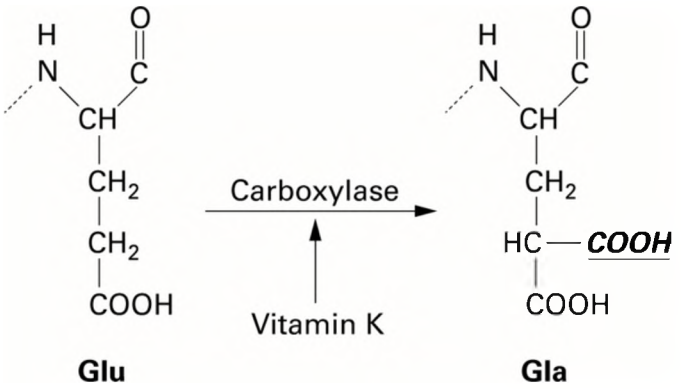

Figure 4. 1 Post translational modification of Glutamic acid (Glu) to gamma carboxy glutamic acid (Gla) by Vitamin K dependent gamma carboxylase enzyme (image adapted from reference [23])

In a healthy individual, gamma-carboxylation occurs at all the ten Glus in the Gla domain of PTB and is essential for the anticoagulant activity of PTB. Uehara et al reported that ten

Glus are carboxylated in the order of 26, 25, 16, 29, 20, 19, 14, 32, 7 and 6 positions from the N-terminus [24]. Fig. 4.2A shows the complete amino acid sequence of PTB with all ten Glus (represented by E) post translationally modified into Glas (represented by γ) in the Gla domain and fig. 4.2B shows different domains of PTB and a part of the polypeptide in Gla domain containing ten Glas. γ-glutamyl carboxylase is a Vitamin K dependent enzyme and its activity is lowered when Vitamin K is inadequate in conditions such as Vitamin K deficiency, hepatocellular carcinoma or by Vitamin K antagonists. This leads to incomplete carboxylation of Glus in the Gla domain leaving all ten or some Glus not converted to Glas. The resulting abnormal PTB molecules with no or partial carboxylation are collectively called as Des-carboxy prothrombin (DCP) [61]. DCP lacks the ability to interact with other clotting factors. DCP is also known as PIVKA-II (Protein Induced by Vitamin K deficiency or Antagonist-II) as it was originally discovered in the plasma of Vitamin K deficient or phenprocoumon, (a Vitamin K antagonist) treated animals along with other abnormal clotting factors IX and X resulting from incomplete carboxylation [25]. Thus, DCP contains several variants which differ in the Glu content in their Gla domains as shown in the following fig. 4.3. DCP is produced by malignant hepatocyte and various mechanisms for production of DCP in HCC have been proposed [17]. Hypoxia occurs in HCC cells that may lead to recycling of Vitamin K leading to diminished activity of γ-glutamyl carboxylase enzyme ultimately resulting in the production of DCP [20].

A)

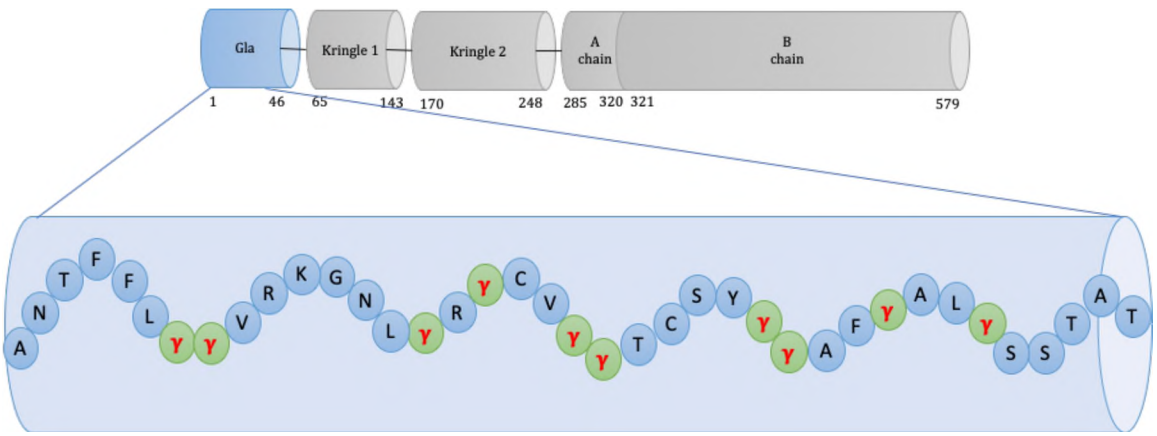

B)

ANTFLγγVRKGNLγRγCVγγTCSYγγAFγALγSSTATDVFWAKYTACETARTPRD
KLAACLEGNCAEGLGTNYRGHVNITRSGIECQLWRSRYPHKPEINSTTHPGADLQENF
CRNPDSSTTGPWCYTTDPTVRRQECSIPVCGQDQVTVAMTPRSEGSSVNLSPPLEQCV
PDRGQQYQGRLAVTTHGLPCLAWASAQAKALSKHQDFNSAVQLVENFCRNPDGDEE
GVWCYVAGKPGDFGYCDLNYCEEAVEEETGDGLDEDSDRAIEGRTATSEYQTFFNPR
TFGSGEADCGLRPLFEKKSLEDKTERELLESYIDGRIVEGSDAEIGMSPWQVMLFRKSP
QELLCGASLISDRWVLTAAHCLLYPPWDKNFTENDLLVRIGKHSRTRYERNIEKISMLE
KIYIHPRYNWRENLDRDIALMKLKKPVAFSDYIHPVCLPDRETAASLLQAGYKGRVTG
WGNLKETWTANVGKGQPSVLQVVNLPIVERPVCKDSTRIRITDNMFCAGYKPDEGKR
GDACEGDSGGPFVMKSPFNNRWYQMGIVSWGEGCDRDGKYGFYTHVFRLKKWIQK
VIDQFGE

Figure 4. 2 A) Structure of prothrombin B) Amino acid sequence of prothrombin

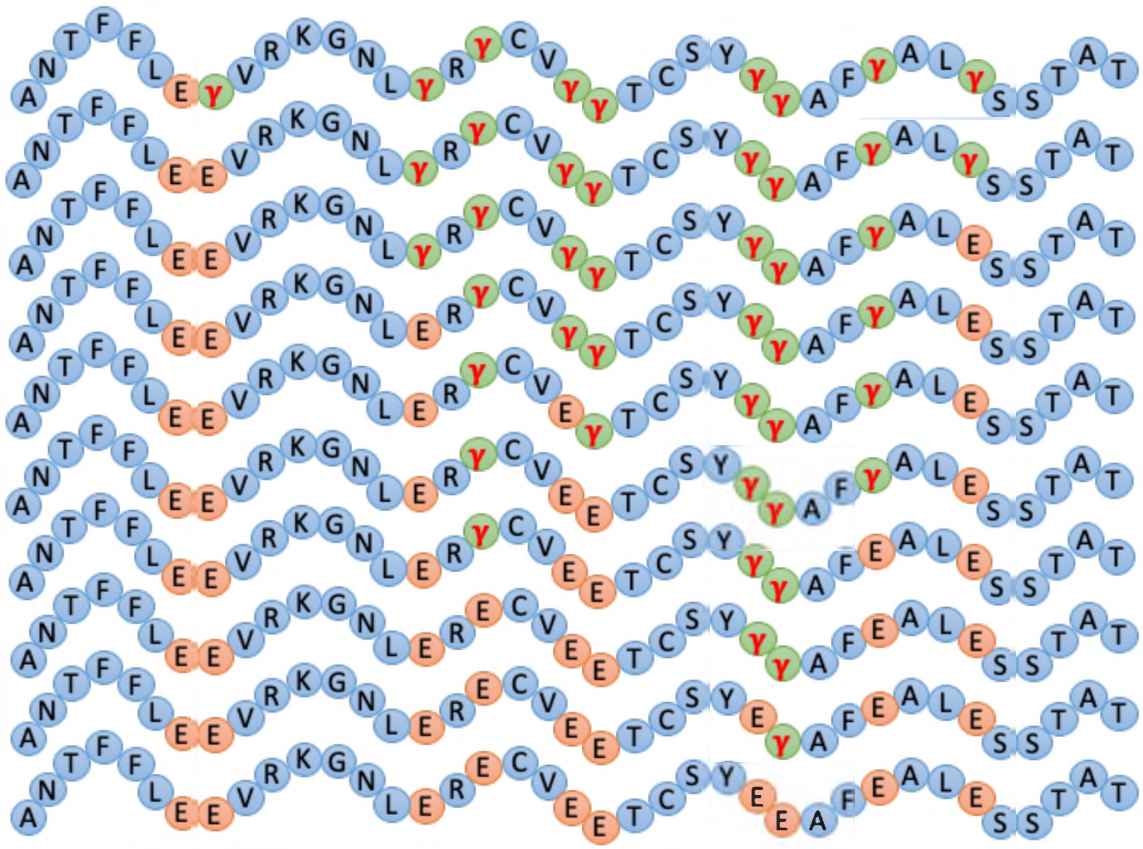

Figure 4. 3 Portions of DCP variants containing 1-10 Glus arranged in the order of carboxylation proposed by Uehara et al (bottom to top).

4.1.2 DCP as a risk marker for HCC

Liebman et al found that DCP was present in the plasma of 90% of HCC patients at a mean level of 900 ng/mL while it was lower (10 ng/mL) chronic active hepatitis and

negligible in healthy subjects [5]. Since then, several studies have been conducted to evaluate the utility of DCP as a biomarker for HCC. Literature review reveals that sensitivity values varied between 28-90% and specificity between 44%-100%. Levels of DCP did not correlate with those of AFP, which is the most widely used biomarker for HCC as both of them have different mechanisms. Studies were also performed to compare the sensitivity and accuracy of DCP with AFP. DCP exhibited more sensitivity in most studies but some studies showed that AFP is more sensitive than DCP. While AFP was more accurate in diagnosing small tumors, DCP diagnosed large tumors and early stage HCC more accurately than AFP [26]. Tumor relapse and metastasis are found to be more in patients with positive for DCP. DCP has been approved by the FDA as a risk marker for HCC and is used in combination with AFP and AFP L3 (lens culinaris agglutinin-reactive AFP) in Asia for early detection of HCC [27]. DCP was predicted to stimulate and metastasize HCC growth by activating abnormal signaling pathways [20]. However, very little information is available on the biochemical role of the different variants in the progression of HCC.

Higher levels of DCP are not only found in HCC patients but also in non-HCC conditions such as obstructive jaundice, Vitamin K deficiency and in patients on warfarin therapy [28]. Though Vitamin K has been found to have an apoptotic role in HCC, administration of Vitamin K could not prevent the recurrence of the cancer. Hence, the interrelationship between Vitamin K deficiency, elevated DCP and HCC still needs to be investigated. Currently, the concentration of DCP in serum is estimated by immunoassays that use MU-3 antibodies. A study conducted by Naraki et al revealed that DCP produced in HCC consisted of variants with 6–10 Glu residues [29]. In the same study it has been

found that the epitope of MU-3 antibodies consisted of amino acid residues 17–27 which included Es at 19, 20, 25 and 26. MU3 antibodies are found to bind with those variants that had at least 6Es (and with 2Es present at 19 and 20). However, DCP variants produced in vitamin K deficiency, consist of 2–9 Glu residues and also react partially with MU-3 antibodies, leading to false positive results [17]. Previous studies aimed at investigating the level of total DCP variants in HCC and non-HCC conditions, but very little information is available regarding the distribution of different variants and their levels in serum. It is still unknown which variant among the variants could serve as a highly specific biomarker for HCC. Hence, a study of distribution of DCP variants in the sera of HCC patients and Vitamin K deficient patients could determine the best variant that can serve as a sensitive and specific biomarker of HCC.

4.1.3 Identification of variants of DCP using middle-down approach

Top-down and bottom-up proteomics are widely used approaches to study variants of proteins. A top down approach involves the analysis of intact protein (>10k Da) and requires expensive and high-resolution mass spectrometers. A bottom-up approach involves the analysis of peptides (< 3kDa) generated by Tryptic digestion of proteins. Though it is widely used, a bottom up approach is not ideal for studying PTMs due to the short length of the peptides [30]. In this study, we have chosen a middle-down approach (which involves analysis of peptides of 3-10 kDa length) to identify different variants of DCP as it is more suitable and convenient if a single peptide that contains all ten Glus or Glas can be produced by subjecting the protein to enzymatic digestion. For this purpose,

we have chosen PTB as the analyte for quantification as it only differs from DCP in the extent of carboxylation at ten Glus and is readily available unlike DCP which is difficult to obtain. Detection of the peptide containing 10 Glas in PTB will allow the study of distribution of different variants of DCP in Vitamin K and HCC serum samples based on the differences in their molecular weights (and hence m/Z). Though Trypsin is a widely used enzyme owing to its high specificity and reproducibility, it is not preferred in this study because it cleaves in between the 10 Glas producing three different peptides as shown in table 4.1. Therefore, we performed an *in silico* digestion of PTB with various enzymes and chemicals using ExPASy: SIB bioinformatics resource portal as shown in table 4.1 and searched for enzymes or chemicals that could produce a single peptide retaining all ten Glus [28]. As can be seen in the same table, BNPS-Skatole, Factor Xa, Aspartic acid N endopeptidase, Cyanogen bromide, Formic acid, Iodosobenzoic acid and Proline-endopeptidase produced single peptides with all ten Glus. Aspartic acid N endopeptidase was selected for this study because it generated shortest peptide consisting of 37 amino acids which is more likely detectable than the other peptides within the dynamic range of mass spectrometer.

Table 4. 1 Peptides obtained by performing *in-silico* digestion using different enzymes [28]

Enzyme	Number of peptides containing 10 Glus	Amino acid sequence of peptides	Number of amino acids
Trypsin	3	ANTFLEEVR	9
		GNLER	5
		ECVEETCSYEEAFEALESSTATDVFWAK	28
Arg-C proteinase	3	ANTFLEEVR	9
		KGNLER	6
		ECVEETCSYEEAFEALESSTATDVFWAKYTACETAR	36
BNPS-Skatole	1	ANTFLEEVRKGNLERECVEETCSYEEAFEALESSTATDVFW	41
Chymotrypsin	4	LEEVRKGNLERECVEETCSY	4
		EEAF	20
		EALESSTATDVF	4
		EALESSTATDVF	12
Clostripain	3	ANTFLEEVR	9
		KGNLER	6
		ECVEETCSYEEAFEALESSTATDVFWAKYTACETAR	36
LysC	2	ANTFLEEVRK	10
		GNLERECVEETCSYEEAFEALESSTATDVFWAK	33
Neutrophil elastase	5	NTFLEEV	7
		RKGNLERECV	10
		EETCSYEEA	9
		FEA	3
		LESSTA	6
Pepsin	4	EEVRKGNL	8
		ERECVEETCSYEEA	14
		EA	2
		ESSTATDV	8
Thermolysin	5	LEEVRKGN	8
		LEREC	5
		VEETCSYEEA	10

		FEA	3
		LESST	5
Asp-N endopeptidase	1	ANTFLEEVRKGNLERECVEETCSYEEA FEALESSTAT	37
CNBr	1	ANTFLEEVRKGNLERECVEETCSYEEA FEALESSTATDVFWAKYTACETARTPR DKLAACLEGNCAEGLGTNYRGHVNIT RSGIECQLWRSRYPHKPEINSTTHPGA DLQENFCRNPDSSTTGPWCYTTDPTVR RQECSIPVCGQDQVTVAM	152
Formic acid	1	ANTFLEEVRKGNLERECVEETCSYEEA FEALESSTATD	38
LysN	2	ANTFLEEVR	9
		KGNLERECVEETCSYEEAFEALESSTA TDVFWA	33
Iodosobenzoi c acid	1	ANTFLEEVRKGNLERECVEETCSYEEA FEALESSTATDVFW	41
NTCB	3	ANTFLEEVRKGNLERE	16
		CVEET	5
		CSYEEAFEALESSTATDVFWAKYTA	25
Proline-endopeptidase	1	ANTFLEEVRKGNLERECVEETCSYEEA FEALESSTATDVFWAKYTACETARTPR DKLAACLEGNCAEGLGTNYRGHVNIT RSGIECQLWRSRYPHKP	97

4.1.4 Feasibility of digestion using Aspartic acid N endopeptidase

Aspartic acid N endopeptidase (Asp-N) is a metalloproteinase (EC 3.4.24.33) produced by *Pseudomonas fragi*. It cleaves peptide bonds at N terminal to Aspartic acid and Cysteic acid residues [31]. However, if Cysteines are alkylated, cleavage is specific at Aspartic acid residues, though cleavage at Glus to a lesser extent (2000 fold less) was observed when digestion times are longer [32]. Because cleavages is specific to only one residue, Asp-N produces longer peptides and is used in middle-down proteomics or in combination with Trypsin and other proteases for achieving superior sequence coverage. In addition to native Asp-N isolated from *Pseudomonas fragi,* recombinant version cloned from *Stenotrophomonas maltophilia* and expressed in *E coli* is commercially available and is found to have better sequence coverage as reported by the manufacturer. In our study, we have investigated digestion efficiency with both forms. The desirable pH range for optimal activity of Asp-N is 4.0 to 9.0. In this work, our goal is to investigate the feasibility of employing Asp-N to digest PTB in order to study the distribution of different variants of DCP in human sera. Specifically, we aim to investigate the digestion efficiency of Asp-N by evaluating the sequence coverage and overall intensities of the resulting peptides of prothrombin. Fig. 4.4 shows peptides and cleavage sites of PTB by Asp-N.

ANTFLEEVRKGNLERECVEETCSYEEAFEALESSTAT|DVFWAKYTACETARTPR|DKLAACLEG
NCAEGLGTNYRGHVNITRSGIECQLWRSRYPHKPEINSTTHPGA|DLQENFCRNP|DSSTTGPWC
YTT|DPTVRRQECSIPVCGQ|DQVTVAMTPRSEGSSVNLSPPLEQCVP|DRGQQYQGRLAVTTHG
LPCLAWASAQAKALSKHQ|DFNSAVQLVENFCRNP|DG|DEEGVWCYVAGKPG|DFGYC|DLNYC
EEAVEEETG|DGL|DE|DS|DRAIEGRTATSEYQTFFNPRTFGSGEA|DCGLRPLFEKKSLE|DK
TERELLESYI|DGRIVEGS|DAEIGMSPWQVMLFRKSPQELLCGASLIS|DRWVLTAAHCLLYPP
W|DKNFTEN|DLLVRIGKHSRTRYERNIEKISMLEKIYIHPRYNWRENL|DR|DIALMKLKKPVA
FS|DYIHPVCLP|DRETAASLLQAGYKGRVTGWGNLKETWTANVGKGQPSVLQVVNLPIVERPVC
K|DSTRIRIT|DNMFCAGYKP|DEGKRG|DACEG|DSGGPFVMKSPFNNRWYQMGIVSWGEGC|D
R|DGKYGFYTHVFRLKKWIQKVI|DQFGE

Figure 4. 4 Cleavage sites (represented by |) and expected peptides of PTB after digestion with Asp-N

4.2 Experimental

4.2.1 Chemicals

PTB (>95%), Ammonium bicarbonate $(NH_4)HCO_3$, iodoacetamide (C_2H_4INO) and formic acid ($COOH_2$) were purchased from Sigma Aldrich. Aspartic acid endopeptidase and recombinant Aspartic acid endopeptidase (Asp-N) were obtained from Promega Corporation (Madison, WI, USA). Trypsin (MS Grade) was purchased from Thermofisher Scientific (Waltham, MA, USA). Urea (CH_4N_2O) was purchased from VWR chemicals, dithiothrietol ($C_4H_{10}O_2S_2$) was purchased from MP Biomedical (Solon, OH, USA). HPLC-grade acetonitrile (C_2H_3N) and trifluoro acetic acid (CF_3CO_2H) was obtained from Alfa Aesar (Ward Hill, MA, USA). C18 ZipTips and amicon centrifugal spin filters were obtained from Millipore sigma (Burlington, MA, USA). Deionized water was obtained from Barnstead D3750 nano pure water purification system by Thermo Scientific (Waltham, MA, USA).

4.2.2 Preparation of stock and working standard solutions

PTB was dissolved in water to obtain a 1.0 mg/mL solution which was stored at -80 °C as single use 50 µL aliquots to avoid degradation likely caused by multiple freeze-thaw cycles. Native Asp-N and recombinant Asp-N were dissolved separately in water to obtain 40 µg/mL solutions which were stored at -80 °C as single use 10 uL aliquots to avoid degradation likely caused by multiple freeze-thaw cycles.

4.2.3. Instrumentation

High performance liquid chromatography was performed on Shimadzu HPLC unit (Columbia, MD, USA) which consisted of binary pumps (Nexera LC-30 AD), degasser (a DUG20A3R), autosampler (SIL-30 AC), column oven (CTO-10AVP) and a controller (CBM 20A). Mass spectrometric detection was carried out in AB SCIEX 5500 QTRAP mass spectrometer (Toronto, Canada) equipped with electrospray ionization (ESI) probe and a syringe pump. The instrument operation, acquisition and processing of data was performed using AB SCIEX Analyst software (version 1.6.3).

4.2.3.1. Liquid Chromatography

Chromatographic separation of peptides was achieved at 30°C on a Waters XBridge™ C18 column (1.0 mm x 100 mm x 3.5 µ). For LC-MS analysis in positive mode, mobile phase A consisting of formic acid in water (0.1/100, v/v) and mobile phase B consisting of acetonitrile were used. During the optimization process, different flow rates, gradient elution programs with different run times were trialed which will be discussed later in the section 4.3.

4.2.3.2. Mass spectrometry

Mass spectrometric detection of peptides was carried out in positive electrospray ionization mode by utilizing Q3 scan feature of triple quadrupole for better sensitivity than

Q1 scan. The mass range was set between m/Z 500-1250 at a scan rate of 200Da/s. The source dependent parameters for positive mode were as follows: curtain gas at 35 psi; collision assisted dissociation gas at high; ion spray voltage at 5000 V; source temperature at 450°C; sheath gas at 30 psi and desolvation gas at 30 psi. The compound dependent parameters were as follows: declustering potential at 110 V; entrance potential at 15 V and collision cell exit potential 23 V. For negative mode the parameters were changed to ion spray voltage at -4500 V, declustering potential at -110 V; entrance potential at -15 V and collision cell exit potential -23 V.

4.2.4 Data interpretation

The MS scan data acquired on the Analyst software of AB Sciex triple quadrupole mass spectrometer was further processed in Skyline software [74]. Deconvolution of mass spectra was performed manually and in Skyline to confirm the identity of peptides. Data processing in Skyline was performed by first inputting the amino acid sequence of PTB in the form of a FASTA file from UniProt database and digesting *in silico* with Asp-N [75]. Peptide settings for detecting target peptide were as follows: missed cleavages at 0; length of peptide at 2-60; amino acid modifications at carbamidomethylation for cysteine (fixed) and carboxylation for glutamic acid residues (variable). Transition settings for all the peptides were as follows: precursor and product ion masses at average mass; precursor and ion charges at 1, 2, 3, 4, 5, 6, 7, 8, 9, 10, 11; ion match tolerance at 0.5 m/Z and scan range at 500 – 1250 m/Z. A separate data processing was done for the rest of the peptides with the same settings as above but, without gamma carboxy modification for Glus.

4.3 Results and Discussion

Because middle-down approach is newly emerging and Asp-N is not as well studied as Trypsin, literature on utility of Asp-N for LC-MS applications is limited. [30, 31]. Our aim was therefore to develop conditions for digesting PTB with Asp-N optimized to produce the greatest sequence coverage, which was conducted in the formation of 7 protocols varying the digestion conditions. The general workflow for digestion of PTB is depicted in the fig. 4.5. PTB was first denatured in 8M urea to break down the quaternary structure of the protein to produce a polypeptide chain. We have also investigated if 6M Guanidine Hydrochloride provides a better sequence coverage than urea in protocol 4 as Guanidine Hydrochloride is regarded as a stronger denaturing agent than urea. Denatured PTB was then reduced in 9.9 mM DTT (except in protocol 1 where 4.3 mM DTT was used) to disrupt disulfide bonds between cysteine residues which were alkylated using 30.2 mM IAA (except in protocol 1 where 36 mM IAA was used) to prevent re-formation of disulfide bonds. The concentration of denaturing agent was reduced to < 2M (except in protocol 5 where the concentration of urea after dilution was 2.8M) by addition of sufficient volume of 100 mM ABC buffer to prevent denaturation of Asp-N. Addition of ABC buffer also maintains a pH of 7-8 optimal for activity of Asp-N. Asp-N was added at an enzyme to protein ratio of 1:10 (except in protocol 1 where the ratio is 1:20) and incubated at 37°C. PTB was digested for variable times including 6 hours, 3.5 hours, 1 hour and 30 min after which Asp-N activity was inactivated by reducing the pH to 2 with formic acid or TFA. The sample was desalted to remove undesirable matrix components, and peptides were concentrated using C18 ZipTips or spin filters (MWCO 3K) before injection into the LC-

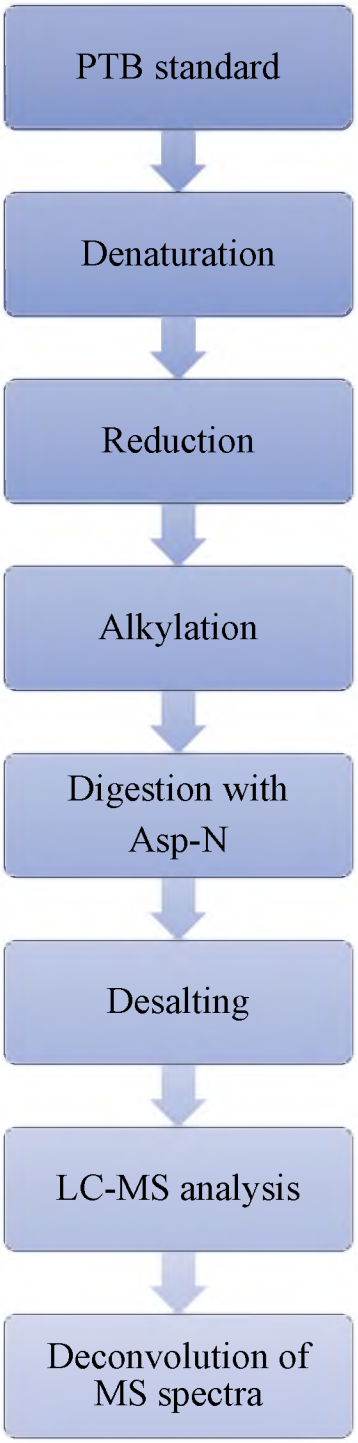

Figure 4. 5 General plan followed for protocols 1-7

MS. However, in protocols 3, 4 and 10, sample was cleaned prior to digestion in order to reduce concentration of urea and increase the concentration of PTB.

4.3.1 Protocol 1

Because Asp-N is not a widely used protease for enzymatic digestion in proteomics, there is limited literature available which describe the conditions for optimal digestion. Hence, we performed denaturation, reduction, alkylation and digestion based on a previously studied Trypsin based method (in our laboratory) and according to the manufacturer's protocol as follows: 5 µg of PTB was denatured with 50 µL of 8M urea in 100mM ABC buffer and vortexing on low speed for 40 min. It was then reduced with DTT to a final concentration of 4.3 mM by vortexing on low speed for 30 min. Alkylation was performed using IAA to a final concentration of 36 mM and incubated in the dark for 30 min. In order to prevent the denaturation of Asp-N, the concentration of urea was reduced to 1.8 M by the addition of ABC. Asp-N was added at enzyme: protein ratioof 1:20 at pH 7.0 and incubated for 6 hours at 37 °C. After 6 hours, digestion was stopped by inactivating the enzyme by lowering the pH to 2 with TFA. The peptides were desalted and enriched by solid phase extraction carried out using C18 ZipTips as follows: the C18 sorbent in the ZipTip was activated using acetonitrile and 0.1 % formic acid after which the digest was loaded. The sorbent was then washed with 0.1% formic acid and the peptides were eluted into 10 µL of 60% acetonitrile. The final volume was made upto 50 µL with 0.1% formic

A

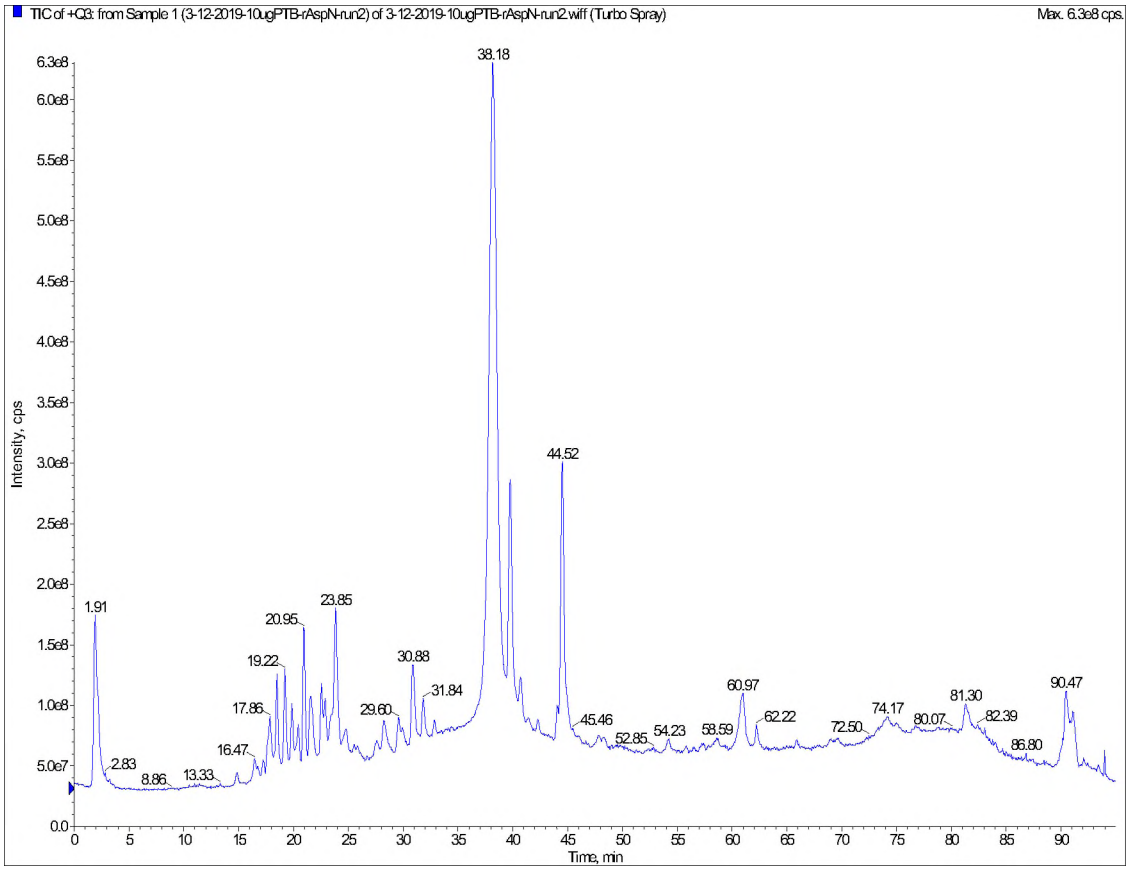

B

ANTFLEEVRKGNLERECVEETCSYEEAFEALESSTAT|DVFWAKYTACETARTPR|DKLAACLEG
NCAEGLGTNYRGHVNITRSGIECQLWRSRYPHKPEINSTTHPGA|DLQENFCRNP|DSSTTGPWC
YTT|DPTVRRQECSIPVCGQ|DQVTVAMTPRSEGSSVNLSPPLEQCVP|DRGQQYQGRLAVTTHG
LPCLAWASAQAKALSKHQ|DFNSAVQLVENFCRNP|DG|DEEGVWCYVAGKPG|DFGYC|DLNYC
EEAVEEETG|DGL|DE|DS|DRAIEGRTATSEYQTFFNPRTFGSGEA|DCGLRPLFEKKSLE|DK
TERELLESYI|DGRIVEGS|DAEIGMSPWQVMLFRKSPQELLCGASLIS|DRWVLTAAHCLLYPP
W|DKNFTEN|DLLVRIGKHSRTRYERNIEKISMLEKIYIHPRYNWRENL|DR|DIALMKLKKPVA
FS|DYIHPVCLP|DRETAASLLQAGYKGRVTGWGNLKETWTANVGKGQPSVLQVVNLPIVERPVC
K|DSTRIRIT|DNMFCAGYKP|DEGKRG|DACEG|DSGGPFVMKSPFNNRWYQMGIVSWGEGC|D
R|DGKYGFYTHVFRLKKWIQKVI|DQFGE

Figure 4. 6 A) Total ion chromatogram (full scan) of Asp-N digest of standard PTB using protocol 1 B) 0% Sequence coverage (detected peptides in bold)

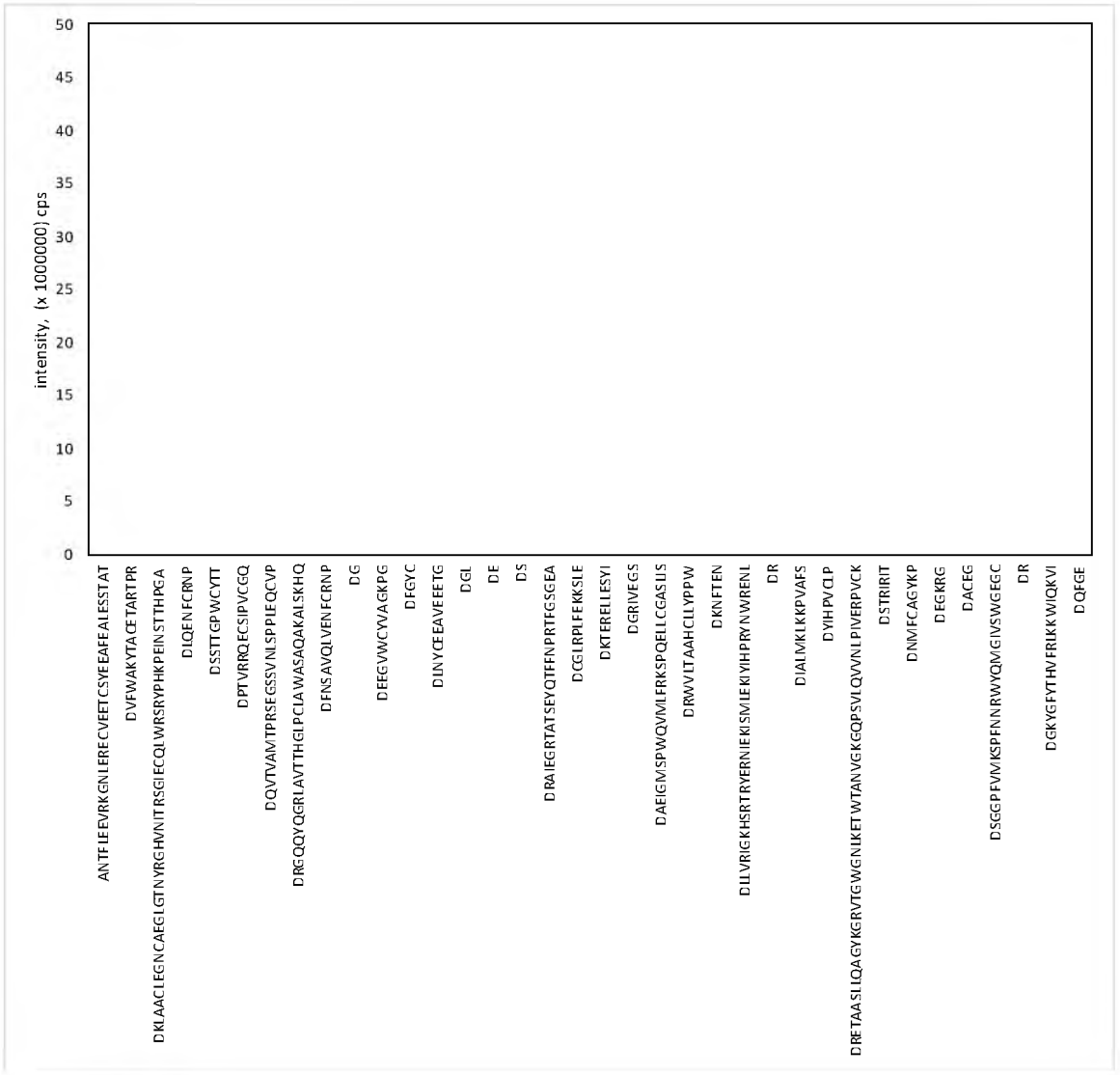

Figure 4. 7 Intensities of peptides detected in Asp-N digest of standard PTB using protocol 1

acid. 10 μL of the sample was injected into LC-MS at a flow at rate of 50 μL/min and 65 min gradient elution. The elution program was as follows: 0% B (initial), 0-90% B (55 min), 90% B (5 min), 90-0% B (3 min) and 0% B (2 min). Fig. 4.6 A shows the total ion chromatogram of the Asp-N digest of PTB obtained in full scan mode. Though a few peaks were observed in the chromatogram, no peptides were identified in the entire chromatogram resulting in 0% sequence coverage as shown in figs. 4.6 B and 4.7 implying that digestion probably did not take place at all. There could be several reasons for inadequate digestion, such as low starting concentration of protein, inaccessibility of cleavage sites by Asp-N due to 4.5 mM of DTT being inadequate for reduction, or over alkylation by IAA (at undesirable places like lysine, aspartic acid and glutamic acid residues) [35]. Another possibility is that the digestion time was too long which might have led to degradation of peptides generated [36]. Another possibility is that native Asp-N is not functional and suitable for digesting PTB.

4.3.2 Protocol 2

Recombinant Asp-N was found to have more efficiency and sequence coverage than native Asp-N as reported by the same manufacturer and hence was chosen for use in protocol 2 [32]. Further, the amount of protein was doubled to 10 μg to improve chances of detecting the peptides as well as digestion efficiency. The concentration of DTT was increased to 9.9 mM and the ratio of IAA to DTT was maintained at approximately 3:1 to ensure adequate reduction and alkylation. The enzyme: protein ratio was also increased to 1: 10 from 1:20 to make more Asp-N available for digestion and digestion time was reduced to 3.5 hours

from 6 hours. The modified procedure was carried out as follows: 10 μg of PTB was denatured with 90 μL of 8M urea in 100mM ABC buffer and incubated at 37 °C for 15 min. It was then reduced with DTT to a final concentration of 9.9 mM by incubating at 37 °C for 30 min. Alkylation was performed using IAA to a final concentration of 30.2 mM and incubated in the dark for 30 min. In order to prevent the denaturation of Asp-N, the concentration of urea was reduced to 2.8 M by the addition of ABC. Asp-N was added at enzyme: protein ratio of 1:10 at pH 7.5 and incubated for 3.5 hours at 37 °C. After 3.5 hours, digestion was stopped by inactivating the enzyme by lowering the pH to 2 with TFA. The peptides were desalted and enriched by solid phase extraction carried out using C18 ZipTips as follows. The C18 sorbent in the ZipTip was activated using acetonitrile and 0.1 % formic acid after which the digest was loaded. The sorbent was then washed with 0.1% formic acid and the peptides were eluted into 10 μL of 60% acetonitrile. The final volume was made up to 50 μL with 0.1% formic acid. 10 μL of the sample was injected into LC-MS at a flow at rate of 50 μL/min and run time of 95 min. The elution program was extended to 95 min to facilitate better chromatographic resolution of peptides as follows: 0% B (initial), 0-90% B (80 min), 90% B (5 min), 90-0% B (5 min) and 0% B (5 min). Fig. 4.8 A shows the total ion chromatogram of the Asp-N digest of PTB obtained in full scan mode using protocol 2. Nine out of thirty peptides were detected with a sequence coverage of 33.7% as shown in fig. 4.8 B and 4.9 thus showing that new conditions are favorable for digestion but need to be improved further.

A

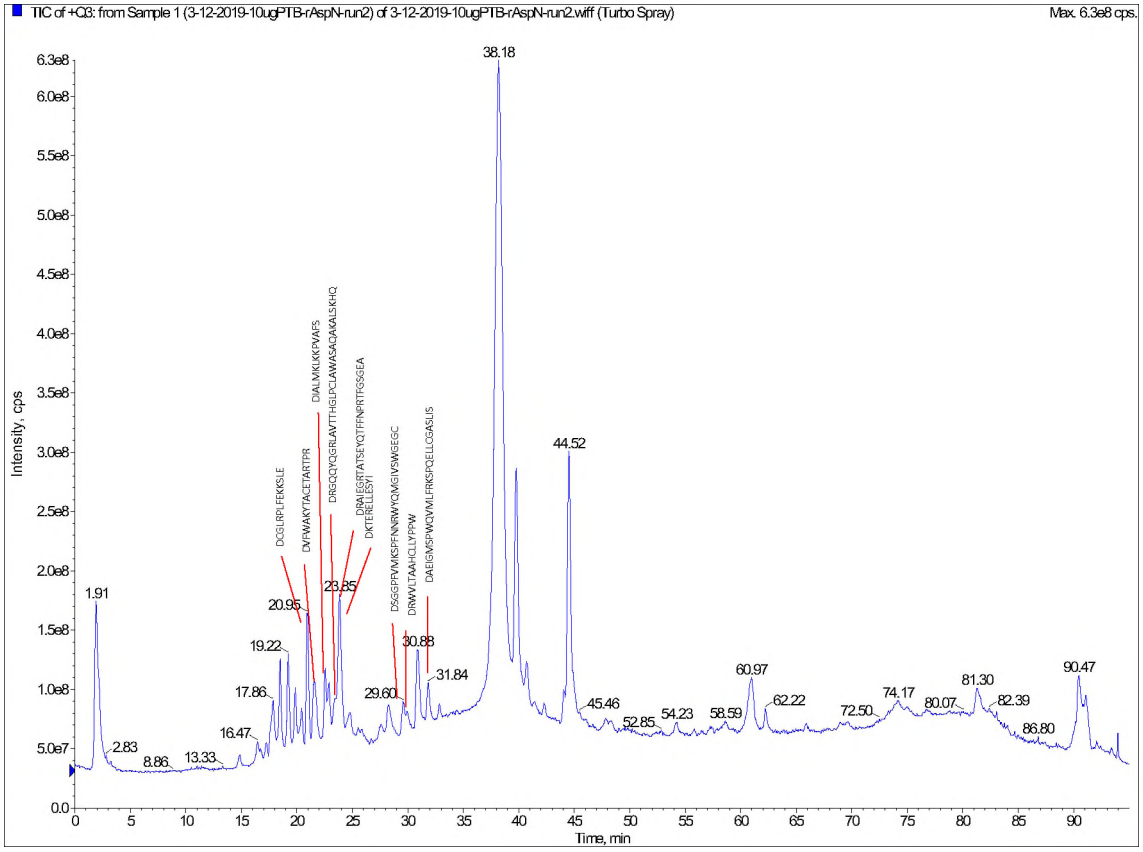

B

ANTFLEEVRKGNLERECVEETCSYEEAFEALESSTAT|**DVFWAKYTACETARTPR**|DKLAACLEG
NCAEGLGTNYRGHVNITRSGIECQLWRSRYPHKPEINSTTHPGA|DLQENFCRNP|DSSTTGPWC
YTT|DPTVRRQECSIPVCGQ|DQVTVAMTPRSEGSSVNLSPPLEQCVP|**DRGQQYQGRLAVTTHG**
LPCLAWASAQAKALSKHQ|DFNSAVQLVENFCRNP|DG|DEEGVWCYVAGKPG|DFGYC|DLNYC
EEAVEEETG|DGL|DE|DS|**DRAIEGRTATSEYQTFFNPRTFGSGEA**|**DCGLRPLFEKKSLE**|**DK**
TERELLESYI|DGRIVEGS|**DAEIGMSPWQVMLFRKSPQELLCGASLIS**|**DRWVLTAAHCLLYPP**
W|DKNFTEN|DLLVRIGKHSRTRYERNIEKISMLEKIYIHPRYNWRENL|DR|**DIALMKLKKPVA**
FS|DYIHPVCLP|DRETAASLLQAGYKGRVTGWGNLKETWTANVGKGQPSVLQVVNLPIVERPVC
K|DSTRIRIT|DNMFCAGYKP|DEGKRG|DACEG|**DSGGPFVMKSPFNNRWYQMGIVSWGEGC**|D
R|DGKYGFYTHVFRLKKWIQKVI|DQFGE

Figure 4. 8 A) Total ion chromatogram (full scan) of Asp-N digest of standard PTB using protocol 2 B) 33.7 % Sequence coverage (detected peptides in bold)

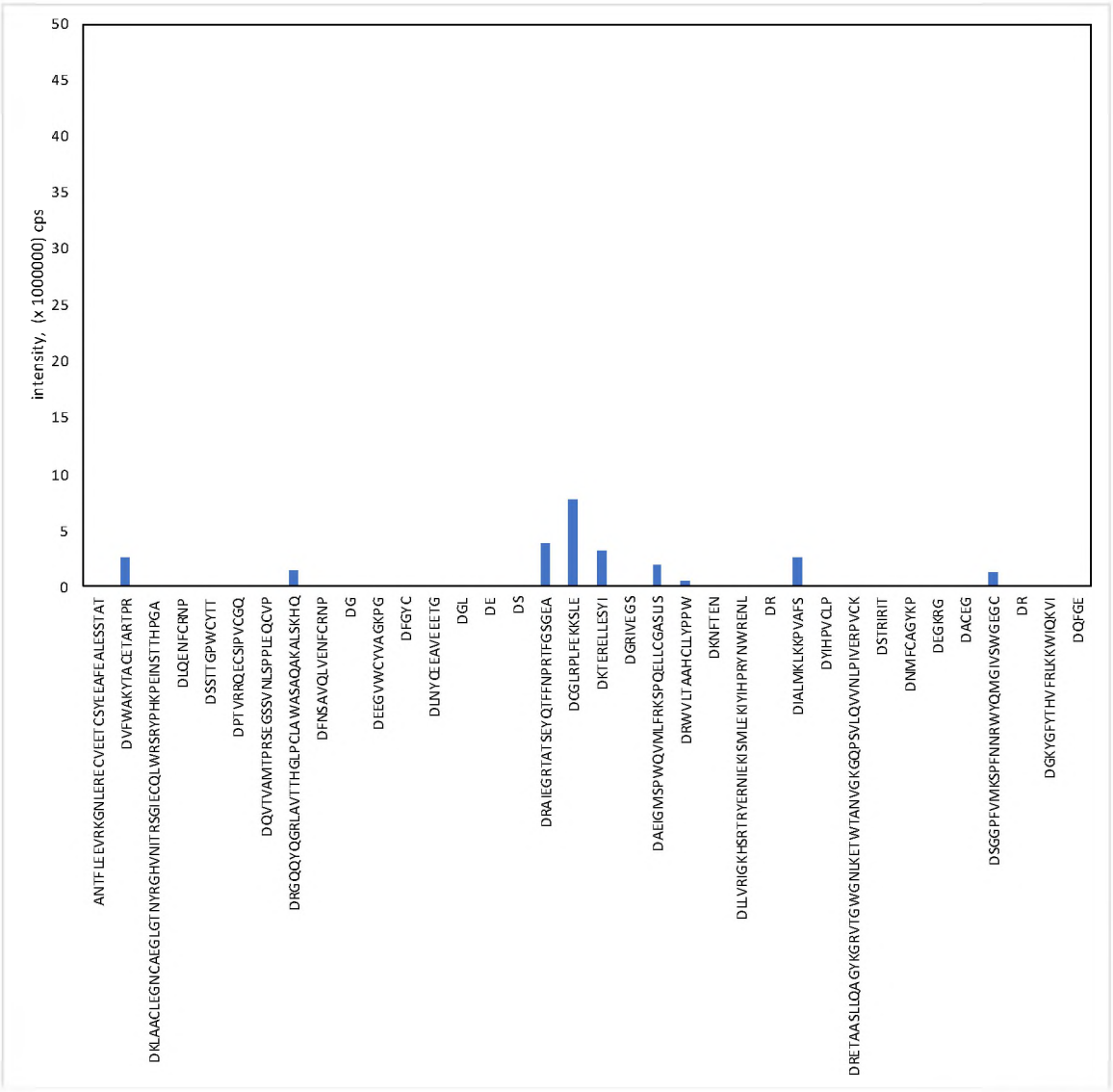

Figure 4. 9 Intensities of peptides detected in Asp-N digest of standard PTB using protocol 2

4.3.3 Protocol 3

In protocol 3, size exclusion spin filters were used not only to remove urea and other chemicals added before digestion but also to concentrate PTB in the sample before digesting it with Asp-N. In the modified procedure 10 μg of PTB was denatured with 90 μL of 8M urea in 100mM ABC buffer and incubated at 37 °C for 15 min. It was then reduced with DTT to a final concentration of 9.9 mM and incubated at 37 °C for 30 min. Alkylation was performed using IAA to a final concentration of 30.2 mM and incubated in the dark for 30 min. The sample was then cleaned up using Amicon 0.5 mL spin filters (MWCO 3K). For this, a spin filter was placed in a microcentrifuge tube, activated by centrifuging with 200 μL water at 14000 rpm for 6 min. Sample was loaded, the filter was spun at 14000 rpm for 10 min and washed by spinning at 14000rpm with 200 μL of ABC buffer for another 10 min. The sample (approximately 130 μL) remaining in the spin filter was collected by inverting the filter into another microcentrifuge tube and spinning at 1000 rpm for 2 min. After clean-up, Asp-N was added at enzyme: protein ratio of 1:10 at pH 7.5 and incubated for 3.5 hours at 37 °C. After 3.5 hours, digestion was stopped by inactivating the enzyme by lowering the pH to 2 with formic acid. 30 μL of sample was injected into LC- MS at a flow at rate of 50 μL/min and run time of 95 min using the same elution program as above. The injection volume was increased to 30 μL as final sample volume was increased approximately three-fold. We have also investigated if digestion was better with guanidine hydrochloride as it was considered as a stronger denaturing agent than urea. For this, another sample was denatured with 6M guanidine hydrochloride and treated and analyzed as described above. The urea treated sample yielded 23 of 30 peptides with a sequence coverage of 46.1 % (fig. 4.10 A and B) while 6M guanidine hydrochloride treated

A

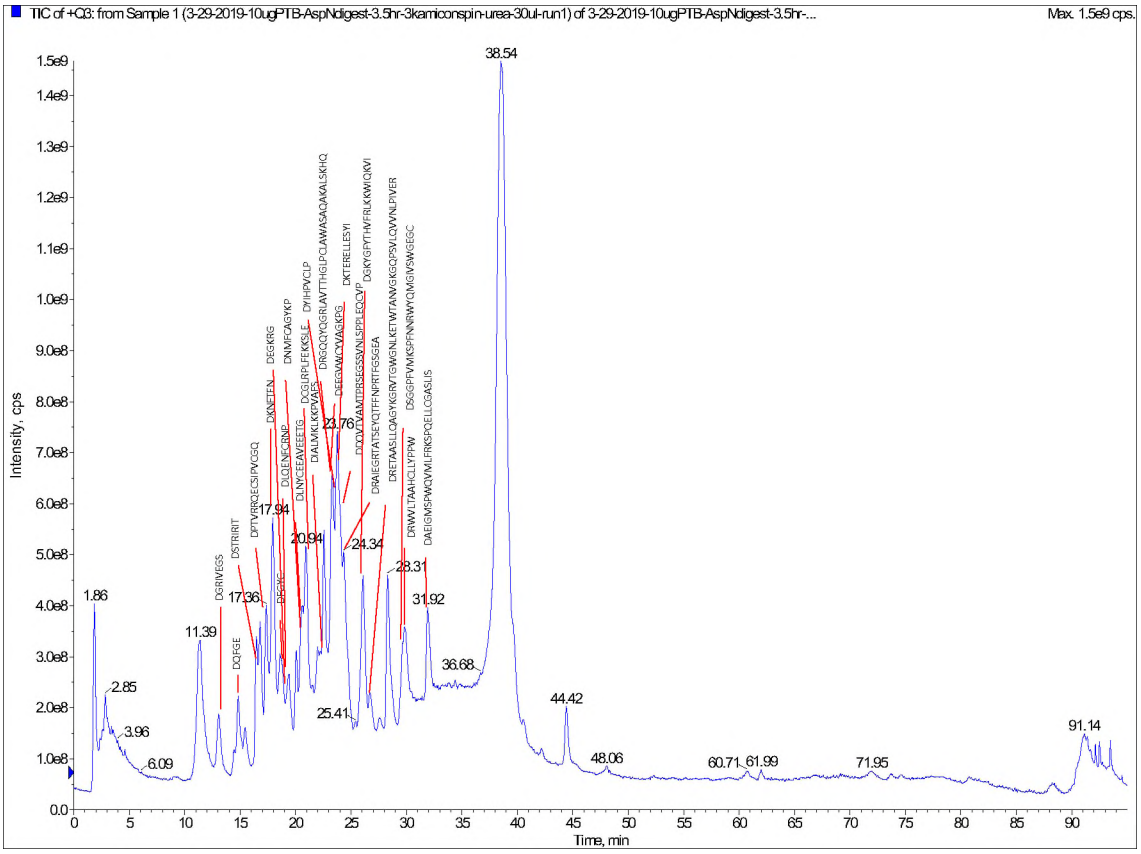

B

ANTFLEEVRKGNLERECVEETCSYEEAFEALESSTAT|DVFWAKYTACETARTPR|DKLAACLEG
NCAEGLGTNYRGHVNITRSGIECQLWRSRYPHKPEINSTTHPGA|**DLQENFCRNP**|DSSTTGPWC
YTT|**DPTVRRQECSIPVCGQ**|**DQVTVAMTPRSEGSSVNLSPPLEQCVP**|**DRGQQYQGRLAVTTHG**
LPCLAWASAQAKALSKHQ|DFNSAVQLVENFCRNP|DG|**DEEGVWCYVAGKPG**|**DFGYC**|**DLNYC**
EEAVEEETG|DGL|DE|DS|**DRAIEGRTATSEYQTFFNPRTFGSGEA**|**DCGLRPLFEKKSLE**|**DK**
TERELLESYI|**DGRIVEGS**|**DAEIGMSPWQVMLFRKSPQELLCGASLIS**|**DRWVLTAAHCLLYPP**
W|**DKNFTEN**|DLLVRIGKHSRTRYERNIEKISMLEKIYIHPRYNWRENL|DR|**DIALMKLKKPVA**
FS|**DYIHPVCLP**|**DRETAASLLQAGYKGRVTGWGNLKETWTANVGKGQPSVLQVVNLPIVERPVC**
K|**DSTRIRIT**|**DNMFCAGYKP**|**DEGKRG**|DACEG|**DSGGPFVMKSPFNNRWYQMGIVSWGEGC**|D
R|**DGKYGFYTHVFRLKKWIQKVI**|**DQFGE**

Figure 4. 10 A) Total ion chromatogram (full scan) of Asp-N digest of standard PTB using protocol with urea as denaturing agent 3 B) 46.1 % Sequence coverage (detected peptides in bold)

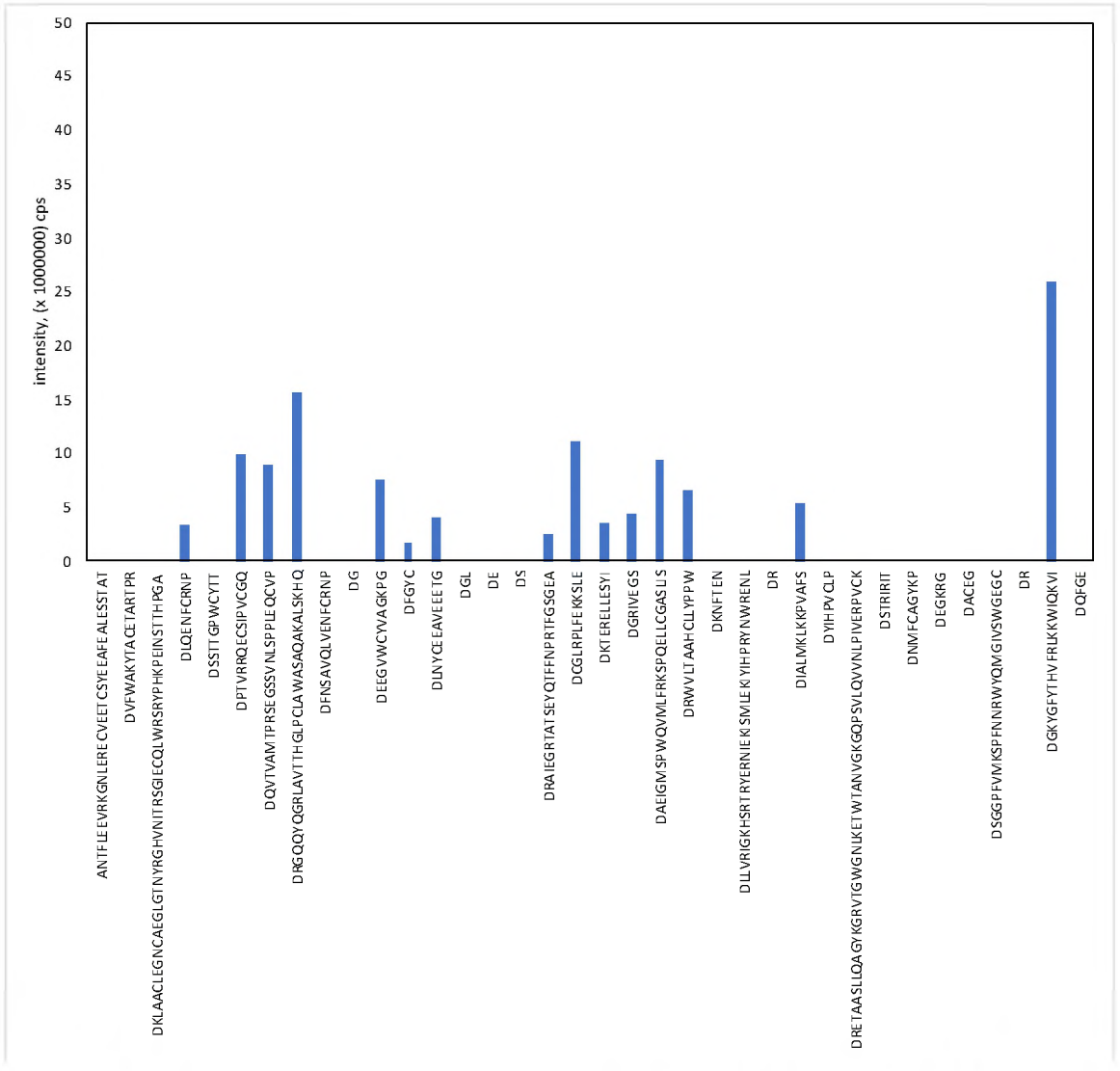

Figure 4. 11 Intensities of peptides detected in Asp-N digest of standard PTB using protocol 3 with urea as denaturing agent

A

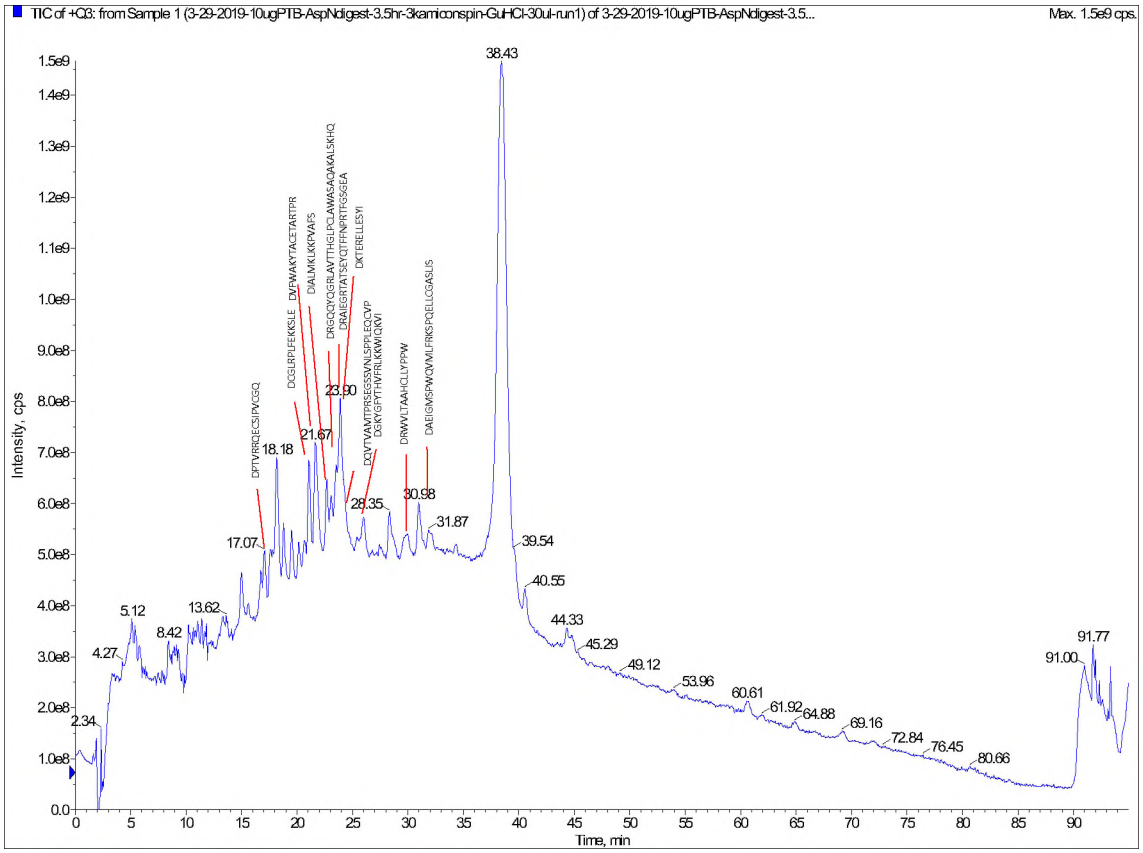

B

ANTFLEEVRKGNLERECVEETCSYEEAFEALESSTAT|**DVFWAKYTACETARTPR**|DKLAACLEG
NCAEGLGTNYRGHVNITRSGIECQLWRSRYPHKPEINSTTHPGA|DLQENFCRNP|DSSTTGPWC
YTT|**DPTVRRQECSIPVCGQ**|**DQVTVAMTPRSEGSSVNLSPPLEQCVP**|**DRGQQYQGRLAVTTHG**
LPCLAWASAQAKALSKHQ|DFNSAVQLVENFCRNP|DG|DEEGVWCYVAGKPG|DFGYC|DLNYC
EEAVEEETG|DGL|DE|DS|**DRAIEGRTATSEYQTFFNPRTFGSGEA**|**DCGLRPLFEKKSLE**|**DK**
TERELLESYI|DGRIVEGS|**DAEIGMSPWQVMLFRKSPQELLCGASLIS**|**DRWVLTAAHCLLYPP**
W|DKNFTEN|DLLVRIGKHSRTRYERNIEKISMLEKIYIHPRYNWRENL|DR|**DIALMKLKKPVA**
FS|DYIHPVCLP|DRETAASLLQAGYKGRVTGWGNLKETWTANVGKGQPSVLQVVNLPIVERPVC
K|DSTRIRIT|DNMFCAGYKP|DEGKRG|DACEG|DSGGPFVMKSPFNNRWYQMGIVSWGEGC|D
R|**DGKYGFYTHVFRLKKWIQKVI**|DQFGE

Figure 4. 12 A) Total ion chromatogram (full scan) of Asp-N digest of standard PTB using protocol 3 with guanidine hydrochloride as denaturing agent B) 40.1 % Sequence coverage (detected peptides in bold)

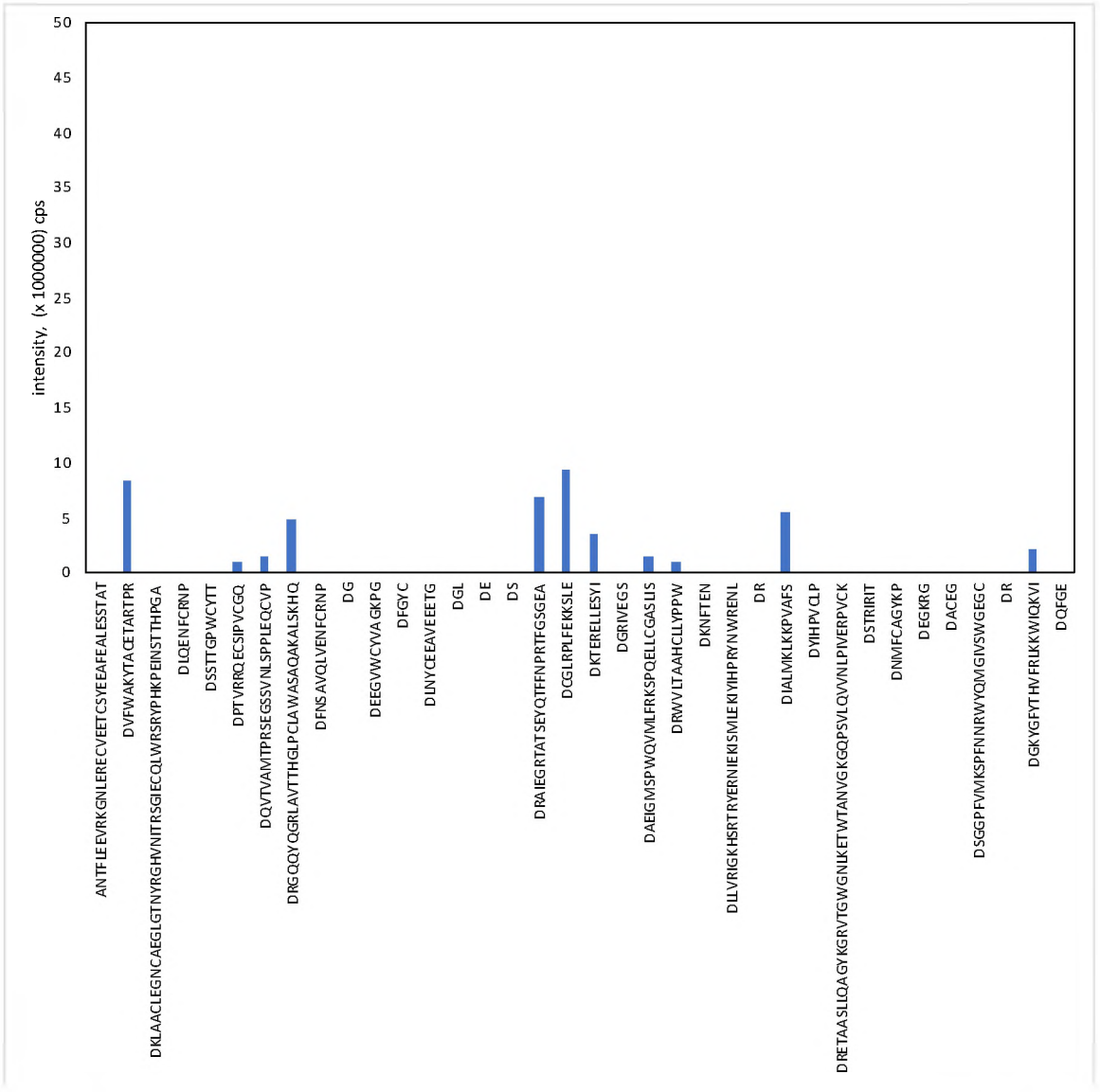

Figure 4. 13 Intensities of peptides detected in Asp-N digest of standard PTB using protocol 3 with guanidine hydrochloride as denaturing agent

sample yielded 11 of 30 peptides with a sequence coverage of 40.1% (fig. 4.12 A and B) suggesting that urea was a better denaturing agent than guanidine hydrochloride. The overall intensity of peptides in both the cases was higher than those of protocol 2 as observed in figs. 4.11 and 4.13.

4.3.4 Protocol 4

In protocol 4, we have investigated if extraction of peptides with spin filters after digestion resulted in a shift in the sequence coverage towards peptides with higher molecular weight, by removing components of molecular weight less than 3 kDa. This was conducted as follows: 10 μg of PTB was denatured with 90 μL of 8M urea in 100mM ABC buffer and incubated at 37 °C for 15 min. It was then reduced with DTT to a final concentration of 9.9 mM by incubated at 37 °C for 30 min. Alkylation was performed using IAA to a final concentration of 30.2 mM and incubated in the dark for 30 min. In order to prevent denaturation of Asp-N, concentration of urea was reduced to 2.8M by the addition of ABC buffer. Asp-N was added at an enzyme to protein ratio of 1:10 at pH 7.5 and incubated for 3.5 hours at 37 °C. After 3.5 hours, digestion was stopped by inactivating the enzyme by lowering the pH to 2 with TFA. The sample was then cleaned up using Amicon 0.5 mL centrifugal filters (MWCO 3K). For this, a spin filter was placed in a microcentrifuge tube and activated by centrifuging with 200 μL water at 14000 rpm for 6 min. Sample was loaded and spun at 14000 rpm for 10 min and washed with 50 μL of water for another 10 min at 14000 rpm. The concentrate remaining in the spin filter was collected

A

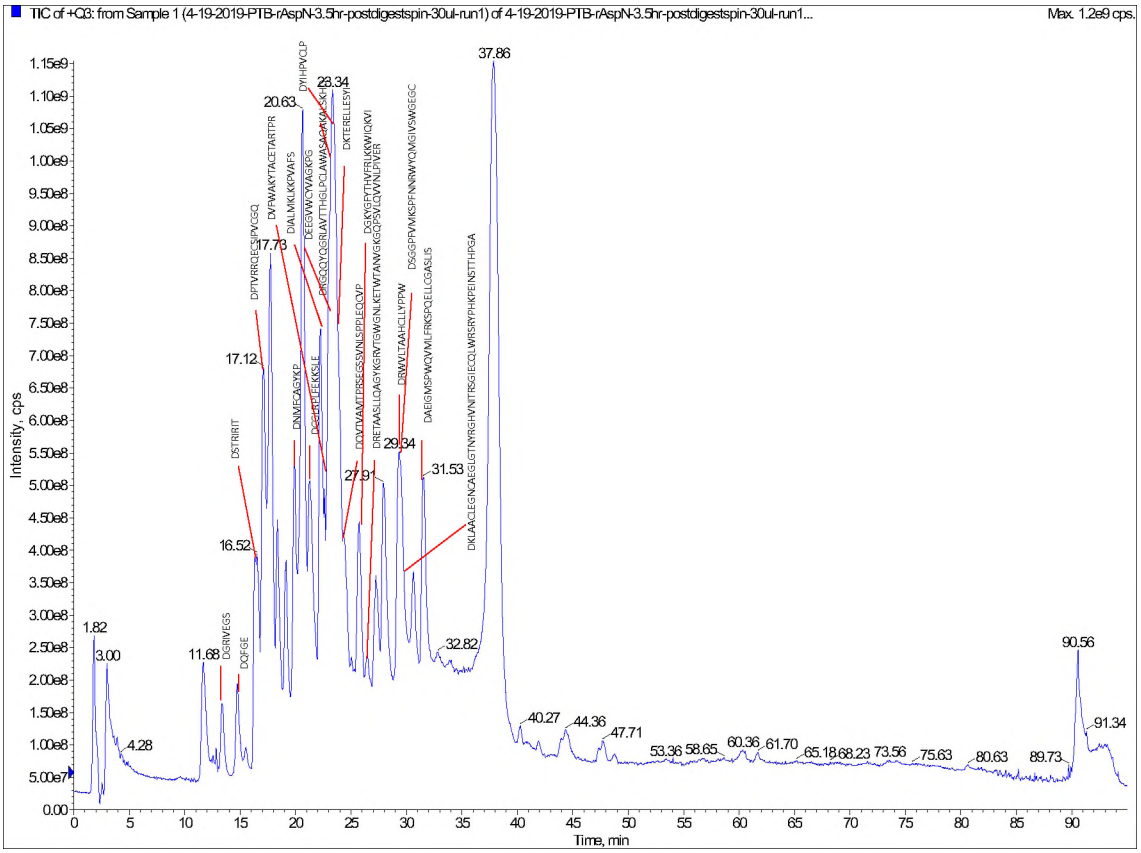

B

ANTFLEEVRKGNLERECVEETCSYEEAFEALESSTAT|**DVFWAKYTACETARTPR**|**DKLAACLEG**
NCAEGLGTNYRGHVNITRSGIECQLWRSRYPHKPEINSTTHPGA|DLQENFCRNP|DSSTTGPWC
YTT|**DPTVRRQECSIPVCGQ**|**DQVTVAMTPRSEGSSVNLSPPLEQCVP**|**DRGQQYQGRLAVTTHG**
LPCLAWASAQAKALSKHQ|DFNSAVQLVENFCRNP|DG|**DEEGVWCYVAGKPG**|DFGYC|DLNYC
EEAVEEETG|DGL|DE|DS|**DRAIEGRTATSEYQTFFNPRTFGSGEA**|**DCGLRPLFEKKSLE**|**DK**
TERELLESYI|**DGRIVEGS**|**DAEIGMSPWQVMLFRKSPQELLCGASLIS**|**DRWVLTAAHCLLYPP**
W|DKNFTEN|DLLVRIGKHSRTRYERNIEKISMLEKIYIHPRYNWRENL|DR|**DIALMKLKKPVA**
FS|**DYIHPVCLP**|**DRETAASLLQAGYKGRVTGWGNLKETWTANVGKGQPSVLQVVNLPIVERPVC**
K|**DSTRIRIT**|**DNMFCAGYKP**|DEGKRG|DACEG|**DSGGPFVMKSPFNNRWYQMGIVSWGEGC**|D
R|**DGKYGFYTHVFRLKKWIQKVI**|**DQFGE**

Figure 4. 14 A) Total ion chromatogram (full scan) of Asp-N digest of standard PTB using protocol 4 B) 73.3% Sequence coverage (detected peptides in bold)

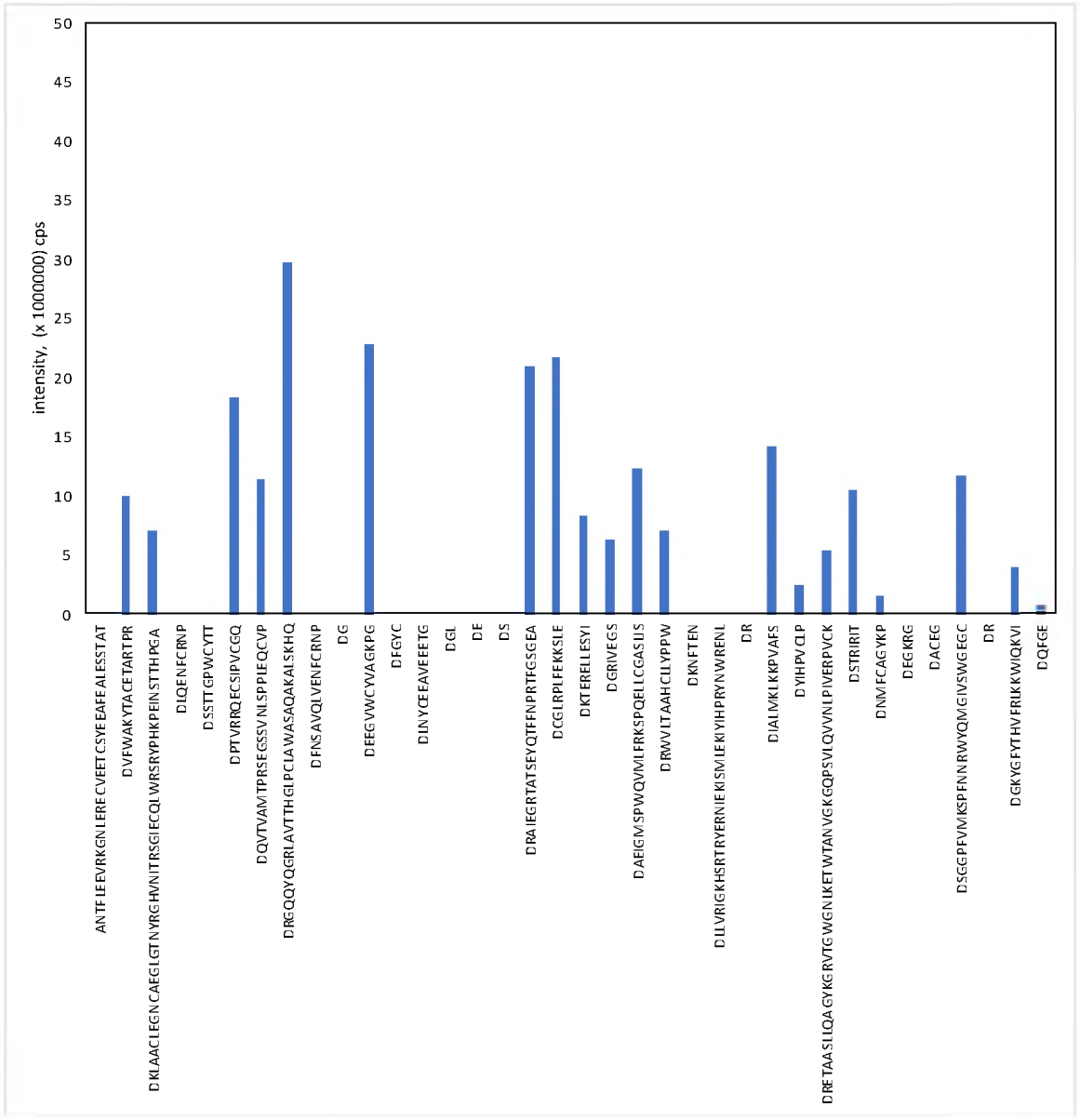

Figure 4. 15 Intensities of peptides detected in Asp-N digest of standard PTB using protocol 4

by inverting the filter into another microcentrifuge tube and spinning at 1000 rpm for 2 min. 30 μL of the sample was injected into LC-MS at a flow at rate of 50 μL/min using the same elution program as above. From fig. 4.14 A and B, it can be observed that the sequence coverage of 73.3% was higher than the previous protocol with 20 of 30 peptides (both low molecular weight and higher molecular weight) being detected. The overall intensity of the peptides was also higher than the previous protocol suggesting that using spin filters post digestion was more advantageous than using them before digestion.

4.3.5 Protocol 5

Bovine serum albumin (BSA) was found to improve digestion by possibly stabilizing the enzyme and by reducing adsorptive losses during digestion [37]. In order to study if BSA could improve sequence coverage of PTB, 5μg of BSA was spiked in the sample just before digestion with Asp-N. The digestion was conducted as follows: 10μg of PTB was denatured with 90 μL of 8M urea in 100mM ABC buffer and incubated at 37 °C for 15 min. It was then reduced with DTT to a final concentration of 9.9 mM by incubated at 37 °C for 30 min. Alkylation was performed using IAA to a final concentration of 30.2 mM and incubated in the dark for 30 min. 5 μL of 1mg/mL. In order to prevent the denaturation of Asp-N, the concentration of urea was reduced to 2.8 M by the addition of ABC buffer. BSA was added into the sample just before Asp-N was added at an enzyme to protein ratio of 1:10 at pH 7.5 and incubated for 3.5 hours at 37 °C. After 3.5 hours, digestion was stopped by inactivating the enzyme by lowering the pH to 2 with TFA. The sample was then cleaned up using Amicon

A

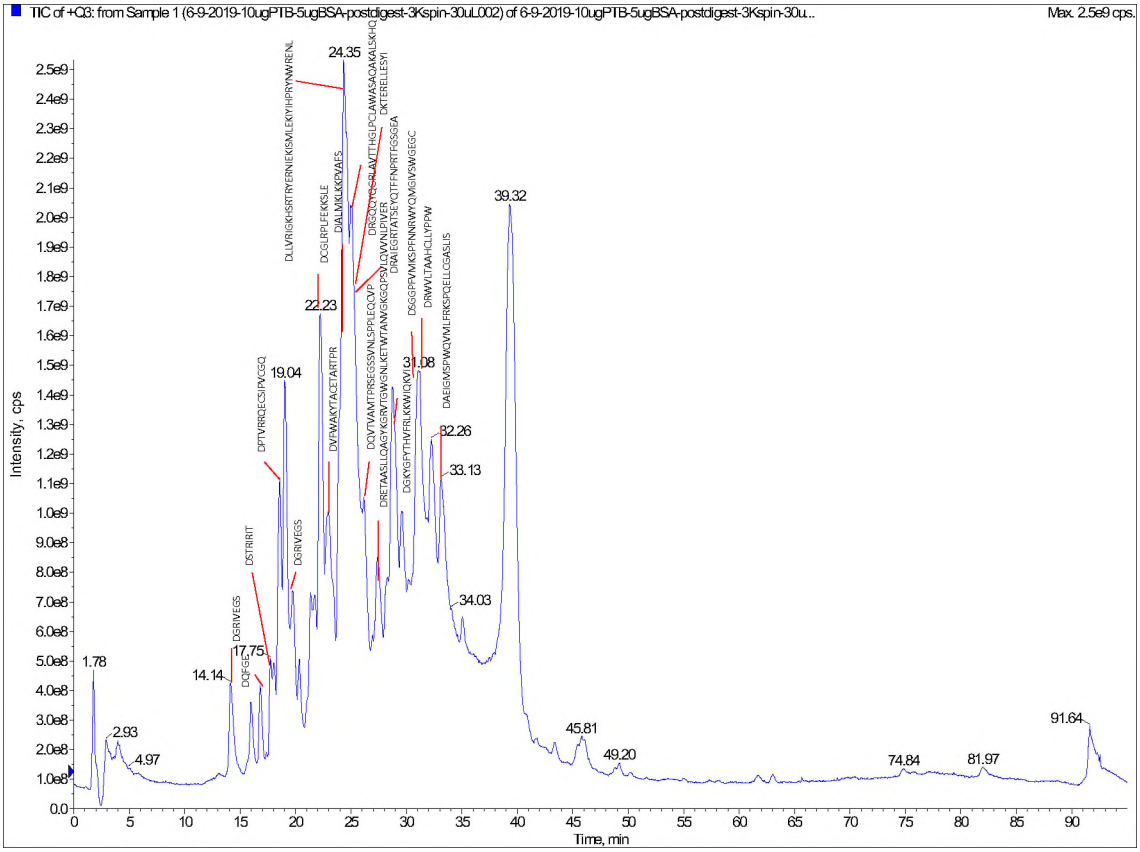

B

ANTFLEEVRKGNLERECVEETCSYEEAFEALESSTAT|**DVFWAKYTACETARTPR**|DKLAACLEG
NCAEGLGTNYRGHVNITRSGIECQLWRSRYPHKPEINSTTHPGA|DLQENFCRNP|DSSTTGPWC
YTT|**DPTVRRQECSIPVCGQ**|**DQVTVAMTPRSEGSSVNLSPPLEQCVP**|**DRGQQYQGRLAVTTHG**
LPCLAWASAQAKALSKHQ|DFNSAVQLVENFCRNP|DG|DEEGVWCYVAGKPG|DFGYC|DLNYC
EEAVEEETG|DGL|DE|DS|**DRAIEGRTATSEYQTFFNPRTFGSGEA**|**DCGLRPLFEKKSLE**|**DK**
TERELLESYI|**DGRIVEGS**|**DAEIGMSPWQVMLFRKSPQELLCGASLIS**|**DRWVLTAAHCLLYPP**
W|**DKNFTEN**|**DLLVRIGKHSRTRYERNIEKISMLEKIYIHPRYNWRENL**|DR|**DIALMKLKKPVA**
FS|DYIHPVCLP|**DRETAASLLQAGYKGRVTGWGNLKETWTANVGKGQPSVLQVVNLPIVERPVC**
K|**DSTRIRIT**|DNMFCAGYKP|DEGKRG|DACEG|**DSGGPFVMKSPFNNRWYQMGIVSWGEGC**|D
R|**DGKYGFYTHVFRLKKWIQKVI**|**DQFGE**

Figure 4. 16 A) Total ion chromatogram (full scan) of Asp-N digest of standard PTB using protocol 5 B) 67.8% Sequence coverage (detected peptides in bold)

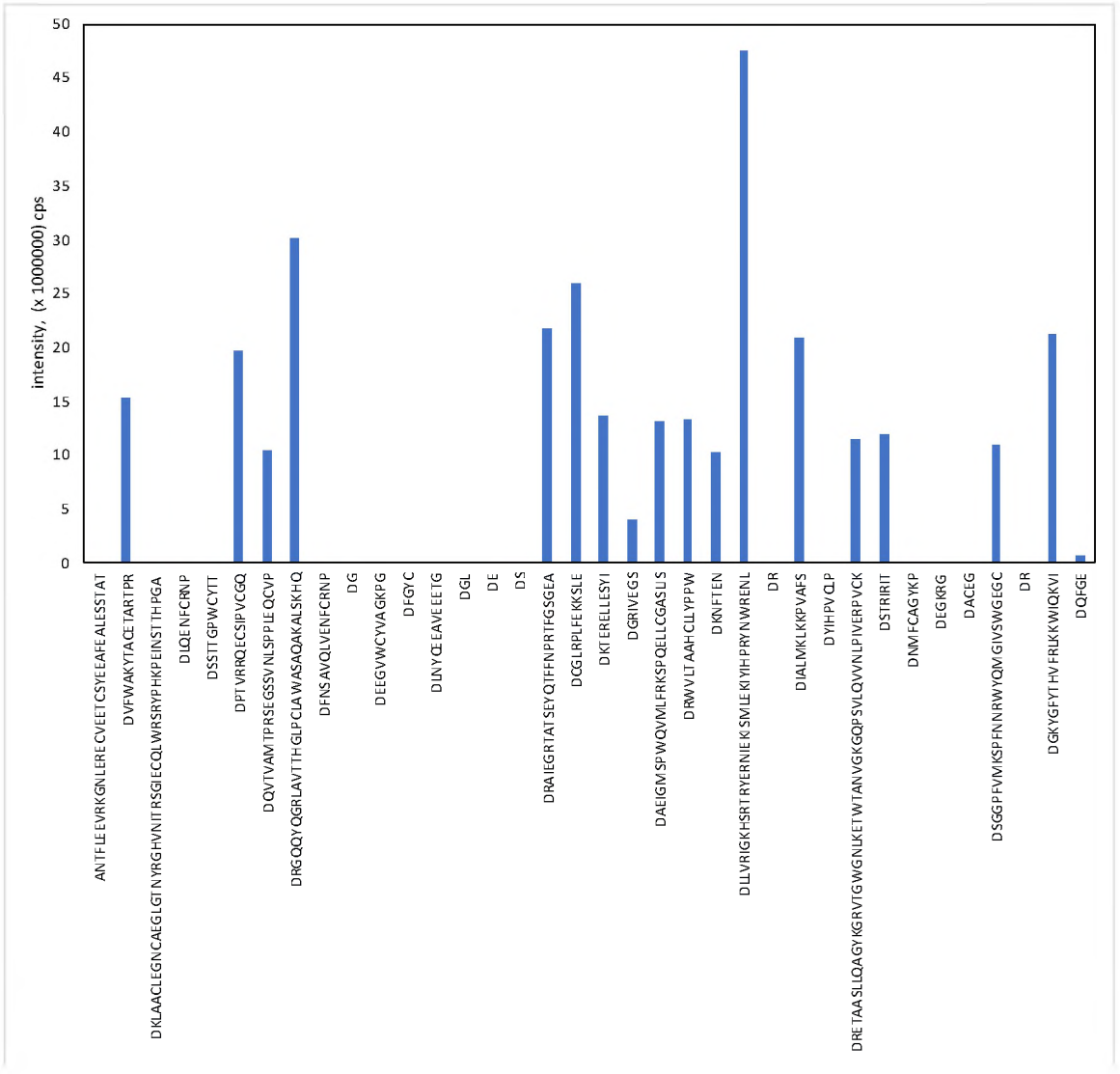

Figure 4. 17 Intensities of peptides detected in Asp-N digest of standard PTB using protocol 5

0.5 mL centrifugal filters (MWCO 3K). For this, a spin filter was placed in a microcentrifuge tube and was activated by centrifuging with 200 µL water at 14000 rpm for 6 min. Sample was then loaded and spun at 14000 rpm for 10 min and washed with 50 µL of water for another 10 min at 14000 rpm. The concentrate remaining in the spin filter was collected by inverting the filter into another microcentrifuge tube and spinning at 1000 rpm for 2 min. 30 µL of the sample was injected into LC-MS at a flow at rate of 50 µL/min with a run time of 95 min using the same elution program as above. From fig. 4.16 A and B, it can be observed that spiking BSA before digestion reduced the sequence coverage to 67.8 % with 18 of 30 peptides detected but increased the intensity of most peptides that were detected. Hence, addition of BSA might not be beneficial for improving sequence coverage.

4.3.6 Protocol 6

We have also studied if the recovery of peptides decreased due to adsorptive losses from the use of ZipTips and spin filters due to adsorptive losses. In order to evaluate whether or not this was the case, digestion was stopped using formic acid instead of TFA (to avoid ion suppression) and the sample was directly injected into LC-MS without desalting or peptide enrichment. The digestion was conducted as follows: 10 µg of PTB was denatured with 90 µL of 8M urea in 100mM ABC buffer and incubating at 37 °C for 15 min. It was then reduced with DTT to a final concentration of 9.9 mM by incubating at 37 °C for 30 min. Alkylation was performed using IAA to a final concentration of 30.2 mM and incubated in

A

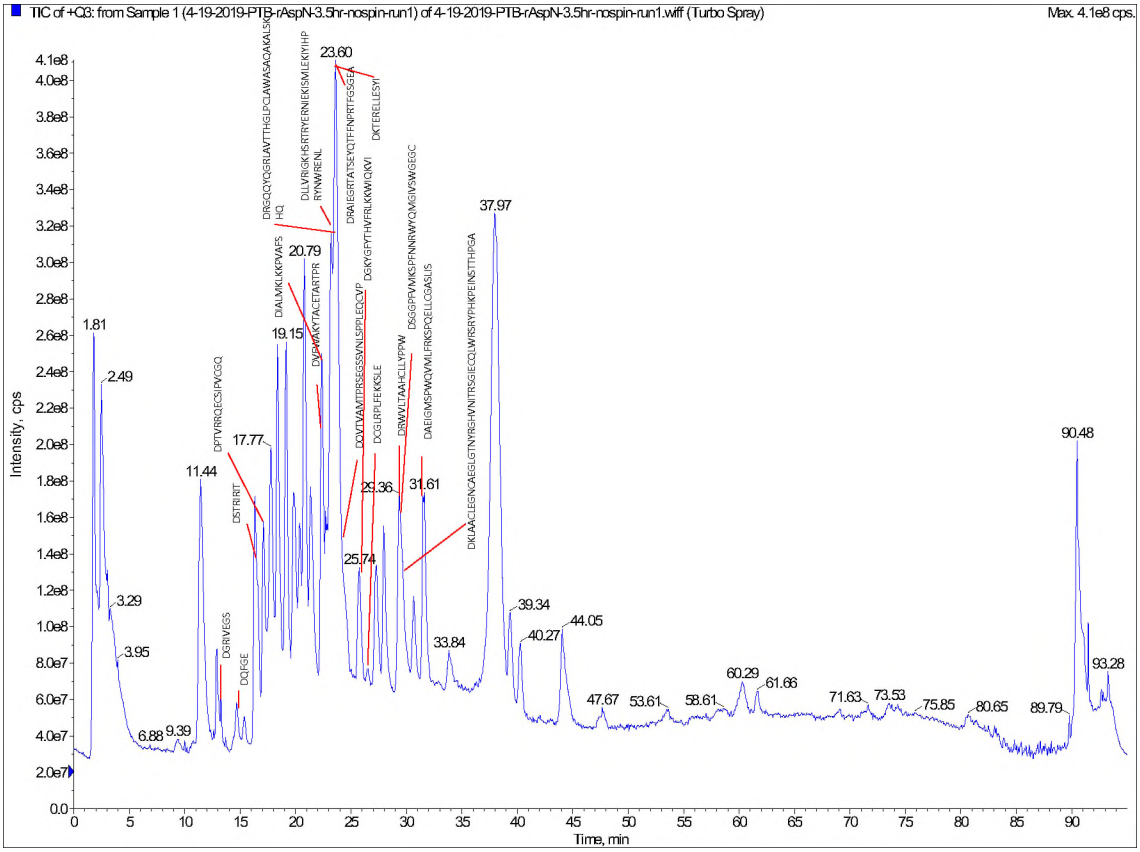

B

ANTFLEEVRKGNLERECVEETCSYEEAFEALESSTAT|**DVFWAKYTACETARTPR**|**DKLAACLEG**
NCAEGLGTNYRGHVNITRSGIECQLWRSRYPHKPEINSTTHPGA|DLQENFCRNP|DSSTTGPWC
YTT|**DPTVRRQECSIPVCGQ**|**DQVTVAMTPRSEGSSVNLSPPLEQCVP**|**DRGQQYQGRLAVTTHG**
LPCLAWASAQAKALSKHQ|DFNSAVQLVENFCRNP|DG|DEEGVWCYVAGKPG|DFGYC|DLNYC
EEAVEEETG|DGL|DE|DS|**DRAIEGRTATSEYQTFFNPRTFGSGEA**|**DCGLRPLFEKKSLE**|**DK**
TERELLESYI|**DGRIVEGS**|**DAEIGMSPWQVMLFRKSPQELLCGASLIS**|**DRWVLTAAHCLLYPP**
W|DKNFTEN|**DLLVRIGKHSRTRYERNIEKISMLEKIYIHPRYNWRENL**|DR|**DIALMKLKKPVA**
FS|DYIHPVCLP|DRETAASLLQAGYKGRVTGWGNLKETWTANVGKGQPSVLQVVNLPIVERPVC
K|**DSTRIRIT**|DNMFCAGYKP|DEGKRG|DACEG|**DSGGPFVMKSPFNNRWYQMGIVSWGEGC**|**D**
R|**DGKYGFYTHVFRLKKWIQKVI**|**DQFGE**

Figure 4. 18 A) Total ion chromatogram (full scan) of Asp-N digest of standard PTB using protocol 6 B) 65% Sequence coverage (detected peptides in bold)

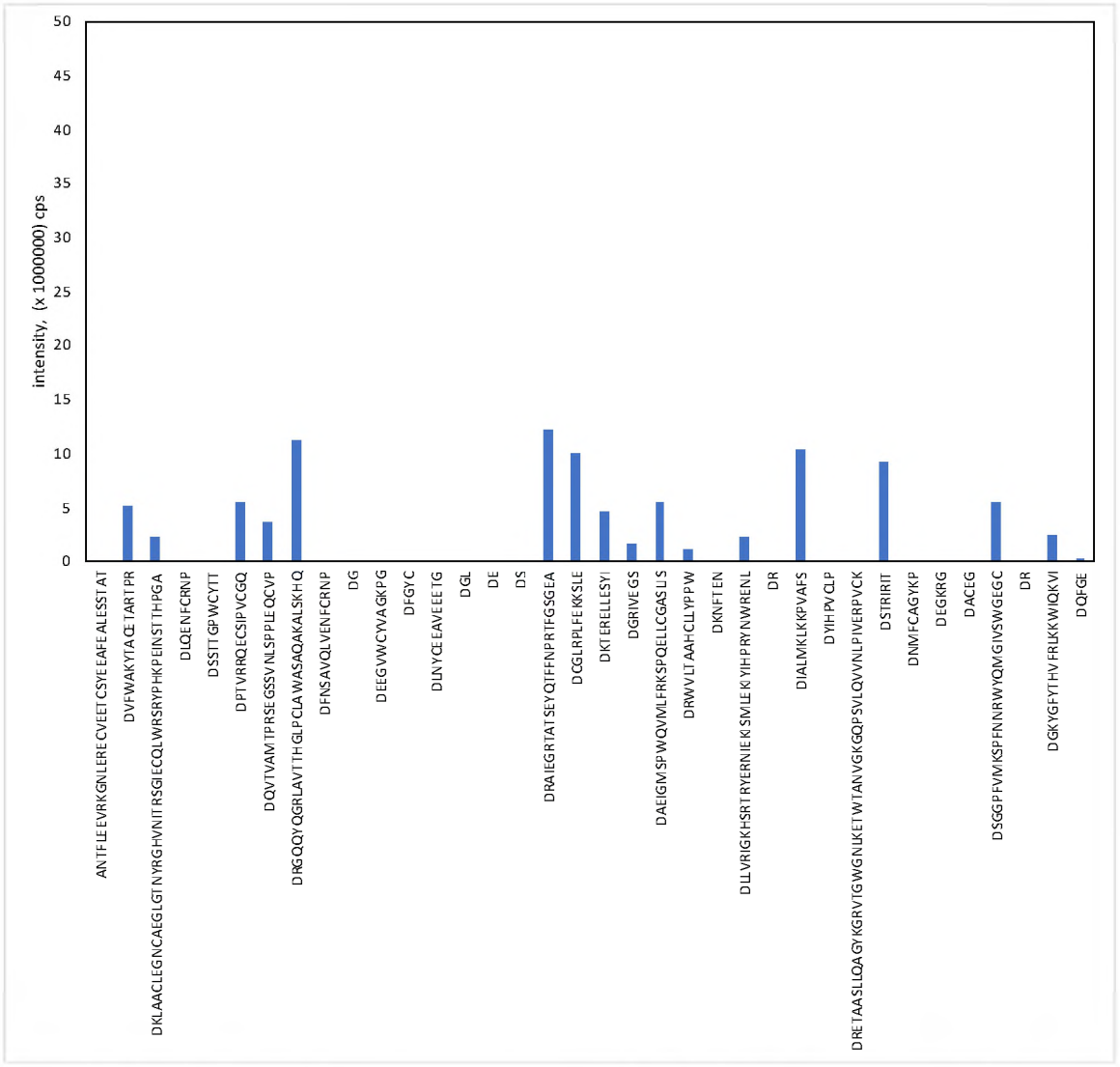

Figure 4. 19 Intensities of peptides detected in Asp-N digest of standard PTB using protocol 6

the dark for 30 min. In order to prevent the denaturation of Asp-N, the concentration of urea was reduced to 2.8M by the addition of ABC buffer. Asp-N was added at an enzyme to protein ratio of 1:10 at pH 7.5 and incubated for 3.5 hours at 37 °C. After 3.5 hours, digestion was stopped by inactivating the enzyme by lowering the pH to 2 with formic acid. 30 μL of the sample was injected into LC-MS at a flow at rate of 50 μL/min and run time of 95 min using the same elution program as above. As can be seen in fig. 4.18 A and B, sequence coverage decreased to 65% with 17 of 30 peptides detected. The overall intensities of the detected peptides were also lower which suggests that peptide enrichment using spin filters was necessary.

4.3.7 Protocol 7

Specificity of Asp-N was found to be high at shorter digestion times with decreased number of cleavages at Glus. Therefore, we decreased the digestion time to one hour to determine if better sequence coverage could be attained. Additionally, spin filters were used to achieve buffer exchange and concentrate the sample prior to digestion with Asp-N with longer centrifugation times. The digestion was conducted as follows: 10 μg of PTB was denatured with 90 μL of 8M urea in 100mM ABC and incubated at 37 °C for 15 min. It was then reduced with DTT to a final concentration of 9.9 mM by incubating at 37 °C for 30 min. Alkylation was performed using IAA to a final concentration of 30.2 mM and incubated in the dark for 30 min. The sample was then cleaned up using Amicon 0.5 mL centrifugal filters (MWCO 3K). For this, a spin filter was placed in a microcentrifuge tube

A

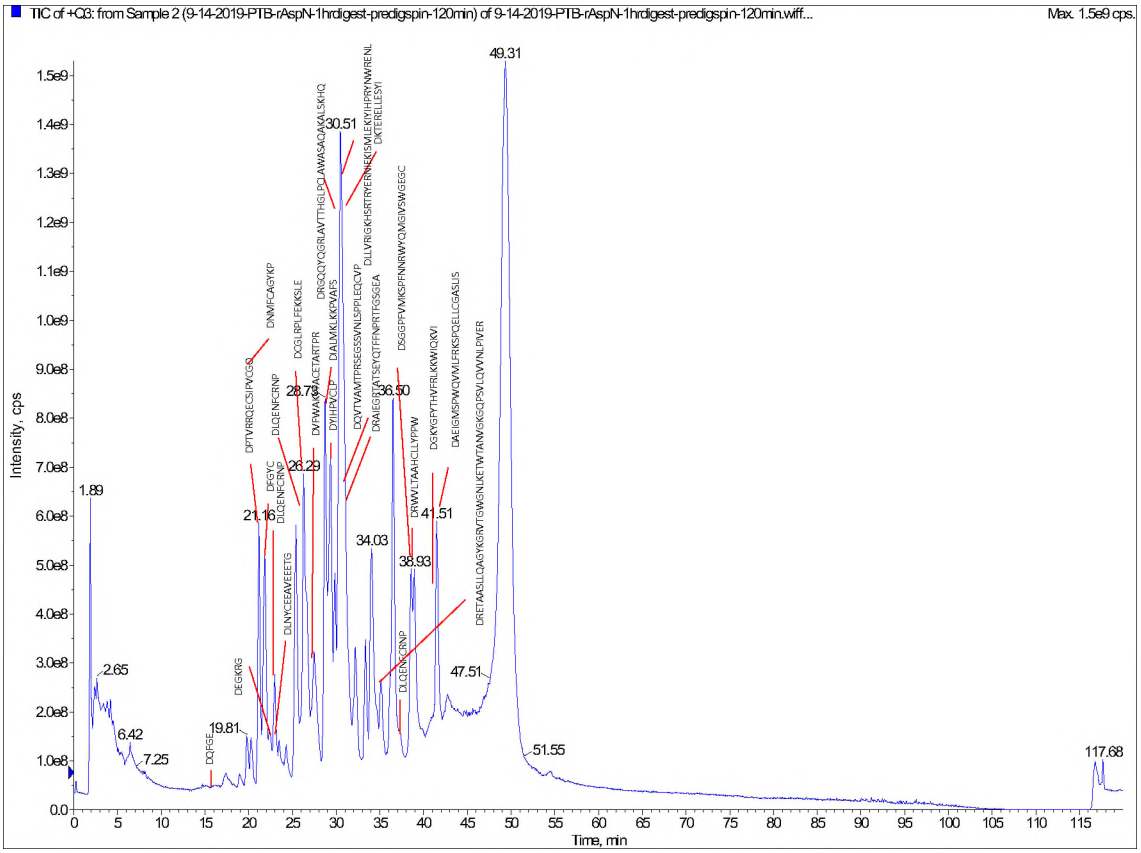

B

ANTFLEEVRKGNLERECVEETCSYEEAFEALESSTAT|**DVFWAKYTACETARTPR**|DKLAACLEG
NCAEGLGTNYRGHVNITRSGIECQLWRSRYPHKPEINSTTHPGA|**DLQENFCRNP**|**DSSTTGPWC**
YTT|**DPTVRRQECSIPVCGQ**|**DQVTVAMTPRSEGSSVNLSPPLEQCVP**|**DRGQQYQGRLAVTTHG**
LPCLAWASAQAKALSKHQ|**DFNSAVQLVENFCRNP**|DG|DEEGVWCYVAGKPG|**DFGYC**|**DLNYC**
EEAVEEETG|DGL|DE|DS|**DRAIEGRTATSEYQTFFNPRTFGSGEA**|**DCGLRPLFEKKSLE**|**DK**
TERELLESYI|DGRIVEGS|**DAEIGMSPWQVMLFRKSPQELLCGASLIS**|**DRWVLTAAHCLLYPP**
W|DKNFTEN|**DLLVRIGKHSRTRYERNIEKISMLEKIYIHPRYNWRENL**|DR|**DIALMKLKKPVA**
FS|**DYIHPVCLP**|**DRETAASLLQAGYKGRVTGWGNLKETWTANVGKGQPSVLQVVNLPIVERPVC**
K|DSTRIRIT|**DNMFCAGYKP**|**DEGKRG**|DACEG|**DSGGPFVMKSPFNNRWYQMGIVSWGEGC**|D
R|**DGKYGFYTHVFRLKKWIQKVI**|**DQFGE**

Figure 4. 20 A) Total ion chromatogram (full scan) of Asp-N digest of standard PTB using protocol 7 B) 77.9 % Sequence coverage (detected peptides in bold)

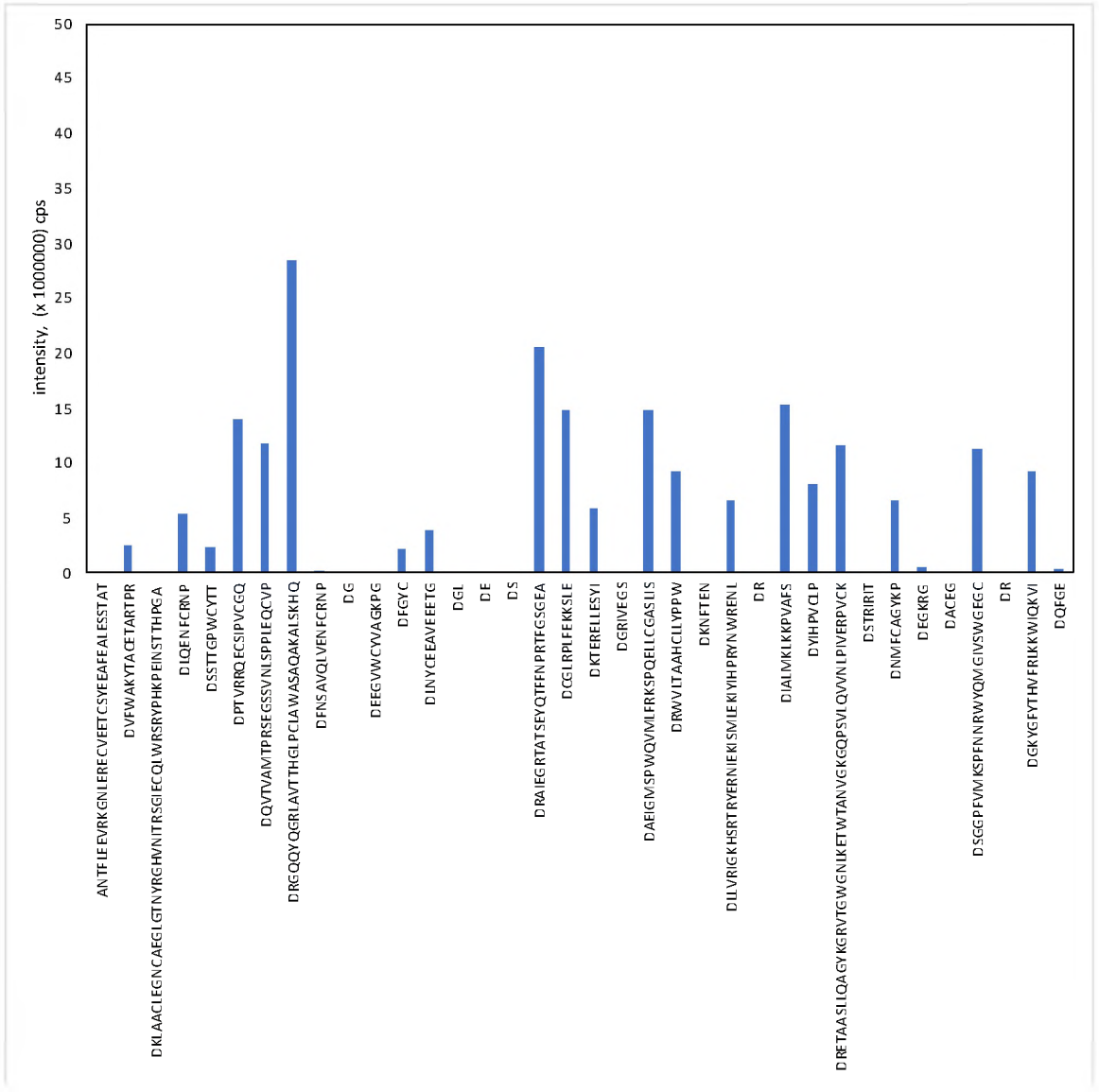

Figure 4. 21 Intensities of peptides detected in Asp-N digest of standard PTB using protocol 7

was activated by centrifuging with 200 µL water at 14000 rpm for 6 min. Sample was loaded and spun at 14000 rpm for 15 min and washed with 360 µL of ABC for another 15 min at same speed. The sample (approximately 50 µL) remaining in the spin filter was collected by inverting the filter into another microcentrifuge tube and spinning at 1500 rpm for 2 min. After clean-up, Asp-N was added at enzyme: protein ratio of 1:10 at pH 7.5 and incubated for 3.5 hours at 37 °C. After 3.5 hours, digestion was stopped by inactivating the enzyme by lowering the pH to 2 with formic acid. 30 µL of the sample was injected into LC-MS at a flow at rate of 50 µL/min with and extended run time of 120 min. The gradient elution program was also modified as follows: 0% B (initial), 0-90% B (105 min), 90% B (5 min), 90-0% B (5 min) and 0% B (5 min).

As seen in fig 4.24 A and B, the sequence coverage was increased to 77.9% with 23 of 30 peptides detected which implies that digestion efficiency was improved even if digestion time was reduced to one hour.

4.3.9 Peptide of interest

One of the common peptides that was not observed in all of the above experiments was ANTFLEEVRKGNLERECVEETCSYEEAFEALESSTAT (peptide of interest) which was essential to study the distribution of variants of DCP. Detection of peptide DVFWAKYTACETARTPR in protocols 2, 4, 5, 6, 7 suggests Asp-N did cleave PTB at Asp-38 to produce the desired peptide. There could be three possible reasons for the peptide not being produced or detected. The first probable reason was that the presence of twenty carboxyl residues in the peptide might be causing poor ionization in positive ionization

mode and poor chromatographic behavior of the peptide in reverse phase HPLC. Second possible reason could be the tendency of Asp-N to have promiscuity in its cleavage at Asp as well as at Glu (which usually occurs at a rate 2000-fold lower and increases when digestion times were longer). The third reason is the possibility of the formation of adducts in positive mode. However, this was ruled out after data analysis did not reveal any sodium, potassium or ammonium adducts. These are only speculations and the true reason as to why the target peptide was not detected could only be confirmed by fine tuning the LC-MS conditions using a synthetic peptide which contains the same sequence as that of the desired peptide. Even though proteomics studies are predominantly carried out using positive mode of ionization as Tryptic peptides with C-termial lysine and arginine residues tend to ionize well in positive ionization mode, negative mode might be a potential alternative in this case as it takes advantage of the 10-20 carboxyl groups available for de-protonation.

4.3.8 Digestion efficiency compared to Trypsin

In order to evaluate the digestion efficiency of Asp-N relative to most commonly used protease, Trypsin, PTB was also digested with Trypsin. Digestion with Trypsin was carried out as follows: 10 μg of PTB was denatured with 90 μL of 8M urea in 100mM ABC buffer and incubated at 37 °C for 15 min. It was then reduced with DTT to a final concentration of 9.9 mM by incubated at 37 °C for 30 min. Alkylation was performed using IAA to a final concentration of 30.2 mM and incubated in the dark for 30 min. In order to prevent the denaturation of Asp-N, the concentration of urea was reduced to 2.8 M by the addition

of ABC buffer. Trypsin was added at enzyme: protein ratio of 1:10 at pH 7.5 and incubated for 18 hours at 37 °C. After 18 hours, digestion was stopped by inactivating the enzyme by lowering the pH to 2 with TFA. The peptides were desalted and enriched by solid phase extraction carried out using C18 ZipTips as follows: the C18 sorbent in the ZipTip was activated using acetonitrile and 0.1 % formic acid after which the digest was loaded. The sorbent was then washed with 0.1% formic acid and the peptides were eluted into 10 µL of 60% acetonitrile. The final volume was made up to 50 µL with 0.1% formic acid. 10 µL of the sample was injected into LC-MS at a flow at rate of 50 µL/min and run time of 95 min. The elution program was same as that in protocol 2. protocols 4 and 7 and lower than those in protocol 6. As can be seen in fig. 4.22 A, it can be inferred that the sequence coverage of Trypsin was 59.1% which was lower than that of Asp-N in protocols 4, 5, 6, 7. Fig 4.22 B suggests that overall intensities of tryptic peptides were comparable to those of Asp-N peptides. These data suggest that Asp-N has better sequence coverage than Trypsin and can be used for more effective digestion of PTB.

4.3.9 Digestion efficiency at low concentrations

Since the amount of DCP in patient samples would be present in nanogram amounts (which could be further concentrated by immunoaffinity enrichment using MU-3 antibodies), we evaluated the digestion efficiency at various initial amounts of PTB such as 10 µg, 5 µg, 1 µg, 0.1 µg and 0.05 µg using protocol 4. The sequence coverage decreased ten-fold from 10 to 0.05 µg as shown in table 4.2. However, we monitored the intensity of one of the

A

ANTFLEEVR|K|GNLER|ECVEETCSYEEAFEALESSTATDVFWAK|YTACETAR|TPR|DK|**LA**
ACLEGNCAEGLGTNYR|**GHVNITR**|**SGIECQLWR**|SR|YPHKPEINSTTHPGADLQENFCR|**NPD**
SSTTGPWCYTTDPTVR|R|**QECSIPVCGQDQVTVAMTPR**|**SEGSSVNLSPPLEQCVPDR**|GQQYQ
GR|**LAVTTHGLPCLAWASAQAK**|ALSK|**HQDFNSAVQLVENFCR**|NPDGDEEGVWCYVAGKPGDF
GYCDLNYCEEAVEEETGDGLDEDSDR|AIEGR|**TATSEYQTFFNPR**|**TFGSGEADCGLRPLFEK**|
K|SLEDK|TER|**ELLESYIDGR**|**IVEGSDAEIGMSPWQVMLFR**|K|**SPQELLCGASLISDR**|**WVL**
TAAHCLLYPPWDK|NFTENDLLVR|IGK|HSR|TR|YER|NIEK|ISMLEK|IYIHPR|YNWR|E
NLDR|DIALMK|LK|KPVAFSDYIHPVCLPDR|**ETAASLLQAGYK**|GR|VTGWGNLK|**ETWTANV**
GK|**GQPSVLQVVNLPIVERPVCKDSTR**|IR|**ITDNMFCAGYKPDEGK**|R|**GDACEGDSGGPFVMK**
|SPFNNR|**WYQMGIVSWGEGCDR**|DGK|**YGFYTHVFR**|LK|K|WIQK|**VIDQFGE**

B

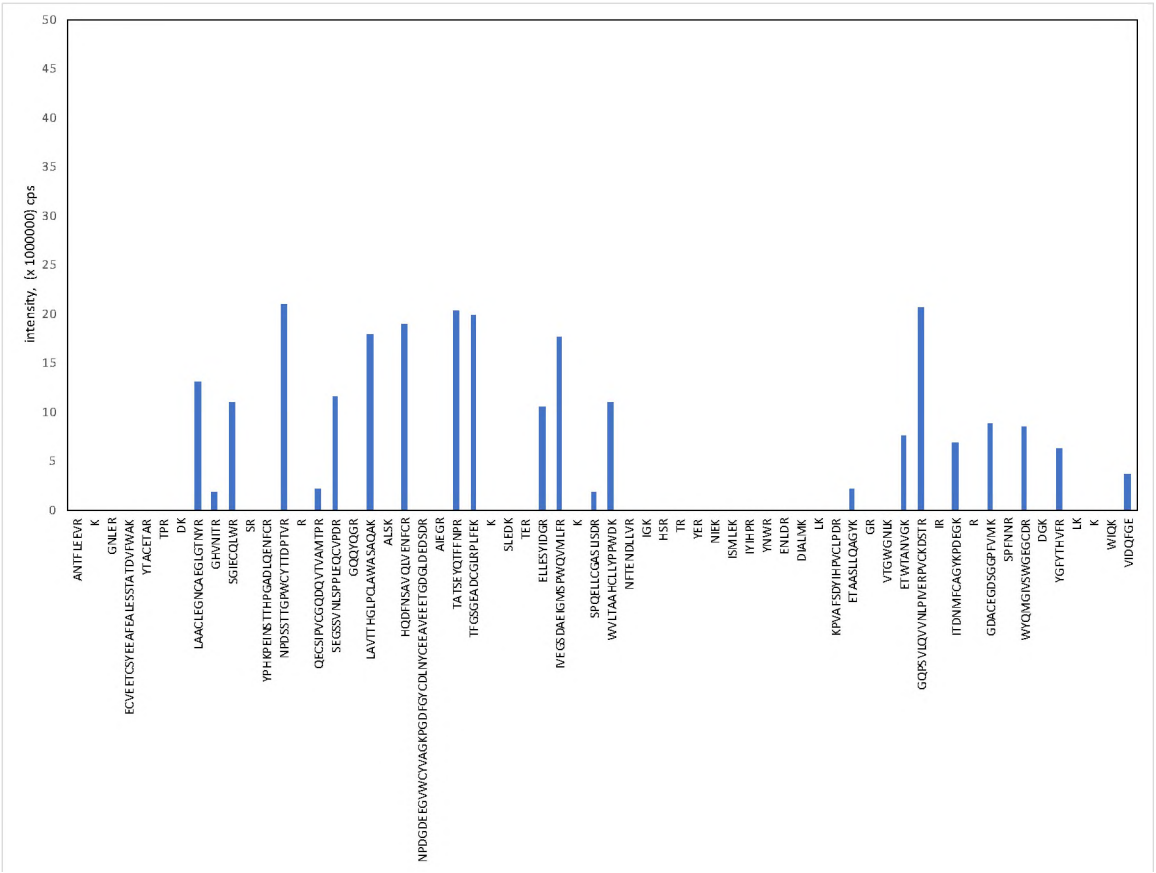

Figure 4. 22 A) 59.1% sequence coverage (detected peptides in bold) B) Intensities of peptides detected in Tryptic digest of standard PTB

Table 4. 2 Digestion efficiency at various initial concentrations of PTB

Initial amount of PTB (μg)	Amount injected into LC-MS (μg)	% sequence coverage	Intensity of peptide DCGLRPLFEKKSLE (10^6 cps)
10	0.6	73.3	20.1
5.0	0.3	58.0	15.3
1.0	0.06	37.1	3.40
0.1	0.006	22.4	0.40
0.05	0.003	7.80	0.13

peptides, detected in all five digests. The signal of the peptide DCGLRPLFEKKSLE was 1.3 $x10^5$ cps in the sample containing 0.05 μg of PTB (~ 3 ng injected into LC-MS).

4.4 Conclusion

A protocol for enzymatic digestion of PTB with Asp-N for LC-MS analysis has been described to obtain a sequence coverage of 77.9%. With this protocol, LC-MS could detect peptides when the initial amount digested was reduced to 0.05 μg. However, the peptide of interest which is essential for identification of variants of DCP was not observed most likely because of poor ionization or undesirable enzymatic cleavage at one or more Glus. It would be worthwhile to fine tune LC-MS parameters using a synthetic peptide with identical sequence and test the digest obtained from protocols 7 and 4. Additionally, the duration of digestion and enzyme to protein ratio could be reduced further to suppress the cleavages at Glus.

4.5 References

[1] S. Mittal and H. B. El-Serag, "Epidemiology of hepatocellular carcinoma: consider the population," *J. Clin. Gastroenterol.*, vol. 47 Suppl, pp. S2-6, Jul. 2013.

[2] D. S. Hill and J. Hill, "Large Hepatocellular Carcinoma in an Essentially Asymptomatic Young Woman," *J. Diagn. Med. Sonogr.*, vol. 30, no. 5, pp. 237–241, Sep. 2014.

[3] J. Bruix, M. Sherman, and American Association for the Study of Liver Diseases, "Management of hepatocellular carcinoma: an update," *Hepatol. Baltim. Md*, vol. 53, no. 3, pp. 1020–1022, Mar. 2011.

[4] H. B. El-Serag, J. A. Marrero, L. Rudolph, and K. R. Reddy, "Diagnosis and treatment of hepatocellular carcinoma," *Gastroenterology*, vol. 134, no. 6, pp. 1752–1763, May 2008.

[5] H. A. Liebman *et al.*, "Des-gamma-carboxy (abnormal) prothrombin as a serum marker of primary hepatocellular carcinoma," *N. Engl. J. Med.*, vol. 310, no. 22, pp. 1427–1431, May 1984.

[6] F. A. Durazo *et al.*, "Des-gamma-carboxyprothrombin, alpha-fetoprotein and AFP-L3 in patients with chronic hepatitis, cirrhosis and hepatocellular carcinoma," *J. Gastroenterol. Hepatol.*, vol. 23, no. 10, pp. 1541–1548, Oct. 2008.

[7] pubmeddev and V. M. al et, "Risk factors for hepatocellular carcinoma may impair the performance of biomarkers: a comparison of AFP, DCP, and AFP-L3. - PubMed

- NCBI." [Online]. Available: https://www.ncbi.nlm.nih.gov/pubmed/17522429. [Accessed: 03-Oct-2019].

[8] R. Tateishi *et al.*, "Prediction of recurrence of hepatocellular carcinoma after curative ablation using three tumor markers," *Hepatol. Baltim. Md*, vol. 44, no. 6, pp. 1518–1527, Dec. 2006.

[9] H. Okuda, A. Saito, K. Shiratori, M. Yamamoto, K. Takasaki, and M. Nakano, "Clinicopathologic features of patients with primary malignant hepatic tumors seropositive for alpha-fetoprotein-L3 alone in comparison with other patients seropositive for alpha-fetoprotein-L3," *J. Gastroenterol. Hepatol.*, vol. 20, no. 5, pp. 759–764, May 2005.

[10] H. Toyoda, T. Kumada, Y. Osaki, T. Tada, Y. Kaneoka, and A. Maeda, "Novel method to measure serum levels of des-gamma-carboxy prothrombin for hepatocellular carcinoma in patients taking warfarin: A preliminary report," *Cancer Sci.*, vol. 103, no. 5, pp. 921–925, May 2012.

[11] B. M. Grosley, C. Hirschauer, B. Chambrette, A. Bezeaud, and J. Amiral, "Specific measurement of hypocarboxylated prothrombin in plasma or serum and application to the diagnosis of hepatocellular carcinoma," *J. Lab. Clin. Med.*, vol. 127, no. 6, pp. 553–564, Jun. 1996.

[12] N. Poté *et al.*, "Performance of PIVKA-II for early hepatocellular carcinoma diagnosis and prediction of microvascular invasion," *J. Hepatol.*, vol. 62, no. 4, pp. 848–854, Apr. 2015.

[13] B. I. Carr, F. Kanke, M. Wise, and S. Satomura, "Clinical evaluation of lens culinaris agglutinin-reactive alpha-fetoprotein and des-gamma-carboxy prothrombin in histologically proven hepatocellular carcinoma in the United States," *Dig. Dis. Sci.*, vol. 52, no. 3, pp. 776–782, Mar. 2007.

[14] S. Nakamura *et al.*, "Sensitivity and specificity of des-gamma-carboxy prothrombin for diagnosis of patients with hepatocellular carcinomas varies according to tumor size," *Am. J. Gastroenterol.*, vol. 101, no. 9, pp. 2038–2043, Sep. 2006.

[15] H. Toyoda *et al.*, "Prognostic significance of simultaneous measurement of three tumor markers in patients with hepatocellular carcinoma," *Clin. Gastroenterol. Hepatol. Off. Clin. Pract. J. Am. Gastroenterol. Assoc.*, vol. 4, no. 1, pp. 111–117, Jan. 2006.

[16] Y. Deyashiki, Y. Nishioka, K. Takahashi, Y. Kosaka, and K. Suzuki, "Evaluation of des-gamma-carboxy prothrombin as a marker protein of hepatocellular carcinoma," *Cancer*, vol. 64, no. 12, pp. 2546–2551, Dec. 1989.

[17] M. Tameda *et al.*, "Des-γ-carboxy prothrombin ratio measured by P-11 and P-16 antibodies is a novel biomarker for hepatocellular carcinoma," *Cancer Sci.*, vol. 104, no. 6, pp. 725–731, 2013.

[18] "Use of serum PIVKA-II (DCP) determination for differentiation between benign and malignant liver diseases. - Google Search." [Online]. Available: https://www.google.com/search?q=Use+of+serum+PIVKA-II+(DCP)+determination+for+differentiation+between+benign+and+malignant+live

r+diseases.&oq=Use+of+serum+PIVKA-II+(DCP)+determination+for+differentiation+between+benign+and+malignant+liver+diseases.&aqs=chrome..69i57.398j0j4&sourceid=chrome&ie=UTF-8. [Accessed: 03-Oct-2019].

[19] "Des-γ-carboxy prothrombin and α-fetoprotein positive status as a new prognostic indicator after hepatic resection for hepatocellular carcinoma. - Google Search." [Online]. Available: https://www.google.com/search?q=Des%E2%80%90%CE%B3%E2%80%90carboxy+prothrombin+and+%CE%B1%E2%80%90fetoprotein+positive+status+as+a+new+prognostic+indicator+after+hepatic+resection+for+hepatocellular+carcinoma.&oq=Des%E2%80%90%CE%B3%E2%80%90carboxy+prothrombin+and+%CE%B1%E2%80%90fetoprotein+positive+status+as+a+new+prognostic+indicator+after+hepatic+resection+for+hepatocellular+carcinoma.&aqs=chrome..69i57.398j0j9&sourceid=chrome&ie=UTF-8. [Accessed: 03-Oct-2019].

[20] Y.-S. Zhang, J.-H. Chu, S.-X. Cui, Z.-Y. Song, and X.-J. Qu, "Des-γ-Carboxy prothrombin (DCP) as a Potential Autologous Growth Factor for the Development of Hepatocellular Carcinoma," *Cell. Physiol. Biochem.*, vol. 34, no. 3, pp. 903–915, 2014.

[21] "Structure of prothrombin in the closed form reveals new details on the mechanism of activation | Scientific Reports." [Online]. Available: https://www.nature.com/articles/s41598-018-21304-1. [Accessed: 11-Sep-2019].

[22] J. A. Bristol, J. V. Ratcliffe, D. A. Roth, M. A. Jacobs, B. C. Furie, and B. Furie, "Biosynthesis of prothrombin: Intracellular Localization of the Vitamin K-Dependent Carboxylase and the Sites of y-Carboxylation," p. 10.

[23] "Low serum and bone vitamin K status in patients with longstanding Crohn's disease: another pathogenetic factor of osteoporosis in Crohn's disease? | Gut." [Online]. Available: https://gut.bmj.com/content/48/4/473. [Accessed: 03-Oct-2019].

[24] S. Uehara, K. Gotoh, H. Handa, K. Honjo, and A. Hirayama, "Process of carboxylation of glutamic acid residues in the gla domain of human des-gamma-carboxyprothrombin.," *Clin. Chim. Acta Int. J. Clin. Chem.*, vol. 289, no. 1–2, pp. 33–44, 1999.

[25] B. C. Johnson, "Post-translational carboxylation of preprothrombin," *Mol. Cell. Biochem.*, vol. 38 Spec No, no. Pt 1, pp. 77–121, Aug. 1981.

[26] C. Li, Z. Zhang, P. Zhang, and J. Liu, "Diagnostic accuracy of des-gamma-carboxy prothrombin versus α-fetoprotein for hepatocellular carcinoma: A systematic review," *Hepatol. Res.*, vol. 44, no. 10, pp. E11–E25, Oct. 2014.

[27] R. G. Gish, "Early Detection of Hepatocellular Carcinoma Through Surveillance Using Biomarkers," *Gastroenterol. Hepatol.*, vol. 10, no. 2, pp. 121–123, Feb. 2014.

[28] "PeptideCutter." [Online]. Available: https://web.expasy.org/peptide_cutter/. [Accessed: 03-Oct-2019].

[29] T. Naraki *et al.*, "γ-Carboxyglutamic acid content of hepatocellular carcinoma-associated des-γ-carboxy prothrombin," *Biochim. Biophys. Acta BBA-Mol. Basis Dis.*, vol. 1586, no. 3, pp. 287–298, 2002.

[30] "Middle-down approach: a choice to sequence and characterize proteins/proteomes by mass spectrometry† - Google Search." [Online]. Available: https://www.google.com/search?q=Middle-down+approach%3A+a+choice+to+sequence+and+characterize+proteins%2Fproteomes+by+mass+spectrometry%E2%80%A0&oq=Middle-down+approach%3A+a+choice+to+sequence+and+characterize+proteins%2Fproteomes+by+mass+spectrometry%E2%80%A0&aqs=chrome..69i57.2109j0j7&sourceid=chrome&ie=UTF-8. [Accessed: 03-Oct-2019].

[31] "On the nucleation of amyloid beta-protein monomer folding. - PubMed - NCBI." [Online]. Available: https://www.ncbi.nlm.nih.gov/pubmed/15930005. [Accessed: 03-Oct-2019].Fa

[32] C. Hosfield *et al.*, "A Recombinant Asp-Specific Protease for Bottom-up Mass Spectrometry Workflows," p. 1.

[33] "Start Page: /home/software/Skyline." [Online]. Available: https://skyline.ms/project/home/software/Skyline/begin.view. [Accessed: 03-Oct-2019].

[34] "UniProt." [Online]. Available: https://www.uniprot.org/. [Accessed: 03-Oct-2019].

[35] S. Suttapitugsakul, H. Xiao, J. Smeekens, and R. Wu, "Evaluation and optimization of reduction and alkylation methods to maximize peptide identification with MS-based proteomics," *Mol. Biosyst.*, vol. 13, no. 12, pp. 2574–2582, Nov. 2017.

[36] S. Hildonen, T. G. Halvorsen, and L. Reubsaet, "Why less is more when generating tryptic peptides in bottom-up proteomics," *Proteomics*, vol. 14, no. 17–18, pp. 2031–2041, Sep. 2014.

[37] "Applications and Reaction Conditions For Restriction Enzymes." [Online]. Available: https://www.promega.com/resources/product-guides-and-selectors/restriction-enzyme-resource/applications-and-reaction-conditions-for-restriction-enzymes/. [Accessed: 10-Oct-2019].

CHAPTER V

CONCLUSIONS AND FUTURE DIRECTIONS

In this dissertation, LC-MS methods for qualitative and quantitative analyses of various small and molecules that are clinically or pharmacologically relevant were discussed. In chapter II, a high-throughput dilute-and-shoot flow injection MS/MS method for quantification of GCA and UBL in human bile was described. This was the first mass spectrometric method to simultaneously determine both the analytes in human bile. Simple dilution without time consuming extraction steps, short run time of 2.5 min resulting in a high throughput of 500 samples a day, and quantitation without HPLC separation render the method suitable for routine clinical use. However, standard-addition used in the method might not be ideal in a clinical setting, but it does eliminate the need of a blank bile matrix that is difficult to obtain. In addition, our method is fast with a run time of only 2.5 min, enabling high throughput analyses of over 500 samples a day. Though we have applied this method to clinical samples and able to quantify the analytes in most of them, we do not know if the samples belonged to healthy or diseased patients. We recommend the application of the method to bile samples from normal and diseased patients which could give us more information on utility of GCA and UBL as potential biomarkers for Cholangiocarcinoma and Cholelithiasis respectively.

In chapter III, an LC-MS/MS method for quantitative determination of TMZ in mouse brain with a recovery of 82% and matrix effects within 15% has been developed and validated for the first time. This was possible by using a two-step extraction process involving a homogenization assisted by Proteinase K and protein precipitation with ethanol. The method has been fully validated and applied to study samples. However, the amount of TMZ detected in the study samples was below LLOQ because the samples were collected long after the drug has probably been eliminated from the body. Hence, we recommend that samples be collected within an hour of intra cerebral microdialysis and quantified using our method. This will help estimate the amount of TMZ being administered to the brain and assess the potential of using intra-cerebral microdialysis as an alternative route of administration.

In chapter IV, a step wise optimization and development of a protocol for enzymatic digestion of PTB with Asp-N for LC-MS analysis has been described. The protocol developed provided a maximum sequence coverage of 77.9% which was higher than the 59.1% sequence coverage achieved by Trypsin. The method was able to detect peptides when the amount of PTB digested was reduced to 0.05 μg. However, the peptide of interest was not observed in any of the protocols probably because of poor ionization or enzymatic cleavage of Glus over-digesting the peptide into smaller fragments. Though the sequence coverage achieved was high, the method needs to be optimized further in order to confirm if the peptide of interest could be produced by Asp-N. This could be achieved using a synthetic peptide of identical sequence as that of DCP or PTB. First, the LC-MS parameters could be optimized to ensure adequate ionization of the peptide so that it could be detected. Then, the digest produced could be analyzed to check if the peptide could be identified. If

the peptide could not be identified, a possible reason is the cleavage of the peptide of interest at one or more Glus which could be suppressed by reducing the digestion time to less than one hour or/and by decreasing the enzyme to protein ratio to less than 1:10.

Once the method is optimized to detect the peptide of interest, it could be applied to study samples which are human serum belonging to HCC and Vitamin K deficient patients. But, since concentration of DCP in human serum is much lower, it needs to be enriched to be detected by LC-MS. This could be achieved by treating human serum samples with MU-3 antibodies that selectively bind to DCP variants containing >6 Glus there by separating them from other matrix components and DCP variants not relevant to diagnosis of HCC followed by elution of DCP from the antigen antibody complex, denaturation, reduction, alkylation, digestion using Asp-N and LC-MS analysis. This study could give insight into the extent of degree in gamma carboxylation in HCC and vitamin K deficiency which in turn would be beneficial to understand the mechanisms underlying both the disease processes. If the distribution of DCP variants in both the cases varies, it will be possible to distinguish Vitamin K deficiency from HCC without the need to undergo additional blood work. Further, a quantification method for the corresponding DCP variants in serum could be developed to predict the risk of HCC and to monitor the progression of HCC. If the expected results are obtained, this method will be a better tool to diagnose HCC compared to previous owing to its better specificity and its ability to diagnose HCC at an early stage.